Modulation of regulatory T cells for the immunotherapy of inflammatory diseases and cancer

Modulation regulatorischer T-Zellen zur Immuntherapie von inflammatorischen Krankheiten und Krebs

Doctoral thesis for a doctoral degree
at the Graduate School of Life Sciences,
Julius-Maximilians-Universität Würzburg,
Section Infection and Immunity

submitted by
Tim Alexander Steinfatt
from
Sinsheim, Germany

Würzburg, 2019

Submitted on: .....
Office stamp

Members of the Promotionskomitee:

Chairperson:

Primary Supervisor: Prof. Dr. Dr. Andreas Beilhack

Supervisor (Second): Prof. Dr. Harald Wajant

Supervisor (Third): Prof. Dr. Thomas Müller

Date of Public Defense: .....

Date of Receipt of Certificates: .....

I Affidavit

I hereby confirm that my thesis entitled “Modulation of regulatory T cells for the immunotherapy of inflammatory diseases and cancer” is the result of my own work. I did not receive any help or support from commercial consultants. All sources and / or materials applied are listed and specified in the thesis.

Furthermore, I confirm that this thesis has not yet been submitted as part of another examination process neither in identical nor in similar form.

Würzburg, 30.07.2019

Tim Steinfatt

Eidesstattliche Erklärung

Hiermit erkläre ich an Eides statt, die Dissertation „Modulation regulatorischer T-Zellen zur Immuntherapie von inflammatorischen Krankheiten und Krebs“ eigenständig, d.h. insbesondere selbstständig und ohne Hilfe eines kommerziellen Promotionsberaters, angefertigt und keine anderen als die von mir angegebenen Quellen und Hilfsmittel verwendet zu haben.

Ich erkläre außerdem, dass die Dissertation weder in gleicher noch in ähnlicher Form bereits in einem anderen Prüfungsverfahren vorgelegen hat.

Würzburg, 30.07.2019

Tim Steinfatt

II Acknowledgments

I am very grateful to Prof. Dr. Dr. Andreas Beilhack for giving me the opportunity to perform this exciting project in his lab. He introduced me to the fascinating field of immunology and in addition enabled personal development. Thank you for your mentorship and support!

Further, I address thanks to Prof. Dr. Harald Wajant. He was on my thesis committee and designed most of the innovative constructs I tested. His scientific advice greatly contributed to this thesis.

Special thanks to Prof. Dr. Thomas Müller. His always friendly scientific and personal input really helped me in the annual meetings and contributed to the course of this thesis.

I truly appreciate the impact of Dr. Andreas Brandl on my thesis. Thank you for the scientific and personal input you gave me. With those advice I could extremely improve and master difficult and tense moments.

Dr. Juliane Medler helped with various last-minute problems and provided information and material for most of the experiments. Thanks to her and the successful collaboration we had.

Special thanks to Sina Thusek. Especially in the beginning she supported my work and until the end she contributed with her excellent expertise. Besides work, I also enjoyed the friendship with her.

Further, I am grateful for being a member of the tumor team. I really enjoyed the work and social life together with Miriam Kurzwart, Theresa Schneider, Julia Hartweg, Hannah Manz, Dr. Julia Delgado Tascon and Elena Seebacher. They all contributed to our great team atmosphere and heavily supported my work. I also wish to thank Carolin Graf, Katharina Schmiedgen, Marlene Strobel and Dr. Yidong Yu. All gave excellent technical input, shaped our team spirit and made me enjoy my work.

I am thankful to Dr. Katja Jarick. With her experience she could answered countless questions and always had helpful advice for my experiments.

Further I wish to thank Haroon Shaik and Dr. Duc-Dung Le who helped with the GvHD experiments.

From the former AG Beilhack members, I want to thank especially Dr. Thorsten Winter for his help with the STAR2 experiments and Berkan Arslan for friendship and technical support in many ways. Further, I want to express gratitude to Ina Eckert and Kerstin Schmid. Both contributed enormously to my first steps at the AG Beilhack and after both left, we still had a great friendship.

Also, the medical students Lukas Scheller, Maria Ranecky and Stefanie Schwinn contributed to a great work environment during my time in the Beihlack lab. Thanks to you!

Many thanks go to our secretary Sabine Stöckel-Eckard. In managing and organizing our group she has a tough job, which she handles extremely well.

I wish to thank Prof. Dr. Hünig. He gave inspiring seminars and shaped my understandings of classical and modern immunology. Further, he enabled great scientific and social interactions during the program retreats together with Tübingen and Erlangen.

III Table of contents

IV List of figures

V List of tables

VI List of abbreviations

Al	Alexa fluor
Allo-HCT	Allogeneic hematopoietic cell transplantation
APC	Allophycocyanin
BLI	Bioluminescence imaging
B6a	C57BL/6-Tyr$^{c\text{-}2J}$/J
CD	Cluster of differentiation
CMC	Complement-mediated cytotoxicity
CRD	Cysteine-rich domains
CTLA-4	Cytotoxic T-lymphocyte-associated protein 4
Ctrl.	Control
Cy	Cyanin
d	Day
DMEM	Dulbecco's modified eagle medium
Ecd	Extracellular domain
EDTA	Ethylenediaminetetraacetic acid
eGFP	Enhanced green fluorescent protein
Fc	Fragment crystalline
FcRn	Neonatal Fc receptor
FCS	Fetal calf serum
FoxP3	Forkhead box protein P3
g	Gram
G	Gravitational constant
GITR	Glucocorticoid-induced TNFR-related protein
GvHD	Graft-versus-host disease
h	Hour
hu	Human
IgG	Immunoglobulin
IL	Interleukin
IDO	Indoleamine 2,3-dioxygenase

i.p.	Intraperitoneal
irr	Irrelevant
i.v.	Intravenous
IPEX	Immune dysregulation, polyendocrinopathy, enteropathy, X-linked syndrome
L	Liter
LSFM	Light sheet fluorescence microscopy
MDSC	Myeloid-derived suppressor cell
m	Meter
MHC	Major histocompatibility complex
min	Minute
mo	Murine
mTNFα	Membrane tumor necrosis factor alpha
NF-κB	Nuclear factor kappa-light-chain-enhancer of activated B cells
NK cells	Natural killer cells
PBS	Phosphate buffered saline
PD-1	Programmed cell death protein 1
PDAC	Pancreatic ductal adenocarcionoma
PE	Phycoerythrin
PerCP	Peridinin-chlorophyll-protein complex
pLN	Pancreatic lymph nodes
pTregs	Peripherally derived regulatory T cells
rpm	Revolutions per minute
RPMI	Roswell Park Memorial Institute
RT	Room temperature
scTNF80	Single chain trimers of TNFR2-specific TNF molecules
STAR2	Selective TNF-based agonist of TNFR2
TDSR	Treg-specific demethylated region
TGF-β	Transforming growth factor beta
Tregs	Regulatory T cells
tTregs	Thymus-derived regulatory T cells

TIGIT	T cell immunoglobulin and ITIM domain
TNFα	Tumor necrosis factor alpha
TNFR2	Tumor necrosis factor receptor 2
TNFRSF	Tumor necrosis factor receptor super family
Tcons	Conventional T cells
IgG	Immunoglobulin
s	Second
sTNF	Soluble tumor necrosis factor alpha
s.c.	Subcutaneous
sc	Single chain
TRAF	Tumor necrosis factor receptor associated factor
TNC	Trimerization domain of chicken tenascin C

VII Contribution statement

I conducted my doctoral thesis project in the laboratory of Prof. Dr. Dr. Andreas Beilhack at the University Hospital in Würzburg, Germany. The experiments and the laboratory work I performed myself with the technical assistance of Theresa Schneider, Elena Seebacher, Julia Hartweg, Sina Thusek, Miriam Ritz, Carolin Graf, Dr. Julia Delgado Tascon, Dr. Thorsten Winter (all current or former members of the Beilhack laboratory). Prof. Dr. Thomas Hünig and Susanne Berr (Institute for Virology and Immunobiology, Würzburg University, Germany) helped with the fusion, generation and culture of hybridoma cells. All antibodies and fusion proteins were designed by Prof. Dr. Harald Wajant (Division of Molecular Medicine, Department of Internal Medicine II, University Hospital Würzburg). Dr. Juliane Medler (née Kums) from the Wajant laboratory characterized, produced and purified the constructs. Christian Linden (Institute for Virology and Immunobiology, Würzburg University, Germany) sorted regulatory T cells for the STAR2 experiments.

The *in vitro* experiments with STAR2 on Tregs were published in the article "Exogenous TNFR2 activation protects from acute GvHD via host T reg cell expansion" published in August 2016 in the Journal of Experimental Medicine (Chopra et al., 2016). The experiments with NewSTAR were part of the invention report "monospecific bimodular TNF-receptor activating antibodies (mobiTRaAbs)" – H. Wajant, A. Beilhack, J. Medler, T. Steinfatt, 2019. Antibody clones obtained from the immunizations contributed to the work "TNFRSF receptor-specific antibody fusion proteins with targeting controlled FcγR-independent agonistic activity" published in March 2019 in Cell Death and Disease (Medler et al., 2019).

The experiments targeting the tumor stroma to alter the immune cell composition for more effective control of cancer are part of an ongoing collaboration between the laboratory of Dr. Erik Henke (Tumor Microenvironment and Experimental Therapeutics, Institute for Anatomy and Cell Biology II, Würzburg University, Germany) and the Beilhack laboratory.

VIII Abstract

Regulatory T cells (Tregs) are the masters of immune regulation controlling inflammation and tolerance, tissue repair and homeostasis. Multiple immunological diseases result from altered Treg frequencies and Treg dysfunction. We hypothesized that augmenting Treg function and numbers would prevent inflammatory disease whereas inhibiting or depleting Tregs would improve cancer immunotherapy.

In the first part of this thesis, we explored whether *in vivo* activation and expansion of Tregs would impair acute graft-versus-host disease (aGvHD). In this inflammatory disease, Tregs are highly pathophysiological relevant and their adoptive transfer proved beneficial on disease outcome in preclinical models and clinical studies. IL-2 has been recognized as a key cytokine for Treg function. Yet, attempts in translating Treg expansion via IL-2 have remained challenging, due to IL-2s extremely broad action on other cell types including effector T cells, NK cells, eosinophils and vascular leakage syndrome, and importantly, due to poor pharmacokinetics *in vivo*. We addressed the latter issue using an IL-2-IgG-fusion protein (irrIgG-IL-2) with improved serum retention and demonstrated profound Treg expansion *in vivo* in FoxP3-luciferase reporter mice. Further, we augmented Treg numbers and function via the selective-TNF based agonists of TNFR2 (STAR2). Subsequently, we tested a next-generation TNFR2 agonist, termed NewSTAR, which proved even more effective. TNFR2 stimulation augmented Treg numbers and function and was as good as or even superior to the IL-2 strategy. Finally, in a mouse model of aGvHD we proved the clinical relevance of Treg expansion and activation with irrIgG-IL-2, STAR2 and NewSTAR. Notably, the TNFR2 stimulating constructs were outstanding as we observed not the IL-2 prototypic effects on other cell populations and no severe side effects.

In the second part of this thesis, we explored Tregs in pancreatic ductal adenocarcinoma (PDAC) and developed targeting strategies. Among several tumor entities in which Tregs impact survival, preclinical and clinical data demonstrated their negative role on PDAC. In our studies we employed the orthotopic syngeneic Panc02 model in immunocompetent mice. Based on flow cytometric analysis of the tumor microenvironment we propose TIGIT and TNFRSF members as novel therapeutic targets. Surprisingly, we found that blocking TNFR2 did not interfere with intratumoral Treg accumulation. However, we decreased the highly abundant intratumoral Tregs when we disrupted the tumor extracellular matrix. In PDAC, Treg

manipulation alone did not lead to tumor regression and we propose that an additional immune boost may be necessary for efficient tumor immune surveillance and cancer clearance. This contrasts with aGvHD, in which Treg manipulation alone was sufficient to improve disease outcome.

Conclusively, we demonstrated the enormous medical benefit of Treg manipulation. Our promising data obtained with our newly developed powerful tools highlight the potential to translate our findings into clinical practice to therapeutically target human Tregs in patients. With novel TNFR2 agonists (STAR2, NewSTAR) we augmented Treg numbers and function as (or even more) effectively than with IL-2, without causing adverse side effects. Importantly, exogenous *in vivo* Treg expansion protected mice from aGvHD. For the therapy of PDAC, we identified novel targets on Tregs, notably TIGIT and members of the TNFRSF. We demonstrated that altering the extracellular tumor matrix can efficiently disrupt the Treg abundance in tumors. These novel targeting strategies appear as attractive new treatment options and they may benefit patients suffering from inflammatory disease and cancer in the future.

IX Zusammenfassung

Regulatorische T-Zellen (Tregs) gelten als die Meister der Immunregulation und entscheiden über Entzündungen und Immuntoleranz, Geweberegeneration und -homöostase. Eine Vielzahl von immunologischen Erkrankungen resultiert aus Veränderung der Treg-Anzahl oder ihrer Funktion. Wir stellten die Hypothese auf, dass Steigerung der Treg-Frequenz und -Funktion entzündliche Erkrankungen verhindert und dass eine Treg-Depletion die Immuntherapie gegen Krebs unterstützt.

Im ersten Teil dieser Studie untersuchten wir, ob eine exogene Aktivierung und Expansion von Tregs *in vivo* eine akute Graft-versus-Host-Reaktion (aGvHD) therapeutisch verhindern oder abschwächen kann. Für dieses Krankheitsbild sind Tregs pathologisch hochrelevant und präklinische Modelle sowie klinische Studien zeigen, dass ein adoptiver Treg-Transfer sich positiv auf das Auftreten bzw. den Verlauf des Immunsyndroms auswirkt. IL-2 ist ein Schlüsselzytokin für die Funktion der Tregs. Dennoch bleibt die klinische Entwicklung eine große Herausforderung, da IL-2 eine breite Wirkung auf weitere Zelltypen wie Effektor T-Zellen, NK-Zellen, eosinophile Granulozyten und Endothelzellen hat. Dadurch können schwerwiegende Nebenwirkungen auftreten, wie zum Beispiel das gefürchtete Vascular-Leak-Syndrom oder eine Eosinophilie. Ein weiteres großes Hindernis für den klinischen Einsatz von IL-2 stellt auch die schlechte *in vivo* Pharmakokinetik von IL-2 dar. Diese adressierten wir durch die Fusion von IL-2 mit einem IgG (irrIgG-IL-2), wodurch die Serumretention deutlich verbessert werden konnte. Durch die Applikation von irrIgG-IL-2 konnten wir Tregs *in vivo* in FoxP3-Reportermäusen expandieren. IrrIgG-IL2 verbesserte auch die Funktionen und Anzahl der Tregs, ähnlich wie der selektive, TNF-basierte Agonist des TNFR2 (STAR2). Die nächste Generation von STAR2 (NewSTAR) hatte sogar noch einen größeren Effekt auf Tregs *in vivo* und war STAR2 überlegen. Exogene TNFR2-Stimulation zeigte vergleichbare (oder sogar bessere) Effekte auf die Tregs *in vivo* wie IL-2-Stimulation ohne, dass unerwünschte Nebenwirkungen zu beobachten waren. Die medizinische Relevanz dieser Treg-Agonisten zeigte sich in der *in vivo* Treg-Aktivierung und -Expansion mittels irrIgG-IL-2, STAR2 und NewSTAR in einem präklinischen aGvHD Modell. Herausragend war die exogene TNFR2 Stimulation, da die für IL-2 typischen Effekte auf andere Immunzellen nicht zu beobachten waren.

Im zweiten Teil dieser Arbeit untersuchten wir Tregs im duktalen Adenokarzinom des Pankreas (PDAC) zur Entwicklung neuner therapeutischer Targeting-Strategien. Unter den vielen Tumorentitäten in welchen Tregs das Überleben beeinflussen, zeigen besonders die präklinischen und klinischen Daten im PDAC ihre negative Rolle. Für unsere Studien verwendeten wir das orthotope, syngene Panc02 Modell in immunkompetenten Mäusen. Mit Hilfe der Durchflusszytometrie analysierten wir das Tumormikromilieu und präsentieren TIGIT und Mitglieder der TNFRSF als neue therapeutische Targets. Eine Blockade des TNFR2 reduzierte nicht die intratumorale Akkumulation von Tregs. Jedoch gelang es durch Manipulation der extrazellulären Tumormatrix deutlich die Anzahl an Tregs im Tumor zu reduzieren. Allerdings reichte im PDAC die Treg-Manipulation allein nicht zur Tumorregression aus und wir postulieren, dass eine weitere Verstärkung der Immunantwort nötig ist, um eine Tumorregression bzw. -kontrolle zu erreichen.

Zusammenfassend zeigten wir das hohe therapeutische Potenzial der Manipulation von Tregs *in vivo* und stellen wirkungsvolle Strategien zu ihrer Umsetzung vor. Mit neuartigen TNFR2 Agonisten (STAR2, NewSTAR) konnten wir die Funktion und Anzahl der Tregs verstärken. Der Effekt war genauso gut (oder sogar besser) wie nach IL-2 Stimulation, jedoch ohne unerwünschte Nebenwirkungen. Bemerkenswert war der therapeutische Nutzen zur Verhinderung der aGvHD nach allogener Stammzelltransplantation. Als neue therapeutische Targets im PDAC identifizierten wir TIGIT und Mitglieder der TNFRSF. Durch Veränderung der extrazellulären Tumormatrix gelang es uns die Anzahl der tumorinfiltrierenden Tregs zu reduzieren. Diese neuen Behandlungsstrategien erscheinen als höchst attraktive Therapieoptionen, welche Patienten mit Entzündungserkrankungen bzw. mit einer Krebsdiagnose in Zukunft nutzen könnten.

1 Introduction

1.1 Regulatory T cells

1.1.1 Regulatory T cells in health and disease

In the 1990s Sakaguchi *et al.* observed a population of CD25 expressing $CD4^+$ T cells that protects from autoimmune symptoms and maintain immunologic self-tolerance. These cells constitute approximately 10 % of the $CD4^+$ T cells in the periphery (Sakaguchi et al., 1995). According to their function the subset was termed regulatory T cells (Tregs). Forkhead box protein P3 (FoxP3, also known as scurfin) was identified as the master transcription factor of Tregs (Hori et al., 2003). Mice with mutations in the FOXP3 locus show the scurfy phenotype, with abnormal T cell proliferation, organ infiltration and elevated cytokine levels (Brunkow et al., 2001). Similar symptoms occur in humans with mutations in the human FoxP3 locus and manifest as the immune dysregulation, polyendocrinopathy, enteropathy, X-linked syndrome (IPEX; Bennett et al., 2001).

There are many inflammatory diseases in which Tregs are considered functional, but their numbers appear to be insufficient to control the persisting inflammation. In these cases, more Tregs are needed and conceptually, Treg expansion appears therapeutically desirable. Based on preclinical mouse models it has been postulated that expanding Tregs would benefit inflammatory diseases such as asthma, type 1 diabetes and experimental autoimmune encephalomyelitis (Brusko and Atkinson, 2007; Ephrem et al., 2008; Schreiber et al., 2010). Furthermore, in transplant rejection and graft-versus-host disease (GvHD) an expansion of Tregs improves the outcome (Hoffmann et al., 2002; Taylor et al. 2002; van Maurik et al., 2002; Edinger et al., 2003; Nguyen et al., 2007). Whereas dysfunctionality or insufficient Treg numbers are often a hallmark of inflammatory disease conditions, there is also a vast number of diseases associated with elevated Treg numbers or function. Particularly, the poor prognosis of malignant diseases is strongly associated with enhanced Treg accumulation within the tumor microenvironment (Barnett et al., 2005; Beyer et al., 2006; Hiraoka et al., 2006). Furthermore, other chronic diseases such as Alzheimer's disease have been associated with higher Treg numbers (Baruch et al., 2015). In preclinical mouse models it has been functionally demonstrated that Treg depletion attenuates disease (Bos et al., 2013; Baruch et al., 2015; Jang et al., 2017).

1.1.2 Suppressive mechanisms of Tregs

Tregs can exert several mechanisms to suppress immune responses. First, they can secrete tolerogenic cytokines, notably TGFβ, IL-10 and IL-35 (Figure 1 A). Second, Tregs can lyse effector cells via granzymes and perforin (Figure 1 B) and third, they can disrupt the metabolite milieu (Figure 1 C). Tregs express constitutively high levels of CD25, the high-affinity IL-2 receptor and, thus very efficiently consume IL-2 thereby starving activated T cells of IL-2 at the site of inflammation. Furthermore, Tregs generate extracellular adenosine via CD39 and CD73. Adenosine has inhibitory effects on T cells. Fourth, Tregs can target dendritic cells and downregulate their costimulatory ligands. Thereby, Tregs interfere with T cells activation (Figure 1 D). Several mechanisms for these potent immunosuppressive interactions of Tregs and antigen-presenting cells have been identified. Tregs can employ cytotoxic T-lymphocyte-associated protein 4 (CTLA-4) to target and reduce CD80 and CD86 and to enhance

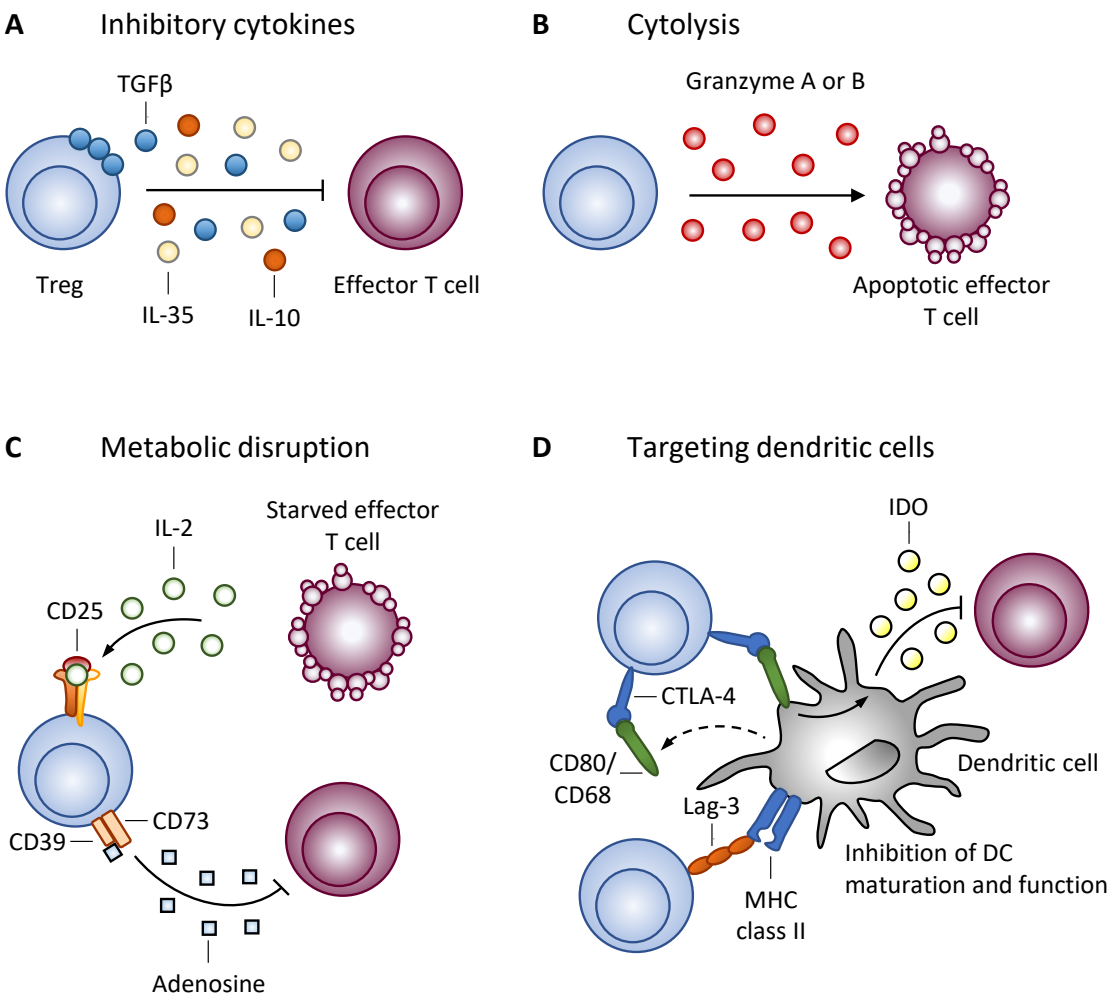

Figure 1: **Treg mechanisms to suppress immune cells and their effector functions.** (A) Tregs secrete inhibitory cytokines, (B) lyse target cells, (C) establish a suppressive metabolic environment and (D) target dendritic cells. Figure blueprinted and edited from Vignali, Collison, and Workman 2008.

indoleamine 2,3-dioxygenase (IDO) expression in dendritic cells. Additionally, Tregs can suppress dendritic cell maturation via Lag-3. In addition to dendritic cells, Tregs can also inhibit monocytes and macrophages (Vignali et al., 2008), which are important to exert either proinflammatory or anti-inflammatory functions in peripheral tissues.

1.1.3 Development and phenotype of Tregs

Tregs differentiate from pre-T cell precursors in the thymus with high affinity for self-antigens (Jordan et al., 2001; Apostolou et al., 2002). In addition, TGFβ converts Tregs from conventional T cells (Chen et al. 2003; Tcons; Bettelli et al., 2006). Tregs that arise from the thymus are termed thymus-derived (tTregs). Tregs induced in the periphery are termed peripherally derived (pTregs; Abbas et al., 2013). Helios and Neuropilin-1 were originally thought to be markers for tTregs, but further studies showed that they can also be expressed in pTregs (Akimova et al., 2011; Gottschalk et al., 2012; Yadav et al., 2012; Szurek et al., 2015). Until today, the only way to distinguish between tTregs and pTregs is the methylation status of the FOXP3 locus. In tTregs the Treg-specific demethylated region (TSDR) within the FOXP3 locus is fully methylated. With the TSDR methylation status it is further possible to discriminate between freshly activated human Tcons that can also express FoxP3 and Tregs (Baron et al., 2007). Besides FoxP3 there are several other characteristics, although not unique markers for Tregs. They constitutively express high levels of IL2Rα (CD25), the high affinity IL-2 receptor, which is also upregulated in Tcons upon activation (Malek, 2008). The integrin CD103 is a marker for Treg suppressive function that is especially high in tumor-infiltrating Tregs (Lehmann et al., 2002; Anz et al., 2011). A constitutively expressed marker critical for Treg suppression is CTLA-4 (Takahashi et al., 2000; Wing et al., 2008). Tregs express the glucocorticoid-induced TNFR-related protein (GITR, TNFRSF18), which is further upregulated upon activation (McHugh et al., 2002). GITR became an interesting target for tumor immunotherapy. Tumor-infiltrating Tregs express high GITR levels and GITR-targeting antibodies reduce their numbers (Coe et al., 2010). With its high expression on tumor-infiltrating Tregs also tumor necrosis factor receptor 2 (TNFR2, TNFRSF1b) gained therapeutic interest (Chen et al. 2008). $TNFR2^+$ Tregs are more suppressive than $TNFR2^-$ Tregs and stimulating the TNFR2 expands regulatory T cells *in vitro* and *in vivo* (Chen et al. 2007, Chen et al. 2008; Chopra et al., 2016).

1.2 Modulation of Tregs via IL-2

IL-2 was originally identified as a proinflammatory cytokine produced by activated $CD4^+$ T cells and to some extent by $CD8^+$ T cells. After secretion IL-2 enables the proliferation of effector T cells and enhances their function. IL-2 signals through the IL-2 receptor (IL-2R), which consists of the three subunits IL-2Rα (CD25), IL-2Rβ (CD122) and the common γ gamma chain (CD132). The low affinity IL-2R consists of CD122 and CD132 and is constitutively expressed on all naïve T cells and NK cells (Malek, 2008). Upon activation T cells transiently upregulate CD25, which together with CD122 and CD132 forms the high affinity IL-2R (Rogers et al., 1997). In contrast to Tcons, naïve Tregs constitutively express CD25 (Sakaguchi et al., 1995). CD25 allows Tregs to rapidly respond to IL-2. It provides survival and expansion signals and is indispensable for Treg function and maintenance (Sakaguchi et al., 1995; Fontenot et al., 2005). Tregs themselves are incapable of producing IL-2 and therefore, highly depend on the IL-2 production of effector T cells (Owen et al., 2018). When the first studies reported the effects of IL-2 on Tregs, they contradicted the long-held dogma of IL-2 being a proinflammatory cytokine and proved its anti-inflammatory functions (Malek, 2008). As an immunomodulatory cytokine, IL-2 appears highly interesting for immunotherapy. For cancer therapy the activating and expanding effects on effector T cells and NK cells are highly interesting. The anti-inflammatory effects mediated by Tregs are envisioned to treat inflammatory disease. However, to date short half-life and high therapeutic doses, limit the clinical success of IL-2 (Kontermann, 2012). Furthermore, severe adverse events have been observed in patients treated with exogenous IL-2, such as malaise, eosinophilia, anemia, thrombocytopenia and capillary leak syndrome (Rosenberg et al., 2010). The occurrence of capillary leak syndrome in patients can be explained by the expression of the IL-2R by endothelial cells, markedly contributing to these described side effects (Krieg et al., 2010).

1.3 Modulation of Tregs via TNFR2

1.3.1 The tumor necrosis factor receptor super family

The tumor necrosis factor receptor super family (TNFRSF) consists of type I transmembrane glycoproteins with extracellular cysteine-rich domains. These domains occur in repeats up to six times. The family is classified in three categories. First, members with a intracellular death domain, second, members with intracellular TRAF-interacting domain and third, decoy receptors (Idriss and Naismith, 2000; Wajant et al., 2003). The receptors themselves have no enzymatic activity. Responsible for the signaling are the death domains and/or TNF receptor associated factors (TRAFs; Locksley et al., 2001). The ligands for the TNFRSF are type II transmembrane proteins, which usually form homotrimers to activate and cluster their receptors. Most can be cleaved and therefore exist also in soluble forms. It is noteworthy, that the membrane-bound and the soluble ligands can have different activities on their target receptor (Grell et al. 1995; Bodmer et al., 2002).

1.3.2 TNFR2 – Structure and function

TNFR2 (CD120b, TNFRSF1b) is a type I transmembrane protein with 62 % similarity in mouse and human (Smith et al., 1990; Lewis et al., 1991). Besides Tregs and T cells various other immune cells such as NK cells (Mason et al., 1995), monocytes, macrophages (Ruspi et al., 2014) and myeloid-derived suppressor cells (MDSCs; Hu et al., 2014) express TNFR2. Furthermore, TNFR2 occurs on non-immune cells, notably neurons (Yang et al., 2002), astrocytes (Han et al., 2001), microglia (Dopp et al., 1997), mesenchymal stem cells (Wang et al., 2009), endothelial cells (Paleolog et al., 1994) and epithelial cells (Mizoguchi et al., 2002). Tumor necrosis factor alpha (TNFα) and lymphotoxin-alpha are the ligands for TNFR2. The main TNFα-producers are macrophages (Stein and Gordon, 1991), monocytes (Kriegler et al., 1988), dendritic cells (Serbina et al., 2003) and T cells (Steffen et al., 1988). It is of interest that also tumor cells can produce TNFα (Naylor et al., 1993). TNFα exists in a soluble (sTNFα) and membrane-bound form (mTNFα; Kriegler et al., 1988). The TNFα-converting enzyme (TACE), a metalloproteinase, cleaves mTNFα to sTNFα (Black et al., 1997; Moss et al., 1997). However, only mTNFα properly activates TNFR2 (Grell et al. 1995). After receptor activation TRAF2 binds to the intracellular domain of TNFR2. Thereafter, TRAF1 engages and forms a heterodimer with TRAF2 (Rothe et al., 1994). Subsequently, the cellular inhibitor of apoptosis protein 1 and 2 (c-IAP1 and c-IAP2) associate with the heterodimer (Rothe et al., 1995). This complex can

further interact with TRAF3 (Naudé et al., 2011). TNFR2 signaling leads to the activation of nuclear factor kappa-light-chain-enhancer of activated B cells (NF-κB; Rauert et al., 2010). It is of interest, that in some cell lines TNFR2 also signals cell death (Grell et al. 1993). In T cells TNFR2 activation results in costimulatory signals (Aspalter et al., 2003). It lowers the threshold of T cell receptor activation and promotes survival of T cells (Kim and Teh, 2001). In Tregs TNFR2 agonization leads to activation and proliferation (Chen et al., 2007, 2008; Chopra et al., 2016).

1.3.3 Agonization of TNFR2

To study TNFR2 activation with a soluble ligand and prove therapeutic concepts H. Wajant designed the selective mouse TNF-based agonist of TNFR2 (STAR2). STAR2 consists of single-chain mouse TNF trimers (scTNF) fused to the trimerization domain of chicken tenascin C (TNC, Figure 2 A). The trimers oligomerize via the TNC domain which results in a nonameric TNF ligand (Figure 2 B). It stimulates the receptor equivalent to mTNF, the prime activating ligand (Figure 2 C). Furthermore, with two point mutations (D221N and A223R) TNF gains selectivity for TNFR2. The selective mutant is termed TNF80. Taken together STAR2 is a nonameric selective TNF ligand for the activation of TNFR2 (Chopra et al., 2016).

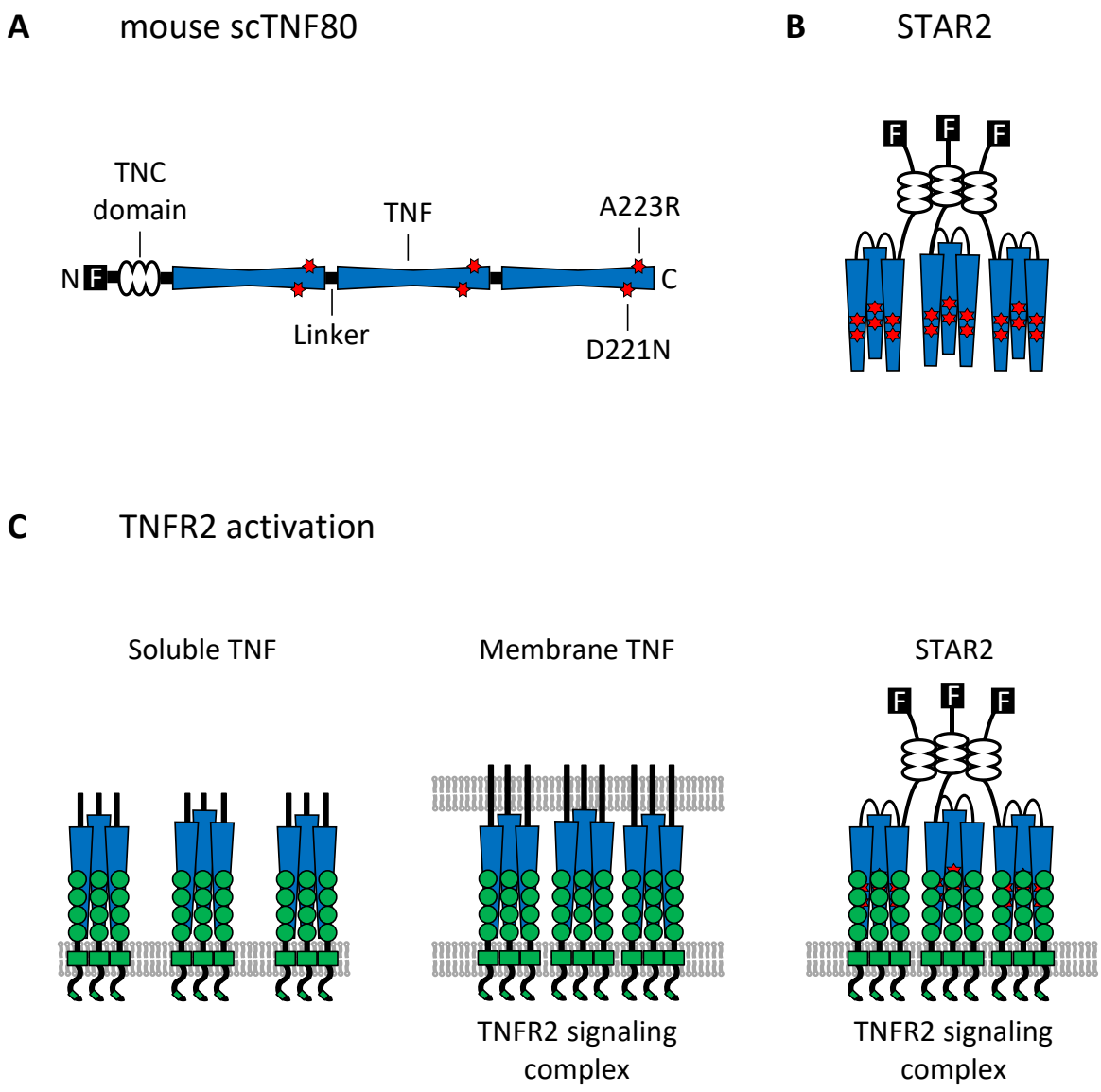

Figure 2: **STAR2 is a soluble TNF-based ligand, that selectively activates TNFR2.** (A) Single-chain mouse TNF trimers were fused to the trimerization domain of chicken TNC to achieve a nonameric TNF ligand. Furthermore, with two point mutations in TNF (D221N and A223R) selectivity for TNFR2 was gained. (B) STAR2 is a soluble ligand that stimulates TNFR2 in the same way than membrane-bound TNF. Figure adapted from Chopra et al. 2016.

1.4 Graft-versus-host disease

1.4.1 Pathophysiology

Allogeneic hematopoietic stem cell transplantation (allo-HCT) provides a potentially curative treatment option for multiple hematologic malignancies. The transplanted cells attack and eradicate the tumor, a phenomenon described as the graft-versus-leukemia effect (GvL). However, even after a successful battle against the tumor, the patients can face severe and often lethal side effects. Graft-versus-host disease (GvHD) occurs in patients when the donor T cells (graft) combat the recipient (host; Zeiser and Blazar, 2017). Essential in this response are T cells directed against the major histocompatibility complex molecules (MHC, HLA in humans) expressed on all nucleated cells. The incidence of GvHD directly correlates with mismatches in this protein family. Nevertheless, 40 % of the human patients with donor-matched HLA develop GvHD (Ferrara et al., 2009; Nassereddine et al., 2017). In the acute phase of GvHD (aGvHD), that occurs within 100 days after transplantation, the T cells predominantly attack the skin, the gastro-intestinal tract and the liver. In these target organs the common aGvHD symptoms are maculopapular skin rash, blistering and ulcerating skin, diarrhea, vomiting, abdominal pain and anorexia. After the acute phase, chronic GvHD (cGvHD) manifests with various symptoms similar to autoimmune diseases. The prevention and treatment of GvHD remains challenging. Inhibiting the activation, expansion and effector functions of allogeneic donor T cells may prevent or reduce GvHD, but puts patients at risk of life-threatening opportunistic infections and, importantly, can also prevent the desired GvL effect resulting in tumor relapses (Ferrara et al., 2009).

1.4.2 Treatment options and perspectives

Immunosuppression is the current standard of care to prevent GvHD. However, the treatment remains challenging and immunosuppression can also increase the infection risk and relapse of the tumor (Nassereddine et al., 2017). Tregs can suppress excessive immune responses and beneficially impact inflammatory diseases and tissue repair. Studies in mouse models revealed that Tregs can diminish GvHD symptoms while at the same time preserving the GvL effect (Hoffmann et al., 2002; Taylor et al. 2002; Edinger et al., 2003; Nguyen et al., 2007). Soon thereafter, the results were translated into the clinics, demonstrated the safety of *ex vivo* expanded Treg infusion (Brunstein et al., 2011) and most importantly, the benefits for GvHD treatment (Di Ianni et al., 2011). Without additional immunosuppression, the adoptively

transferred Tregs prevented GvHD in patients, promoted lymphoid reconstitution, improved immunity to opportunistic pathogens and did not diminish the GvL effect (Di Ianni et al., 2011). These striking results urged for new strategies to isolate Tregs and to expand them *ex vivo*. Notably, Tregs are highly resistant to radiation (Komatsu and Hori, 2007) and therefore, recent approaches aim to expand Tregs directly in the recipients prior to transplantation (Chopra et al., 2016; Nishikii et al., 2016). Tregs expansion after the transplantation at the onset of GvHD still remains challenging since Treg expansion strategies often also target activated T cells and thereby may accelerate GvHD. In summary, the Treg-mediated immune suppression holds high therapeutic potential for the treatment of GvHD and novel Treg *in vivo* expansion strategies may lead to a clinical breakthrough.

1.5 The tumor microenvironment

In contrast to the protective role of Tregs in GvHD, they correlate with poor survival in cancer. Tregs dampen the anti-tumor immune response and suppress inflammation where it is desperately needed. Together with other immunosuppressive cells they contribute to immune escape of the tumor.

1.5.1 Immunosuppressive cells

To fight tumor development and progression the immune system utilizes the common concept of T cell immune response. Dendritic cells capture and present antigens from the tumor cells in a proinflammatory environment. They present these antigens to T cells via the MHC route, which in return leads to T cell priming. Cytotoxic $CD8^+$ T cells now infiltrate and kill the tumor cells they recognize. Target cell killing further releases antigens and strengthens the anti-tumor immune response (Chen and Mellmann 2013). Besides $CD8^+$ T cells, also $CD4^+$ T cells infiltrate the tumor. They exert cytokine secretion and target cell killing. Without prior priming NK cells recognize tumor cells and destroy them. In this ideal scenario the cancer becomes eliminated. However, along with immune cell infiltration, the tumor builds its own protective army (Figure 3). When successful this process is termed immune escape and leads to further tumor progression (Monjazeb et al., 2013). Although their function is to activate T cells, antigen presenting cells can also exert tolerogenic effects. The lack of costimulatory molecules (CD80 and CD86) is the main reason for this. In addition, MDSCs produce nitric oxide, reactive oxygen species and tryptophan metabolites that inhibit effector T cells. Tumor-associated macrophages, especially M2-like macrophages possess tissue-reparative functions and suppress immune responses (Speiser et al., 2016). Tregs are currently one of the most prominent tumor-protective cells. With their multifaceted suppressive functions explained before they inhibit the effective anti-tumor immune response and are key players in immune escape. Various cancer entities show high Treg frequencies which correlate with dismal prognosis (Liyanage et al., 2002; Barnett et al., 2005; Beyer et al., 2006; Hiraoka et al., 2006; Joshi et al., 2015).

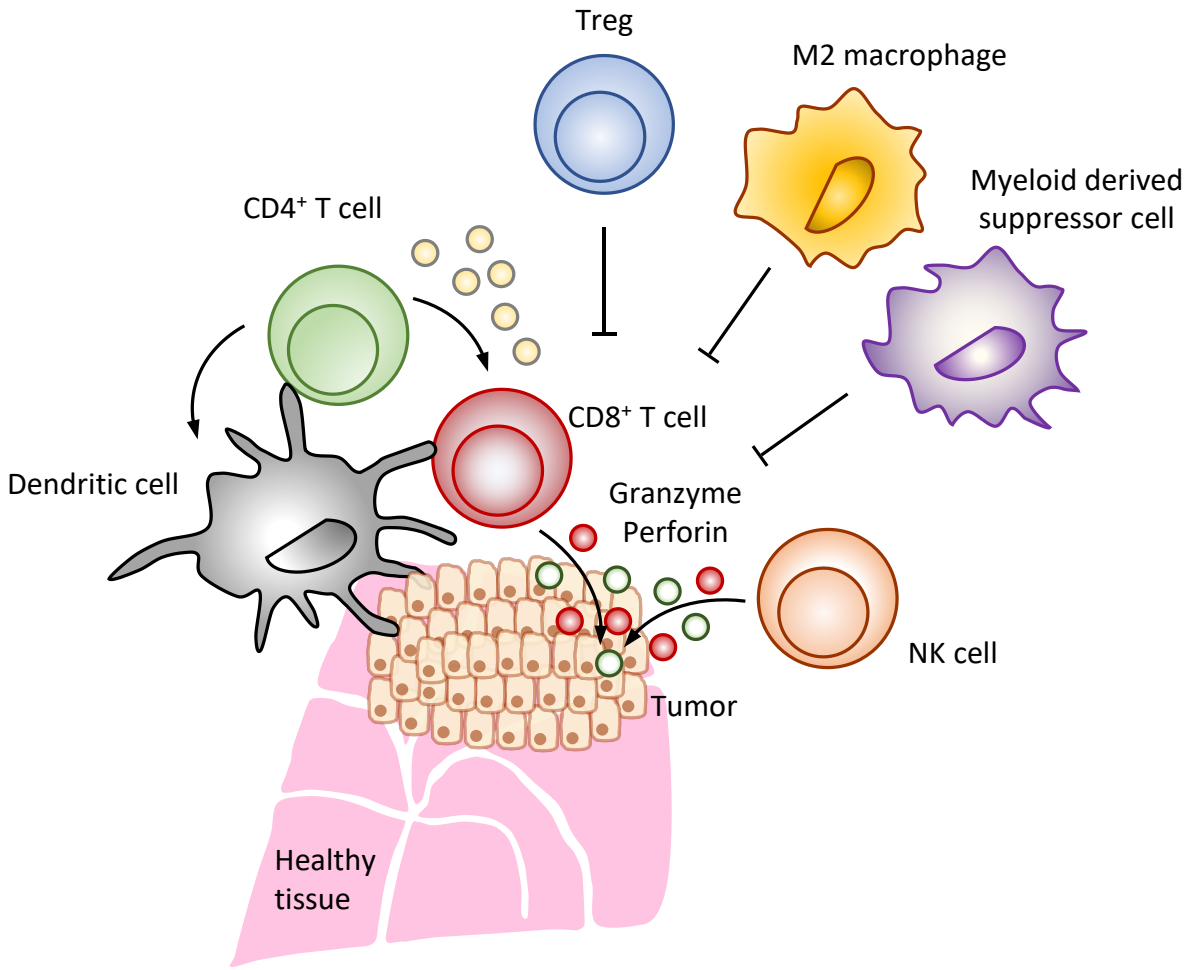

Figure 3: **Cancer cell elimination and escape depend on the tumor microenvironment, that can constitute diverse immune cell populations.** Various immune cells infiltrate malignant tissue. While some elicit anti-tumor immune responses, others prevent an effective elimination and lead to immune escape of the tumor. Cytotoxic $CD8^+$ T cells and NK cells are the most potent killers of tumor cells. They get support from cytokine secreting $CD4^+$ T helper cells. The interaction with dendritic cells and the antigens they present to T cells leads to T cell activation. However, within the tumor microenvironment are also cells that suppress immune responses. Tregs are among the most powerful of them. In addition, immature dendritic cells, myeloid suppressor cells and macrophages of the M2 type protect the tumor. Figure drafted from the scheme of Monjazeb *et al*. 2013.

1.5.2 Immunomodulatory receptors and checkpoint blockade

Besides tolerogenic immune cells there are also immunomodulatory receptors that inhibit anti-tumor effector functions. Programmed cell death protein 1 (PD-1) is expressed by activated T cells. Engagement of its ligands (PD-L1 and PD-L2) reduces T cell activation and costimulation (Wilson et al., 2018). It is of interest, that also tumor cells express PD-1 ligands (Dong et al., 2002). CTLA-4 is constitutively expressed on Tregs and transiently on activated T cells. It competes with CD28 for the binding of the costimulatory molecules CD80 and CD86. Tregs use it to strip CD80 and CD86 from antigen presenting cells and give inhibitory signals

(Wilson et al., 2018). A similar function to CTLA-4 fulfills T cell immunoglobulin and ITIM domain (TIGIT). NK cells and T cells express this coinhibitory receptor and tumor cells directly stimulate it via the TIGIT ligands (Anderson et al., 2016). Lymphocyte-activation gene 3 (Lag-3) competes with CD4 to the binding of MHC class II molecules. It inhibits $CD8^+$ T cells and NK cells by unknown mechanisms (Anderson et al., 2016). Tim-3 occurs on T and innate immune cells. Stimulation results in tolerogenic signaling in T cells and proliferation in MDSCs (Anderson et al., 2016).

With antibodies against CTLA-4 (ipilimumab) and PD-1 (pembrolizumab and nivolumab) the first antibodies without direct tumor targets conquered the market. In both cases, the mechanism of action is blockade of immunomodulatory receptors which results in unleashed power of the immune system. This leads to a successful anti-tumor immune response and tumor regression. Besides surgery, radiation, chemo and targeted therapy, the concept of checkpoint inhibition is now established for the treatment of malignancies (Sharma and Allison, 2015). As expected, an unleashed immune system causes severe immune-related adverse events. Main consequences are gastrointestinal, dermatologic, hepatic and endocrine toxicities (Spain et al., 2016). After the great success of targeting CTLA-4 and the PD-1 axis, targeting Lag-3, Tim-3 and TIGIT might become the second generation of checkpoint inhibitors (Anderson et al., 2016). However, the many immune suppressive control mechanisms show that there is redundancy in regulation of the immune response. With one checkpoint blocked, several others still function and are ready to step in for tumor tolerance.

1.5.3 Immunosuppressive metabolism

Effector T cells highly depend on aerobic glycolysis and amino acid metabolism. Since these metabolic pathways are also used from tumor cells, the opponents compete for nutrients. The competition for glucose is essential in this context. Tregs on the other hand use oxidative phosphorylation to metabolize fatty acids and thus are not in direct competition with tumor cells. Hence, Tregs proliferate better than their tumoricidal T cell companions. Furthermore, malignant cells, macrophages and MDSCs express indoleamine-2,3-dioxygenase (IDO). The enzyme degrades tryptophan and catabolites foster Treg differentiation. Through expression of CD39 and CD73 Tregs degrade adenosine triphosphate to adenosine. This inhibits the effector function of T cells (Speiser et al., 2016).

Taken together, tumors harbor immunosuppressive cells and a metabolic milieu that supports their function. Tumors compete with opponents for nutrients and even directly interact with them by surface expression of immunomodulatory ligands. All this prevents an effective anti-tumor immune response and leads to immune escape.

1.6 Pancreatic ductal adenocarcinoma

1.6.1 Epidemiology and pathology

In the last 30 years the overall survival rate for cancer patients have increased by 20 % (Siegel et al., 2017). Hematopoietic and lymphoid malignancies increased the most and survival reaches 71 % and 66 % respectively. In contrast to that patients diagnosed with pancreatic ductal adenocarcinoma (PDAC) still show only 8 % 5-year survival and a median survival of less than 9 months. The main reason for this is late diagnosis in advanced stages of the disease (Kleeff et al., 2016; Siegel et al., 2017). Symptom-free progression, absence of tumor markers and difficulties in imaging of early-stage tumors further complicate the diagnosis. In addition to late diagnosis, the tumor grows aggressive and metastasizes early on. Finally, upon diagnosis of their disease patients face a tumor highly resistant to chemo-, radio- and targeted therapy. Although the frequency of new cases is not very high, the aforementioned reasons lead to the fact that PDAC is responsible for the 4th most cancer related deaths in the developed countries (Kleeff et al., 2016; Siegel et al., 2017). By the year 2030 PDAC is predicted to take the 2nd place in cancer related death mortalities (Rahib et al., 2014). PDAC typically occurs at the age between 60 and 80 and men have a 50 % higher risk than women. Risk factors are family history, smoking, diabetes mellitus and chronic pancreatitis (Kamisawa et al., 2016).

1.6.2 Treatment options and perspectives

PDAC constitutes 75 – 80 % of all pancreatic cancers and is the most common type (Kleeff et al., 2016). It develops in the head of the pancreas from precursor lesions. The genetic alterations that accompany the lesions are activating Kras and p53 mutations. Characteristically for PDAC is a dense tumor stroma build of fibroblasts and inflammatory cells. The tumor infiltrates lymph nodes, spleen and peritoneal cavity. Liver and lungs are the target of distant metastasis (Hezel et al., 2016). In the healthy pancreas T cells are scarce, however, immune cells infiltrate in mouse models of PDAC and human patients (Clark et al., 2007; Chopra et al., 2013; Tang et al., 2014). Despite the immune-infiltration in PDAC a successful anti-tumor immune response is absent.

The first drug approved for the treatment of metastatic pancreatic cancer was 5-fluorouracil. In the early 1990s gemcitabine became the standard of care (Ducreux et al., 2018). Compared to 5-fluorouracil it prolonged the median survival from 4.41 to 5.65 months and the 1-year

survival from 2 % to 18 % (Burris et al., 1997). The combination of nab-paclitaxel and gemcitabine further increased the median survival to 8.5 months and 1-year survival to 35 % (Von Hoff et al., 2013; Ducreux et al., 2018). The dismal prognosis, high incidence of deaths and limited treatment options dramatically underscore the need for further studies on PDAC and how to oppose it. Immunotherapy might be an option but remains challenging as PDAC harbors only few mutations and appears low immunogenic (Vogelstein et al., 2013). The approved immune checkpoint therapies (CTLA-4 and PD-1) alone or in combination with chemotherapy were unsuccessful. However, at least in preclinical mouse models, cancer vaccination in combination with low-dose cyclophosphamide turns even this cancer into an immunogenic tumor. Key players in this process seemed to be the Tregs, which were reduced by low-dose cyclophosphamide treatment (Lutz et al., 2014; Jiang et al., 2019). Jang and colleagues showed that depletion of Tregs prolonged survival of pancreatic tumor-bearing mice. After Treg depletion $CD8^+$ T cells exerted their full function, produced IFNγ and thereby combated the tumor. This effect appears to be rooted in dendritic cell modulation. In the presence of Tregs, dendritic cells showed a tolerogenic phenotype with low expression of costimulatory molecules. Depletion of Tregs increased the expression (Jang et al., 2017). In human patients, Tregs also play a negative role in the progression of PDAC. Patients with low Treg burden inside the tumor show prolonged and more often long-term survival. High Treg frequencies on the other hand correlated with distant metastasis, advanced tumor stage and poor survival (Hiraoka et al., 2006). Taken together, these results demonstrate the high potential of Treg depletion for the therapy of PDAC that might overcome the flaws observed with currently approved checkpoint inhibitors.

1.6.3 Inhibition of collagen synthesis to target the tumor microenvironment in stroma-rich PDAC

In the 1970s the Upjohn Company developed minoxidil for the treatment of hypertension (Meisheri et al., 1993). Sulfotransferase converts minoxidil into its active metabolite minoxidil sulfate (Johnson et al., 1982). Minoxidil sulfate then opens potassium channels and reduces Ca^{2+} influx. This relaxes vascular smooth muscle and makes minoxidil a potent vasodilator for the treatment of hypertension (Meisheri et al., 1988; Messenger and Rundegren, 2004). The effect even persists after serum clearance of minoxidil (Gottlieb et al., 1972). When the first hypertension patients received minoxidil the main side effects were nausea, fatigue, rash, and fluid retention. Surprisingly, as an additional side effect, some of the minoxidil treated patients displayed induced hair growth (Mehta et al., 1975; Jacomb and Brunnberg, 1976; Burton and Marshall, 1979) and so topically applied minoxidil became a treatment option for androgenic alopecia (Messenger and Rundegren, 2004). Murad and Pinnell (1987) were the first who reported the inhibiting effects of minoxidil on lysyl hydroxylase in human fibroblasts. They concluded that the effect roots in the inhibition of the lysyl hydroxylase synthesis. The mechanism is selective for lysyl hydroxylase and prolyl hydroxylase activity is not affected (Murad et al., 1994). Subsequently, minoxidil treatment results in hydroxylysine-deficient collagen and thereby interferes with functional collagen synthesis (Messenger and Rundegren, 2004).

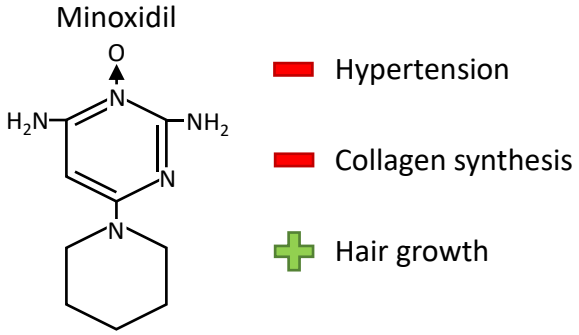

Figure 4: **Structure and therapeutic benefits of minoxidil.**

The effect of minoxidil on collagen synthesis bares potential for the treatment of stroma-rich tumor entities. In cancer, the tumor promoting effects of collagen-rich stroma is well studied. PDAC for instance is characterized by a dense desmoplastic stroma (Hidalgo, 2010). The stroma results in an increased hydrodynamic pressure within the tumor compared to the surrounding environment and provides a physical barrier, such that immune cells and even anti-cancer drugs are unable to penetrate into the tumor to reach cancer cells (Cabral et al., 2011). Furthermore, collagen abrogates anti-tumoral effects of monocytes (Kaplan, 1983). Notably, T cells preferentially migrate into and stay within the surrounding collagen-rich

tumor stroma rather than directly interacting with the cancer cells themselves. The tumor stroma prevents T cells from engaging directly with the cancer cells (Salmon et al., 2012). In PDAC tumor-stroma is especially dense (Hezel et al., 2016). Thus, we hypothesize that this devastating disease is a suited target for minoxidil-mediated stroma reduction and displays a new treatment perspective.

1.6.4 Mouse models and imaging of pancreatic ductal adenocarcinoma

The simplest models to investigate PDAC in mice use subcutaneous injected cell lines to induce a tumor (Corbett et al., 1984; Tan et al., 2009). However, in ectopic locations these tumors have altered characteristics (Morikane et al., 1999). Affected are tumor growth, tumor rejection and anti-tumor immune response. Therefore, orthotopic mouse models appear superior, in mimicking human disease. In these models the tumor arises directly from the pancreas. There are different strategies to induce orthotopic tumors. Most genetically engineered mouse models employ mice that express constitutively or inducible versions of mutated Kras or p53 in the pancreas (Hingorani et al., 2005; Esni et al., 2008; Timpson et al., 2009). These models allow investigations of tumor-associated genes and mutations. However, a major drawback of these models is that tumor development can last from several months to more than a year and this makes it challenging to study within a given time period. The electroporation of oncogenes directly into the pancreas results in faster tumor formation and also allows convenient investigation of genes and mutations (Park et al., 2014). Another way to induce PDAC is the orthotopic implantation of syngeneic tumor cells into the pancreas (Partecke et al., 2011; Chopra et al., 2013). Via this route even freshly isolated human tumor cells can efficiently induce PDAC in immunodeficient mice (Kim et al., 2009). The main advantage of orthotopic human xenograft PDAC is the investigation of chemotherapeutics, cancer targeting agents and antibodies. However, immunodeficient models do not contribute to the investigation of checkpoint therapies and the impact of immune cells on PDAC formation and rejection. For latter transplantable syngeneic cell lines are suited. One of these cell lines, Panc02, has been generated by Corbett *et al.* (1984). The group implanted 3-methyl-cholan-threne-saturated cotton into the pancreata of C57BL/6 mice and observed formation of pancreatic ductal adenocarcinoma thereafter. They passaged the tumors several times by subcutaneous implantation and finally generate the Panc02 cell line. Transferred subcutaneously back into mouse, they reported that the Panc02 tumors metastasized into the

lungs, lymph nodes and kidneys. Tumor resection and chemotherapy barely cured mice from the tumors. Orthotopically injected into the pancreas, Panc02 cells form an undifferentiated carcinoma with the absence of well-formed ductal structures. The tumors show angiogenesis and intratumoral hemorrhage (Morikane et al., 1999). Monitoring tumor progression is complex in orthotopic models. For PDAC several non-invasive methods such as magnetic resonance imaging (Grimm et al., 2003), positron emission tomography (Seitz et al., 2001) and ultrasonic imaging (Mamaeva et al., 2013) are described. However, most methods are linked to high efforts and require advanced skill sets. In contrast, bioluminescence imaging is straightforward to use. It requires luciferase positive tumor cells which emit light upon substrate supply and an imaging system (Condeelis and Weissleder, 2010). Furthermore, bioluminescence imaging detects metastases easily. Chopra *et al.* transduced Panc02 cells with the firefly luciferase. Injected into the pancreas they form a luciferase positive tumor (Chopra et al., 2013). The administration of D-luciferin then enables the non-invasive imaging of the tumor progression at subsequent time points in the same animal.

1.7 Structure and function of therapeutic antibodies

Antibodies are powerful weapons of the adaptive immune system. They recognize an extremely broad spectrum of antigens and mediate multiple effector functions for target cell killing. Responsible for specific antigen binding are hypervariable regions within the antibody binding domains (Fab fragment). These regions determine the specificity and the affinity of the antibody for an antigen. The Fc fragment with constant regions is responsible for the antibody effector functions. First, with the activation of the classical complement pathway it causes complement-mediated cytotoxicity (CMC). Second, by binding to Fc receptors it recruits immune cells and thereby mediates antibody-dependent cellular cytotoxicity (ADCC). Classical ADCC happens via crosslinking of Fc receptors on NK cells that then release perforin and granzyme on the target cell. Besides NK cells, macrophages, dendritic cells and neutrophils express Fc receptors and their engagement also leads to ADCC. Third and last, by the recruitment of professional phagocytes, antibodies lead to phagocytosis of recognized cells. Phagocytosis by antigen presenting cells increase the presentation of the antigen to T cells and thereby promotes immune activation (Weiner et al., 2010).

According to the sequence of their Fc part, antibodies can be classified into isotypes. In mouse and human the five isotypes IgA, IgD, IgE, IgG and IgM exist and are further subgrouped. Each isotype and subgroup binds to different Fc receptors and therefore, possesses different potential for the activation of effector functions. Besides mediating CMC and ADCC, the Fc fragment of the IgG isotype binds to the neonatal Fc receptor (FcRn). Expressed on vascular endothelial cells it protects internalized antibodies from lysosomal degradation and brings them back into the circulation. This recycling mechanism contributes to the long serum half-life of IgG antibodies (Weiner et al., 2010; Lu et al., 2018). In mice IgG1 and IgG2a have a half-life of 6-8 days (Vieira and Rajewsky, 1986, 1988). In humans IgG 1 has a half-life of 12 – 21 days (Kontermann, 2009). Human IgG1 (huIgG1) is the most common used isotype for therapeutic antibodies (Grilo and Mantalaris, 2019). Strong effector functions make it superior to other IgGs and FcRn mediated recycling leads to the longest serum half-life compared to other isotypes (Lencer and Blumberg, 2005). HuIgG1 is also the most potent human isotype in mouse and, although, moIgG2a is stronger than huIgG1 mouse models are appropriate for the investigation of therapeutic antibodies with an huIgG1 isotype (Overdijk et al., 2012).

Mutations of the asparagine residue at position 297 (N297A) reduce the glycosylation of antibodies and thereby lead to human IgG1s with reduced complement activation (Lund et al., 1996) and loss of Fcγ receptor binding (Lund et al., 1995). Loss of Fcγ receptor binding results in ADCC dead antibodies which are unable to induce target cell lysis via immune cell recruitment. However, Fc mutations can also enhance Fc receptor binding and lead to ADCC enhanced isotypes (Natsume et al., 2009). Besides the killing of target cells, antibodies are useful tools to block or activate receptors. This is especially important for immunomodulatory antibody therapy.

2 Specific aims

Tregs are key players in orchestrating and resolving immune responses and to foster tissue homeostasis. Preclinical data and research on inflammatory disease and cancer have demonstrated their impact on disease outcome. Thus, strategies to manipulate Tregs hold a high therapeutic potential and may efficiently improve modern immunotherapy.

The aim of this thesis is to identify molecular targets on Tregs to develop therapeutic strategies to modulate Tregs *in vivo*. First, we attempted to enhance Treg function *in vivo* to reduce excessive inflammation in a prototypic and highly clinically relevant model of inflammation, namely acute graft-versus-host disease (aGvHD). Second, we targeted Tregs either directly or indirectly through altering the extracellular matrix, to boost antitumor immunity in a model of pancreatic ductal adenocarcinoma (PDAC).

The specific aims of this work are:

1. To test methods to selectively augment Treg numbers and function *in vitro* and *in vivo* to reduce inflammation in aGvHD.
2. To evaluate the tumor microenvironment to directly or indirectly target Tregs to improve cancer immunotherapy directed against PDAC.

3 Materials and Methods

3.1 Materials

3.1.1 Chemical reagents

Chemical reagent	Company
0.05 % Trypsin-EDTA (1x)	ThermoFisher (Waltham, USA)
2-mercaptoethanol (50 mM)	ThermoFisher (Waltham, USA)
6-0 coated Vicryl Polyglactin BV-1	Ethicon (Sommerville, USA)
Aqua ad injectabilia	Braun (Melsungen, Germany)
Baytril (Enrofloxacin)	Bayer (Leverkusen, Germany)
Benzylalcohol	Sigma-Aldrich (St. Louis, USA)
Benzylbenzoate	Sigma-Aldrich (St. Louis, USA)
Bepanthen eye and ear ointment	Bayer Vital GmbH (Leverkusen, Germany)
Biocoll separating solution	Biochrom GmbH (Berlin, Germany)
Braunol	B. Braun (Melsungen, Germany)
Collagenase P	Roche (Basel, Switzerland)
D-Luciferin, potassium salt	Biosynth (Staad, Switzerland)
DMEM	ThermoFisher (Waltham, USA)
DNaseI	Roche (Basel, Switzerland)
EDTA	Sigma-Aldrich (St. Louis, USA)
Enbrel	Wajant laboratory (Würzburg, Germany)
Fetal calf serum	ThermoFisher (Waltham, USA)
Gemcitabine	UKW pharmacy (Würzburg, Germany)
Ketamine hydrochloride (Ursotamin)	Serumwerk (Bernburg, Germany)

HAT media supplement 50x hybri-max	Sigma-Aldrich (St. Louis, USA)
Hexane	Sigma-Aldrich (St. Louis, USA)
HT media supplement 50x hybri-max	Sigma-Aldrich (St. Louis, USA)
Isofluran	cp-pharma (Burgdorf, Germany)
L-Glutamine 200 mM (100x)	ThermoFisher (Waltham, USA)
Minoxidil	Sigma-Aldrich (St. Louis, USA)
Normal rat serum	Stemcell Technologies (Vancouver, Canada)
Novalgin 500 mg/mL	Sanofi (Paris, France)
rhIL-6	ImmunoTools GmbH (Friesoythe, Germany)
RPMI-1640 medium	ThermoFisher (Waltham, USA)
TiterMax® Gold Adjuvant	Sigma-Aldrich (St. Louis, USA)
Trypan blue	Sigma-Aldrich (St. Louis, USA)
OneComp eBeads™ Compensation Beads	eBioscience (San Diego, USA)
Paraformaldehyde	Sigma-Aldrich (St. Louis, USA)
PBS	PAN-Biotech (Aidenbach, Germany)
Polyethylene glycol 1500	Roche (Basel, Switzerland)
Triton-X100	Carl Roth (Karlsruhe, Germany)
Wound repair ointment	UKW pharmacy (Würzburg, Germany)
Xylavet	cp-pharma (Burgdorf, Germany)

3.1.2 Buffers and solutions

Buffer/solution	Composition
Anesthetics	ketamine hydrochloride (8 mg/mL), xylavet (1.6 mg/mL) in PBS, stored at 4 °C
Bulk fusion media	RPMI-1640 medium, 5 % heat inactivated FCS, Penicillin (100 U/mL), Streptomycin (100 µg/L), L-glutamine (2 mM), 2-mercaptoethanol (50 µM), rhIL-6 (100 U/mL), stored at 4 °C
DMEMc	DMEM, 10 % heat inactivated FCS, Penicillin (100 U/mL), Streptomycin (100 µg/L), L-glutamine (2 mM), stored at 4 °C
Erythrocyte lysis buffer	168 mM NH_4Cl, 10 mM $KHCO_3$, 0.1 mM EDTA, in distilled H_2O, stored at RT
HAT media	RPMI-1640 medium, 5 % heat inactivated FCS, Penicillin (100 U/mL), Streptomycin (100 µg/L), L-glutamine (2 mM), 2-mercaptoethanol (50 µM), rhIL-6 (100 U/mL), 1x HAT, stored at 4 °C
Luciferin	5 g D-luciferin in 165 mL Aqua ad injectabilia, stored at -20 °C
RPMIc	RPMI-1640 medium, 10 % heat inactivated FCS, Penicillin (100 U/mL), Streptomycin (100 µg/L), L-glutamine (2 mM), 2-mercaptoethanol (50 µM), stored at 4 °C

3.1.3 Antibodies

Mouse antibodies

Antigen	Clone	Conjugate	Host species	Company
4-1BB	17B5	PE/Cy7	Syrian hamster	Invitrogen
CD103	2E7	PE/Cy7	Armenian Hamster	Biolegend
CD11c	N418	Al647	Armenian Hamster	Biolegend
CD19	6D5	PE	Rat	Biolegend
CD3	17A2	BV711	Rat	Biolegend

CD4	GK1.5	Al700	Rat	Biolegend
CD4	RM4-5	APC	Rat	LifeTechnologies
CD4	RM4-5	PE	Rat	Biolegend
CD4	GK1.5	Al750	Rat	R&D Systems
CD8	53-6.7	APC	Rat	Biolegend
CD8	53-6.7	APC/Cy7	Rat	Biolegend
CD44	IM7	APC	Rat	Biolegend
CD62L	MEL-14	PerCp/Cy5.5	Rat	eBioscience
CD64	X54-5/7.1	PE/Cy7	Mouse	Biolegend
CD69	H1.2F3	PE/Cy7	Armenian Hamster	Invitrogen
CD69	H1.2F3	Pacific Blue	Armenian Hamster	Biolegend
CD73	eBioTY/11.8 (TY/11.8)	PE/Cy7	Rat	eBioscience
CD103	2E7	Pacific Blue	Armenian Hamster	Biolegend
CTLA-4	UC10-4B9	PerCp/Cy5.5	Armenian Hamster	Biolegend
DR3	4C12	PE/Cy7	Armenian Hamster	Biolegend
F4/80	BM8	Al488	Rat	Biolegend
Foxp3	FJK-16s	Al488	Rat	eBioscience
GITR	DTA-1	PE	Rat	Biolegend
Helios	22F6	PE	Armenian Hamster	Biolegend
I-Ab	PE	AF6-120.1	Mouse	Biolegend
ICAM-1	YN1/1.7.4	APC	Rat	Biolegend
Ki-67	16A8	PerCp/Cy5.5	Rat	Biolegend
Lag-3	eBioC9B7W (C9B7W)	PE	Rat	eBioscience
Neuropilin-1	3E12	APC	Rat	Biolegend
NK-1.1	PK136	APC	Mouse	eBioscience
Ox40	OX-86	APC	Rat	eBioscience
PD-1	RMP1-30	PE/Cy7	Rat	Biolegend
TIGIT	GIGD7	PE/Cy7	Rat	eBioscience
TNFR2	3G7A02	PE	Rat	Biolegend

Human antibodies

Antigen	Clone	Conjugate	Host species	Company
CD25	BC96	APC	Mouse	Biolegend
CD3	OKT3	Pacific Blue	Mouse	Biolegend
CD4	OKT4	PerCP/Cy5.5	Mouse	Biolegend
FoxP3	OCH101	FITC	Rat	eBioscience
IgG	Polyclonal	Al647	Goat	Invitrogen
TNFR2	3G7A02	PE	Rat	Biolegend

3.1.4 Kits

Kit	Company
CellTrace™ Violet Cell Proliferation Kit	ThermoFisher (Waltham, USA)
Dynabeads™ Untouched™ Mouse T Cells Kit	ThermoFisher (Waltham, USA)
Dynabeads™ Untouched™ Mouse CD4 Cells Kit	ThermoFisher (Waltham, USA)
LIVE/DEAD® Fixable Violet Dead Cell Stain	ThermoFisher (Waltham, USA)
LIVE/DEAD® Fixable Yellow Dead Cell Stain	ThermoFisher (Waltham, USA)
Mouse Regulatory T Cell Staining Kit	eBioscience (San Diego, USA)
ZombieAqua™ Fixable Viability Kit	Biolegend (San Diego, USA)

3.1.5 Consumables

Material	Company
1 mL syringe, needle 26GA x 3/8in (0.45 x 10 mm)	BD Bioscience (Heidelberg, Germany)
5 mL syringe	BD Bioscience (Heidelberg, Germany)
96-well plate, U-bottom for suspension cells	Sarstedt (Nuembrecht, Germany)
96-well plate, V-bottom for suspension cells	Sarstedt (Nuembrecht, Germany)

100 µL syringe (710 RN 100 ml, Gauge 28, 10 mm, Point Style 4 needle)	Hamilton (Bonaduz, Switzerland)
Cell culture flask 50 mL, 25 cm^2	Greiner Bio-One (Kremsmünster, Austria)
Cell culture flask 250 mL, 75 cm^2	Greiner Bio-One (Kremsmünster, Austria)
Cell culture flask 550 mL, 175 cm^2	Greiner Bio-One (Kremsmünster, Austria)
Cell strainer 70 µm	Greiner Bio-One (Kremsmünster, Austria)
SepMate™ PBMC isolation tubes	Stemcell Technologies (Vancouver, Canada)
U-100 insulin syringes	BD Bioscience (Heidelberg, Germany)

3.1.6 Mice

The mice used in this study were housed and bred in the Center for Experimental Molecular Medicine (ZEMM) animal facility in Würzburg or purchased from Charles River (Sulzfeld, Germany). C57BL/6/huTNFR2ecd-ki mice (Dong et al., 2016) were a kind gift from Ulrich L. M. Eisel (University of Groningen, Groningen, The Netherlands). C57BL/6J-$Tyr^{c\text{-}2J}$/Foxp3.Luci.DTR-4.huTNFR2ecd-ki were crossed from C57BL/6J-$Tyr^{c\text{-}2J}$/Foxp3.Luci.DTR-4 (Suffner et al., 2010) and C57BL/6/huTNFR2ecd-ki mice. The new line expresses a chimeric TNFR2 containing the extracellular human domain and the mouse transmembrane- and intracellular domain. (Dong et al., 2016). Furthermore, the line expresses eGFP, the CBGr99 luciferase and the human diphtheria toxin receptor under the control of the FOXP3 promoter. The huTNFR2ecd-ki genotype was evaluated via polymerase chain reaction by the absence of moTNFR2 extracellular domain (ecd) and presence of huTNFR2ecd. huTNFR2 forward primer: 5’ ctggactttgtggggacagt 3’ reverse primer 5’ gacagctggaagccaaagag 3’. moTNFR2 forward primer 5’ aaggaccagaggtctcagca 3’ reverse primer 5’ gcaggaacagaggagacgag 3’. The genotypes of eGFP expressing mouse lines were determined by flow cytometry analyzing eGFP expression within the $CD4^+$ T cells.

Mouse line	Abbreviation
BALB/cAnNCrl	BALB/c
C57BL/6/huTNFR2ecd-ki	B6.huTNFR2
C57BL/6NCrl	B6
C57BL/6-Tyr^{c-2J}/J	B6a
C57BL/6-Tyr^{c-2J}/huTNFR2ecd-ki	B6a.huTNFR2
C57BL/6-Tyr^{c-2J}/Foxp3.Luci.DTR-4	B6a.Foxp3.Luci.DTR
C57BL/6-Tyr^{c-2J}/Foxp3.Luci.DTR-4.huTNFR2ecd-ki	B6a.Foxp3.Luci.huTNFR2
C57BL/6-Tyr^{c-2J}/129S2-Tnfrsf1b^{tm1Mwm}/J	B6a.TNFR2ko
FVB/NCrl	FVB

3.1.7 Cell lines

Cell line	Description
AgX myeloma cells	Mouse myeloma
Panc02	Mouse pancreatic ductal adenocarcinoma
Panc02 FUGLW	Mouse pancreatic ductal adenocarcinoma, expressing eGFP and firefly luciferase

3.1.8 Devices and equipment

Device	Company
710 RN 100 ml Hamilton syringe with a Gauge 28, 10 mm, Point Style 4 needle	Hamilton (Bonaduz, Switzerland)
Attune NxT flow cytometer	ThermoFisher (Waltham, USA)
BD FACSAria III	BD Biosciences (Heidelberg, Germany)
BD FACSCanto II	BD Biosciences (Heidelberg, Germany)
Faxitron CD-160	Faxitron Bioptics, LLC (Tucson, USA)
Heracell 150 CO_2 incubator	ThermoFisher (Waltham, USA)
Heraeus multifuge 3SR Plus	ThermoFisher (Waltham, USA)
Hybridisation incubator 7601	GFL (Burgwedel, Germany)

IVIS Spectrum in vivo imaging system	PerkinElmer (Hopkinton, USA)
Nikon Eclipse TS 100 microscope	Nikon (Tokio, Japan)
PSU-10i, orbital shaker	Biosan (Riga, Latvia)

3.1.9 Software

Software	Developer
FlowJo version 8 and 10.5.3	FlowJo LLC (Ashland, USA)
Graphpad Prism version 7.02	GraphPad Software (San Diego, USA)
Imaris version 7.7.2 and 9.2.1	Bitplane (Belfast, United Kingdom)
Living Image Version 4.5	PerkinElmer (Hopkinton, USA)
Microsoft Office 365	Microsoft (Redmond, USA)

3.2 Methods

3.2.1 Isolation of splenocytes

Animals were sacrificed by cervical dislocation. The fur was sprayed with 70 % ethanol, the abdominal cavity was opened, and the spleen externalized. Until further processing, the spleen was kept in PBS on ice. Spleens were cut into 3-4 pieces and mashed through a 70 µm cell strainer with the plunger of a 5 mL syringe. The cell strainers were rinsed two times with 10 mL erythrocyte lysis buffer and incubated for 3 min at room temperature (RT). During the incubation time the spleens were further mashed. Afterwards, 20 mL PBS was added through the cell strainers to neutralize the erythrocyte lysis buffer. The splenocytes were then spun down (311 x g, 5 min, 4 °C) and again passed through the previously used cell strainer. From that on the splenocytes were kept in PBS at 4 °C.

3.2.2 T cell stimulation assays

Untouched T cells were enriched from splenocytes employing the Dynabeads untouched T cell enrichment kit according to the manufacturer's protocol. 2 x 10^5 T cells were seeded in a 96-well plate (U-bottom) with 200 µL RPMIc and incubated with 100 ng/mL (1.67 nM) STAR2 for 96 h at 37 °C. Expression of activation markers was analyzed via flow cytometry. The proliferation of T cells was measured via CellTrace™ Violet (CTV). Therefore, untouched T cells were stained with 5 µM CTV and incubated for 6 min at RT. Afterwards, 500 µL FCS were added followed by 5 mL warm RPMIc. 5 min later the cells were centrifuged and seeded.

For the investigations of enriched Tregs, untouched $CD4^+$ T cells from three BALB/c mice were pooled and stained for CD4 and CD25 expression. Afterwards the cells were fluorescence-activated cell sorted for $CD25^{high}$ expressing cells within the $CD4^+$ T cells. The obtained Tregs were seeded in 96-well plates (V-bottom) and cultured in RPMIc. Stimulated with 100 ng/mL (1.67 nM) STAR2 for 96 h the Tregs were then analyzed via flow cytometry.

3.2.3 Peripheral blood mononuclear cell isolation

Peripheral blood was obtained from the department of transfusion medicine at University Hospital Würzburg. To isolate peripheral blood mononuclear cells (PBMCs) blood was mixed 1:2 with PBS and centrifuged (1200 x g, 10 min, RT) in SepMate™ PBMC isolation tubes with 15 mL biocoll separating solution. Afterwards the PBMC layer was removed with a 5 mL pipette and washed twice with 50 mL PBS.

3.2.4 Preparation of mouse blood for flow cytometry

Mouse blood obtained from tail vein was lysed in erythrocyte lysis buffer for 15 min at RT. The samples were spun down (311 x g, 5 min, RT) and washed twice with PBS. Afterwards the samples were stained (as described 3.2.5).

3.2.5 Preparation of cells for flow cytometry

Cells were blocked with normal rat serum 1:20 in PBS. Thereafter, cell surface antigens were stained with appropriately titrated antibodies for 30 min at 4 °C in the dark. At the same time live dead staining was performed with LIVE/DEAD™ Fixable Dead Cell Stain Kits. For FoxP3 and CTLA-4 staining the cells were fixed for 30 min at 4 °C with the Mouse Regulatory T Cell Staining Kit and stained intracellular for 30 min at 4 °C. Stained cells were then analyzed via flow cytometry. For data analysis FlowJo Version 10 was used. Compensation of multi-color panels was calculated via the FlowJo algorithm. For the calculation of the compensation matrix single cell stainings or compensation beads were used.

3.2.6 Allogeneic hematopoietic stem cell transplantation

Recipient C57Bl/6 mice received either 75 µg STAR2 on days -9, -7, -5 and -2, or 50 µg irrIgG-IL-2 on days -5 and -2 or 140 µg of NewSTAR on day -5 prior to allo-HCT. All biologicals were given intraperitoneal (i.p.) and diluted in PBS. The 12 weeks old C57Bl/6 recipients were then myeloablatively irradiated with 9 Gray (Gy). For hematopoietic reconstitution 5 x 10^6 bone marrow cells from FVB donor mice were retro-orbitally i.v. injected along with 0.6 x 10^6 T cells to induce aGVHD. T cells were purified from spleen with the Dynabeads untouched T cell enrichment kit. Antibiotics (Baytril) were added to the drinking water for one week after transplantation to prevent infections. GvHD score of mice was assessed according to Table 1 with the endpoints of weight loss more than 20 % for more than two consecutive days or total score higher than 8.

Table 1: **Criteria for clinical acute graft-versus-host disease score**.

Score	0	1	2
Weight loss	<10 %	>10 - <20 %	>20 %
Fur	Normal	Slightly to moderately ruffled	Strong ruffled
Eyes	Normal	Conjunctivitis of one, or slightly on both eyes	Conjunctivitis of both eyes
Fur	Normal	Slightly or moderate ruffles	Strongly ruffled, no grooming
Stool Behavior	Normal Normal	Slight diarrhea Slightly to moderately reduced	Strong tarry stool Movement only after provocation
Posture	Normal	Hunchback at rest	Hunchback during movement, inhibits movement
Skin	Normal	Dandruff on paws and tail	Strong fur defects
Anemia	Absent	Paleness of skin without fur	Paleness of whole body
Licking and scratching of inflamed skin	Absent	<1x/min	>1x/min

3.2.7 Hybridoma technology

B6a.TNFR2ko mice were immunized with a mixture of 50 µg moTNFR2ecd-Fc and 50 µg huTNFR2ecd-Fc (Enbrel) in 50 µL PBS and 50 µL TiterMax® Gold Adjuvant. The mixture was s.c. injected in the neck on day 0 and +28. Between day +49 and +56 the mice were then boosted by i.v. injection with 10 µg of each antigen in PBS. Three days later the spleens were harvested. Erythrocytes were lysed with erythrocyte lysis buffer and splenocytes were then fused with AgX myeloma cells. Therefore, AgX cells and splenocytes were washed with serum-free RPMI 1640 and mixed 5:1. The pellet was loosened by gently tapping the tube. The following steps

were performed at 37 °C. Drop by drop 1 mL PEG 1500 per $1x10^8$ splenocytes was added over the course of 1 minute. During that time the tube was carefully rotated. 5 mL warm and serum-free RPMI 1640 was added over the course of 5 min. After that 10 mL warm and serum-free RPMI 1640 was added in the same manner. Finally, 30 mL RPMI-1640 were added and cells were incubated for 30 min. After that the cells were cultured in bulk fusion media overnight. Starting from the next day, the cells were separated by single cell dilutions and cultured in HAT media.

3.2.8 Orthotopic tumor model

To induce orthotopic PDAC, Panc02 (Corbett et al., 1984) and reporter gene expressing Panc02 FUGLW cells (Chopra et al., 2013) were used. The FUGLW transduced Panc02 variant expresses eGFP and the firefly luciferase. All cells were stored at liquid nitrogen and were negatively tested for mycoplasma contamination. Prior to tumor inoculation the cells were thawed, cultured in DMEMc medium and passaged with trypsin. Cell viability was validated via trypan blue staining under the microscope and the cells were kept on ice until injection. For tumor inoculation, mice were anesthetized with ketamine and xylazine until surgical tolerance was reached. With a lateral incision the abdominal cavity was opened. Spleen and pancreas were externalized and $1x10^4$ Panc02 or Panc02 FUGLW cells in 30 µL PBS were injected into the pancreas with a Hamilton syringe. Successful injection was verified by bubble formation. Afterwards, the abdominal cavity was closed by suture. For pain relief metamizole (Novalgin) was added to the drinking water. After 13-14 days the tumors were explanted and analyzed via flow cytometry. Healthy untreated mice were used as controls.

3.2.9 Bioluminescence imaging

The Treg population or tumor growth was monitored via non-invasive bioluminescence imaging (BLI). Mice were i.p. injected with 300 mg/kg D-luciferin and anesthetized with 2 % isoflurane in O_2. After 10 min the bioluminescence signal was acquired with an IVIS Spectrum device. The exposure times were 5 min for Treg imaging, 2 min for ex vivo Treg imaging and minimum of 30 s for tumor imaging. Afterwards the total flux was measured via the Living Image software.

3.2.10 Light-sheet fluorescence microscopy

For light-sheet fluorescence microscopy (LSFM) mice were anesthetized with ketamine and xylazine until surgical tolerance was reached and perfused by intracardial infusion of PBS,

followed by 4 % paraformaldehyde (PFA) at pH 7.4. Organs were then harvested from perfused mice and further fixed in 4 % PFA for 2 h at 4 °C (as described in Brede et al., 2012). Unspecific antibody binding was blocked with 2 % FCS, 0.1 % Triton X-100 in PBS over night at 4 °C. Samples were stained with CD4-Al750 (clone GK1.5) diluted 1:100 in PBS for 36 h at 4 °C while rotating. Unbound antibodies were removed in three wash steps with PBS for 30 min at 4 °C each. Afterwards, the samples were dehydrated by ethanol series (30 %, 50 %, 70 %, 80 %, 90 %) for 2 h each at RT and stored in 100 % EtOH at 4 °C over night. The EtOH was then replaced with hexane for 2 h at RT. To optically clear the samples hexane was carefully replaced by 1 part benzylalcohol and 2 parts benzylbenzoate (BABB). During this crucial step air contact of the samples was avoided. After 30 min at RT, BABB was replaced 3 times. Samples were then kept at 4 °C until analysis. Light-sheet images were acquired with the microscopy setup described by Stegner *et al.* (2017). A 5x objective was used. The images were analyzed and visualized with the Imaris software.

3.2.11 Isolation of tumor cells

Tumor affected sites of the pancreas were identified with *ex vivo* bioluminescence imaging and separated from healthy tissue. The tumor tissue was then digested in 0.1 mg/mL DNaseI and 0.4 mg/mL Collagenase P in RPMI 1640 medium at 37 °C and 400 rpm for 30 min. Every 10 min the suspension was heavily resuspended with a 10 mL pipette. Afterwards, the solution was mashed through a 70 µm cell strainer centrifuged at 311 x g for 5 min at RT and resuspended in PBS. Until further analysis the samples were kept on ice.

3.2.12 Statistical analysis

Data were displayed as mean ± standard deviation. Prism 7 was used to generate the graphs and calculate the significance. Repeated measurements were analyzed via two-way ANOVA followed by Sidak's or Tukey's multiple comparisons test. Single measured groups were tested for normality using Shapiro-Wilk normality test. Normal data sets were then analyzed with two-tailed unpaired Student's t test. Non-normal data sets were analyzed with Mann-Whitney test. Significance was set at $P \leq 0.05$. Survival was analyzed via log-rank test.

4 Results

In this thesis, we aimed to manipulate Treg numbers and function for the treatment of inflammatory disease and cancer. First, we focused on augmenting Tregs to reduce inflammation in aGvHD. Tregs are highly relevant for the pathophysiology of GvHD and adoptive transfer improved disease outcome in preclinical models and clinical studies (Hoffmann et al., 2002; Taylor et al. 2002; Edinger et al., 2003; Nguyen et al., 2007; Di Ianni et al., 2011).

4.1 An IL-2-IgG-fusion protein expands Tregs *in vivo*

Physicians and scientists have used recombinant IL-2 for the expansion of Tregs. However, the short half-life and high therapeutic doses limit its clinical success (Kontermann, 2012). To overcome the clinical limitations, we addressed the serum retention and fused IL-2 to the heavy chains of an irrelevant human IgG1 (irrIgG). The IgG backbone of this fusion protein was mutated in its FcR-binding site by introducing the N297A mutation (described in 0) to prevent ADCC, which otherwise might result in a deletion of IL-2 receptor expressing cells, such as Tregs. The construct is hereafter referred to as irrIgG-IL-2 (Figure 9 A). Injected into FoxP3-reporter mice, irrIgG-IL-2 expanded the Treg population in the whole organism (Figure 9 C, D). After two injections we analyzed the immune cell composition of the spleen at day 5. This revealed Treg specific expansion without affecting the conventional $CD4^+$ and $CD8^+$ T cells (Figure 9 E-H). Aside from Tregs also the NK cells increased (Figure 9 I). We did not detect off-target effects on B cell numbers and also ruled out general splenocyte proliferation (Figure 9 J, K).

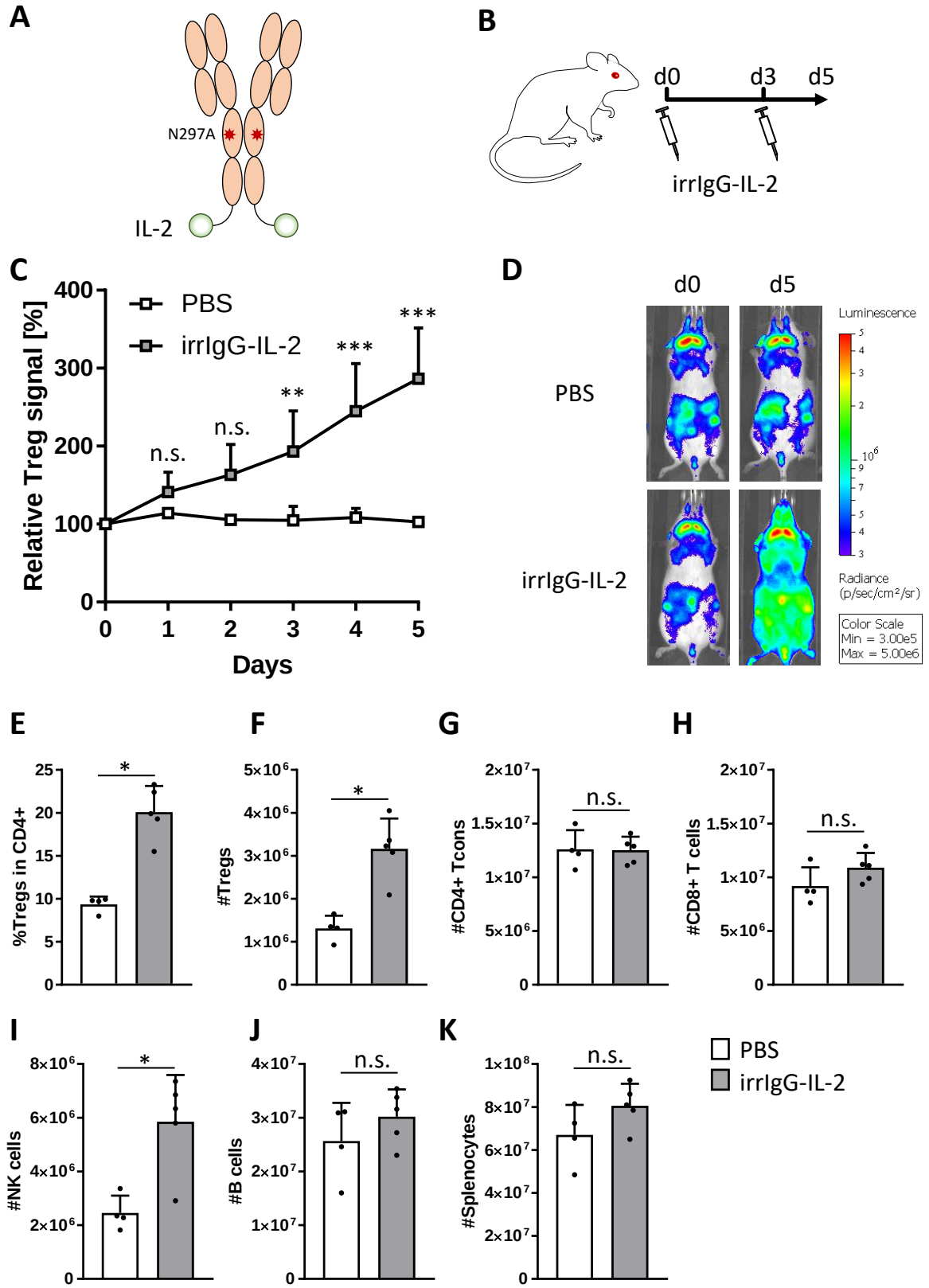

Figure 5: An IL-2-IgG-fusion protein expands Tregs and NK cells *in vivo*. (A-B) FoxP3-reporter mice were injected with 50 µg irrIgG-IL-2 or PBS on day 0 and 3. (C, D) The bioluminescence signal of the Tregs was measured daily. At day 6 splenocytes were isolated and analyzed via flow cytometry. (E) %Tregs in $CD4^+$ T cells, (F) total Tregs, (G) total $CD4^+$ Tcons, (H) total $CD8^+$ T cells, (I) total NK cells, (J) total B cells, (K) total splenocytes. $CD3^+CD4^+FoxP3^+$ (Tregs), $CD3^+CD4^+FoxP3^-$ ($CD4^+$ Tcons), $CD3^+$ $CD8^+$ ($CD8^+$ T cells), NK cells (NK-1.1$^+$), B cells ($CD19^+$). PBS, n = 4; irrIgG-IL-2, n = 5. *, $p \leq 0.05$; **, $p \leq 0.01$; ***, $p \leq 0.001$; n.s., not significant.

4.2 Stimulation of TNFR2 activates and expands regulatory T cells

Treatment of mice with exogenous irrIgG-IL-2 expand Tregs *in vivo*. However, treatment of IL-2, can result in severe side effects and so we developed a second approach to expand Tregs by exogenously selectively stimulating the TNFR2.

4.2.1 Comparison of TNFR2 expression in wildtype mice, humanized transgenic mice and human donors

To investigate the effects of human TNFR2-targeting reagents we bred the new mouse line B6a.Foxp3.Luci.huTNFR2 (as described in 3.1.6). The line in the C57BL/6 (B6) background expresses a chimeric TNFR2 consisting of the human TNFR2 extracellular domain and the mouse TNFR2 transmembrane and signaling domain (Figure 5 A; Dong et al. 2016). Thereby, the signaling is conserved while the targeting of the human TNFR2 is possible in mouse. Flow cytometric analysis revealed comparable expression patterns of the transgenic huTNFR2ecd and the wild type moTNFR2 in the respective C57Bl/6 controls (Figure 6 B). Furthermore, we confirmed the absence of moTNFR2 on the surface of Tregs from B6a.FoxP3.Luci.huTNFR2 mice (Figure 6 B). The expression of TNFR2 on human Tregs isolated from peripheral blood was used as positive control. Most of the human Tregs expressed TNFR2, which contrasted with mouse Tregs.

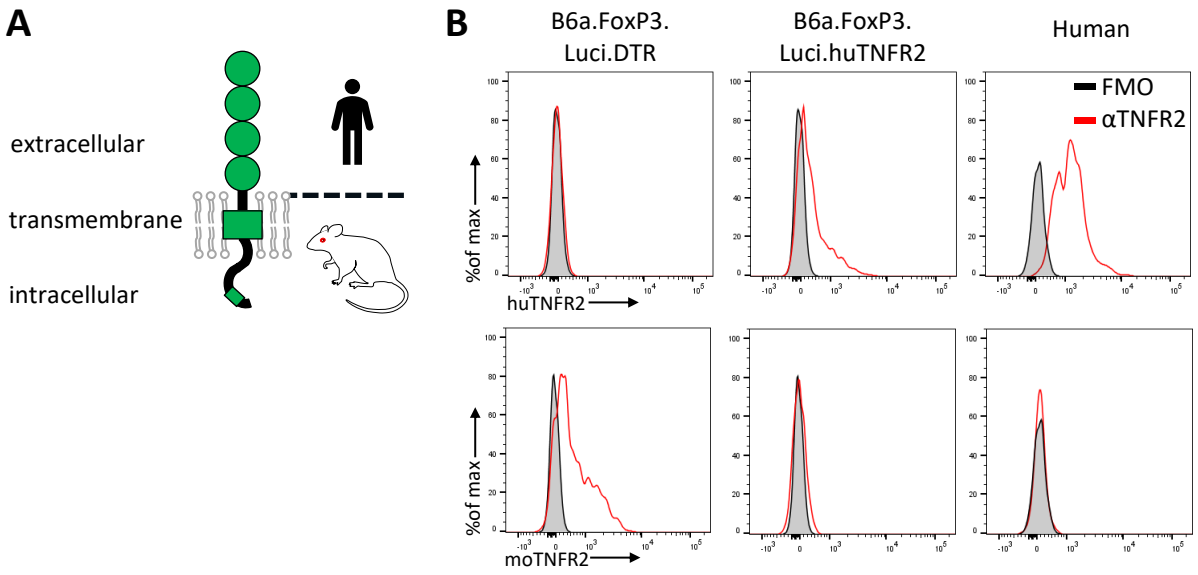

Figure 6: **Comparison of TNFR2 expression in Tregs from wildtype mice, humanized transgenic mice and human donors.** (A) Illustration of the chimeric TNFR2 expressed from B6a.Foxp3.Luci.huTNFR2 mice. It consists of the human extracellular and the mouse intracellular and transmembrane domain. (B) TNFR2 expression on splenic Tregs from B6a.FoxP3.Luci.DTR and B6a.FoxP3.Luci.huTNFR2 mice. Tregs from human peripheral blood were used as positive control. Mouse Tregs ($CD3^+CD4^+FoxP3^+$), human Tregs ($CD3^+CD4^+CD25^+FoxP3^+$).

4.2.2 STAR2 activates and expands regulatory T cells *in vitro* and *in vivo*

The nonameric STAR2, designed by Harald Wajant, was used to stimulate TNFR2 on Tregs. To demonstrate its function, we treated cultures of untouched enriched T cells. No further stimulants were added. In these cultures, STAR2 treatment activated $CD4^+$ $FoxP3^+$ T cells (Tregs; Figure 7 A). Several T cell activation markers (CD103, ICOS, ICAM-1, CD69, CD44 and CD25) were upregulated. In contrast, on $CD4^+FoxP3^-$ T cells ($CD4^+$ Tcons) only minor changes were observed. ICAM-1 was upregulated, but far less than on Tregs and CD44 expression decreased. Furthermore, we stimulated T cells labeled with CellTrace Violet (Figure 7 B). STAR2 increased cell division and proliferation selectively in Tregs and not in $CD4^+$ Tcons. After the results from mixed T cell-cultures, we investigated the effects of STAR2 on isolated Tregs. To obtain purified Tregs we FACS-sorted $CD4^+$ and $CD25^{high}$ expressing cells from splenic T cells (as described in 3.2.2). STAR2 increased the activation markers CD103, ICAM-1, CD69 and CD25 on purified Tregs in culture. ICOS and CD44 expression slightly decreased (Figure 7 C).

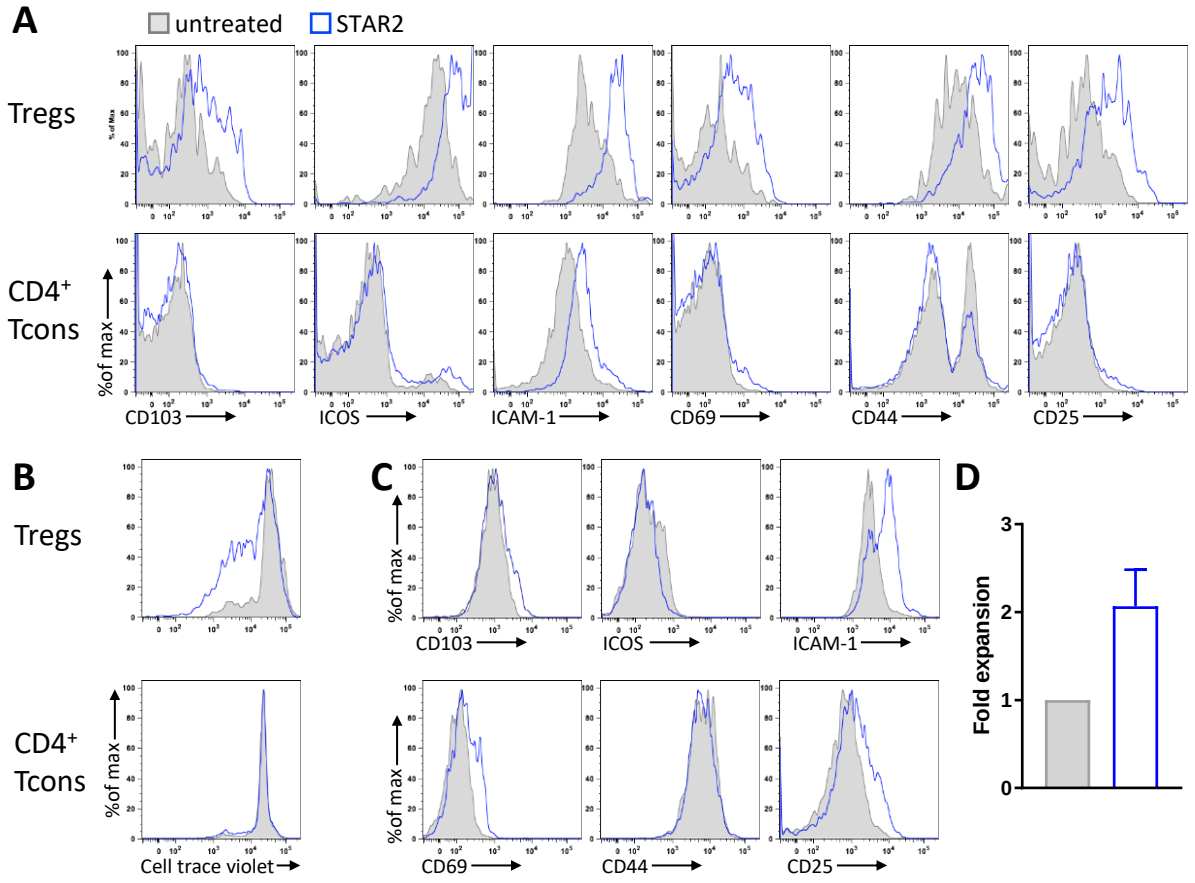

Figure 7: **STAR2 activates and expands Tregs *in vitro*.** Untouched T cells were stimulated with 1.67 nM STAR2 for 96 h. (A) Activation markers and (B) proliferation was assessed via flow cytometry. (C, D) Tregs sorted via CD4 and CD25 high expression, were stimulated with 1.67 nM STAR2 for 96 h. Shown are representative graphs from at least three independent experiments each. $CD4^+FoxP3^+$ (Tregs), $CD4^+FoxP3^-$ ($CD4^+$ Tcons).

The STAR2-stimulation further expanded the enriched Tregs in the culture by the factor two (Figure 7 D).

Next, we proved that the expansion of Tregs via our soluble TNFR2-specific ligand is also possible *in vivo*. For the experiments we used Treg-reporter mice expressing the CBGr99 luciferase and eGFP under the control of the FoxP3 promoter (Suffner et al., 2010). We injected STAR2 and monitored the Treg population via non-invasive bioluminescence imaging

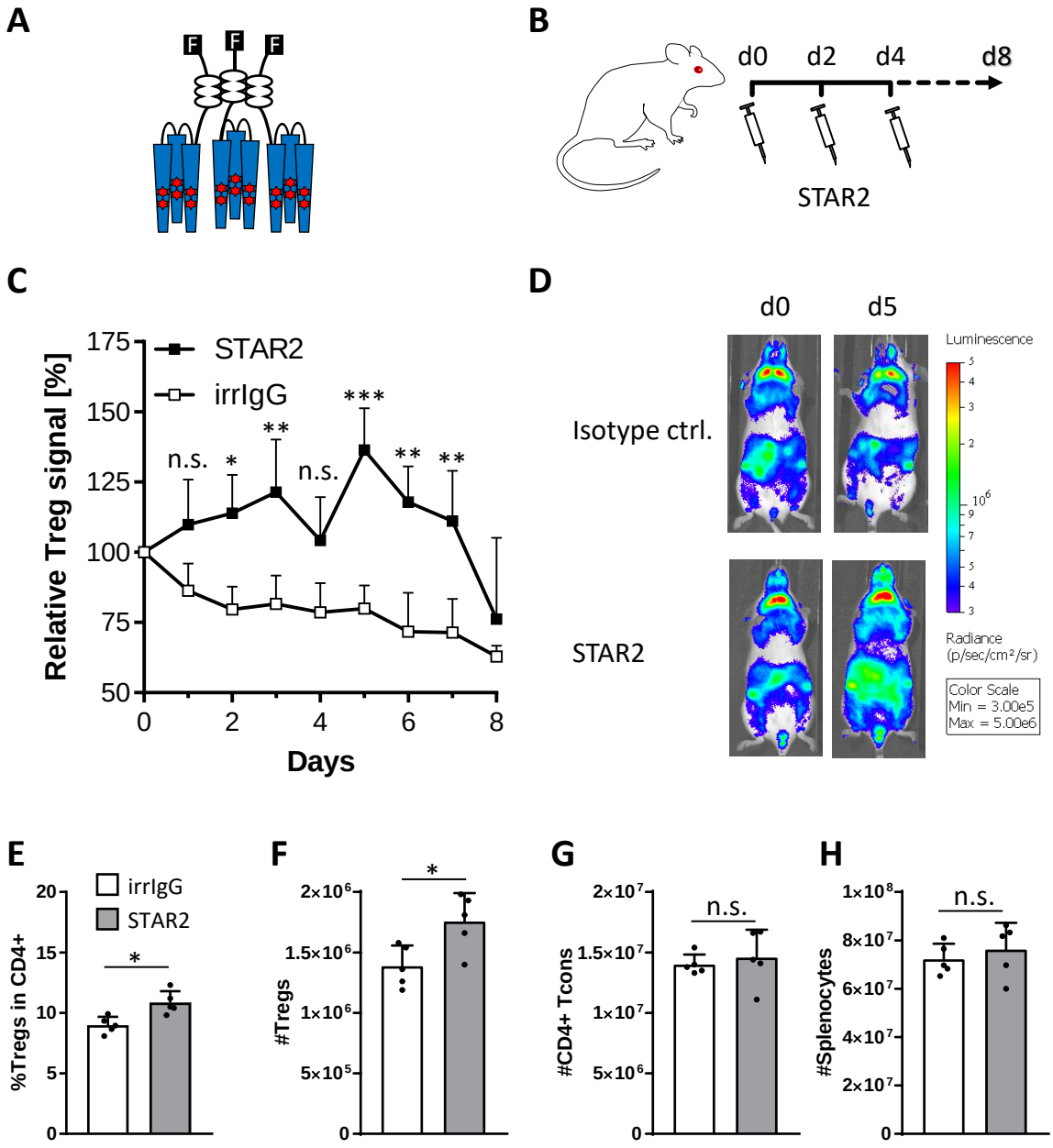

Figure 8: **STAR2 expands Tregs *in vivo*.** (A-B) B6a.Foxp3.Luci.huTNFR2 mice were injected with 75 µg STAR2 or 150 µg irrelevant huIgG1 (irrIgG) on day 0, 2 and 4. (C, D) The bioluminescence signal of the Tregs was measured daily. At day 8 splenocytes were isolated and analyzed via flow cytometry. (E) %Tregs in $CD4^+$ (F) Total Tregs (G) Total $CD4^+$ Tcons (H) Total splenocytes. irrIgG, STAR2, n=5. *, $p \leq 0.05$; **, $p \leq 0.01$; ***, $p \leq 0.001$; n.s., not significant.

(Figure 8 A, B). The Tregs expanded starting two days after the first injection and decreased to normal level four days after the last injection (Figure 8 C, D). At this timepoint Treg frequencies remained elevated in the spleen, while total splenocytes and $CD4^+$ Tcons were not affected (Figure 8 E-H).

4.2.3 NewSTAR treatment rapidly expands Tregs for prolonged time periods

Next, we addressed the *in vivo* pharmacokinetics of our TNFR2 agonist. To improve the serum retention, we fused single chain trimers of TNFR2-specific TNF molecules (scTNF80) to the heavy chain of an ADCC dead (N297A mutation) irrelevant antibody (irrIgG) of the huIgG1 isotype (Figure 9 A). The final construct, termed NewSTAR, is a hexameric TNFR2 agonist. This new agonist we injected into FoxP3-reporter mice and monitored the Treg expansion via non-invasive bioluminescence imaging (Figure 9 B). A single injection of IgG-scTNF80 was sufficient to expand Tregs for 14 days (Figure 9 C, D). The expansion peaked at day 5 with a 3.7-fold higher Treg level in relation to day 0. BLI showed that the expansion is systemic and not restricted to specific sites of the body. However, increased BLI signals were preferentially observed in the cervical lymph nodes and in the gastrointestinal tract.

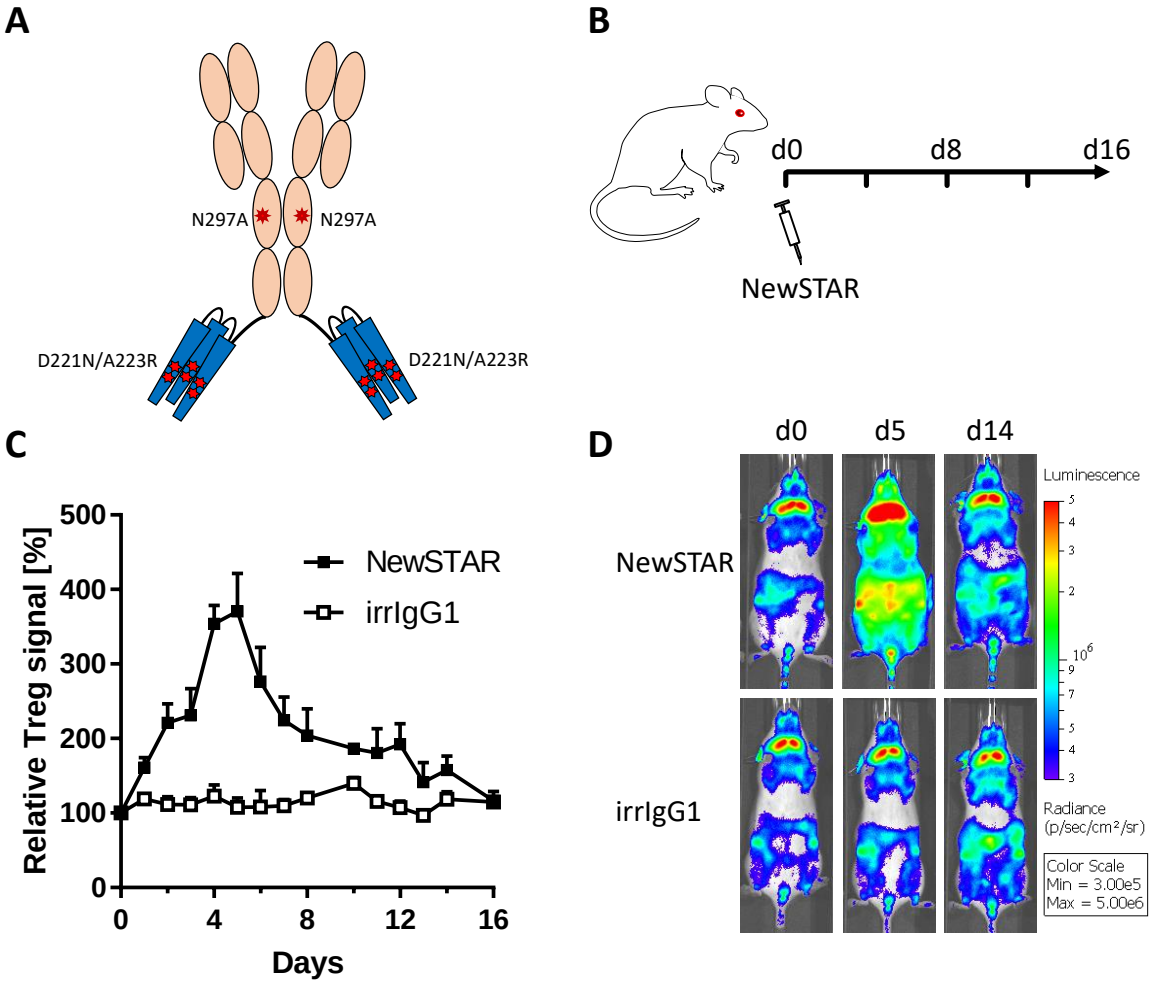

Figure 9: **NewSTAR treatment rapidly expands Tregs for prolonged time periods.** (A) NewSTAR consists of TNFR2-selective TNF trimers fused to an irrelevant huIgG1 containing the N297A mutation (ADCC dead). (B) B6a.Foxp3.Luci.DTR mice received a single i.p. injection of 140 µg irrIgG1-scTNF80. (C, D) The Treg signal was monitored via non-invasive BLI and calculated in relation to the signal measured at d0. irrIgG1-scTNF80, n=3; irrIgG1, n = 4. $p < 0.05$ from d1 – d14.

4.2.4 C1-moIgG1 expand Tregs

To develop therapeutic anti-TNFR2 antibodies for Treg expansion we immunized TNFR2$^{-/-}$ mice. In total, we generated 20 anti-huTNFR2 antibodies, two anti-moTNFR2 antibodies, and three that were cross-reactive and recognizing both species. The antibodies were then pre-screened on cell lines for TNFR2 activation. A potent activator of moTNFR2 *in vitro* was C1. In the moIgG1 format we injected C1 into FoxP3-reporter mice and monitored the Treg expansion via BLI (Figure 10 A, B). Administered three times, every other day C1-moIgG1 expanded Tregs. Non-invasive BLI suggested a systemic expansion (Figure 10 C, D). Although not significant, flow cytometric analysis of the spleen at day 6 revealed that the expansion was specific for Tregs and not CD4^{+} Tcons or splenocytes (Figure 10 E-H).

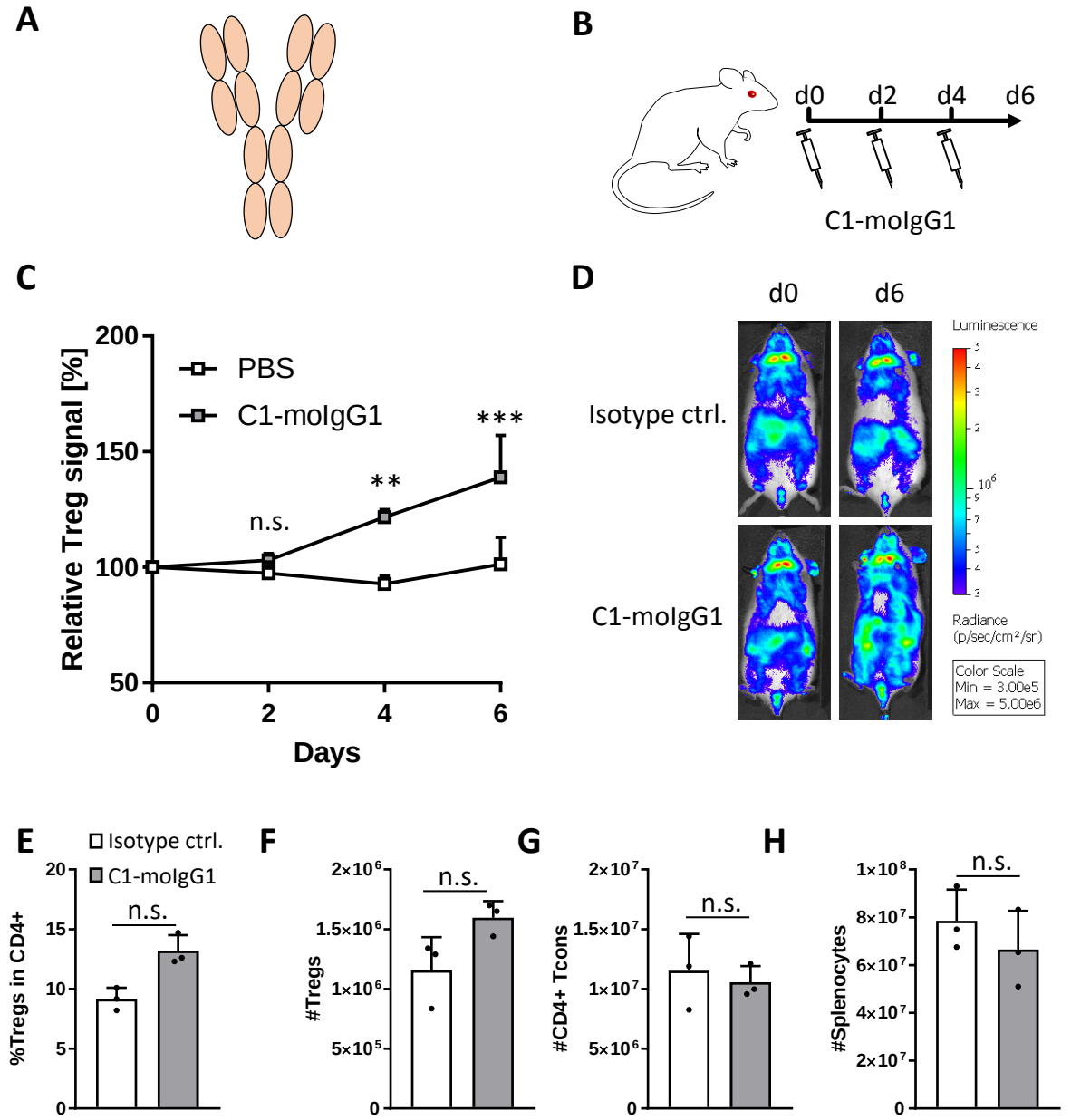

Figure 10: **C1-moIgG1 expands Tregs *in vivo*.** (A-B) B6a.Foxp3.Luci.DTR mice were injected with 150 µg C1-moIgG1 or PBS on day 0, 2 and 4. (C, D) The bioluminescence signal of the Tregs was measured every other day. (E-G) At day 6 splenocytes were isolated and analyzed via flow cytometry. (E) %Tregs in $CD4^+$, (F) Total Tregs, (G) Total $CD4^+$ Tcons, (H) Total splenocytes. PBS, n=3; C1-moIgG1, n= 3. **, $p \leq 0.01$; ***, $p \leq 0.001$; n.s., not significant.

4.3 Exogenous *in vivo* Treg expansion protects from aGvHD

After we demonstrated the expansion of Tregs via our constructs, we next tested whether they have therapeutic benefits in aGvHD. With STAR2, NewSTAR and irrIgG-IL-2 we expanded Tregs in C57Bl/6 mice prior to allo-HCT (Figure 11 A). After Treg expansion we lethally irradiated the mice and injected bone marrow and T cells from fully MHC-mismatched FVB mice. Weight loss, clinical score and survival were monitored for the following days to grade the severity of aGvHD (Figure 11 B-D). The untreated control group dramatically lost weight after transplantation, increased clinical score and fully deceased by day 9. The median survival was only 8.5 days. In contrast to that STAR2, NewSTAR and irrIgG-IL-2 prolonged the median survival to > 40 days, > 40 days and 33 days respectively. In all mice with preemptive Treg expansion we observed a lower clinical score and faster weight recovery compared to the untreated control group. Conclusively, irrIgG-IL-2, STAR2 and NewSTAR treatment increased Treg density *in vivo*. All strategies were biological relevant and protected mice from aGvHD.

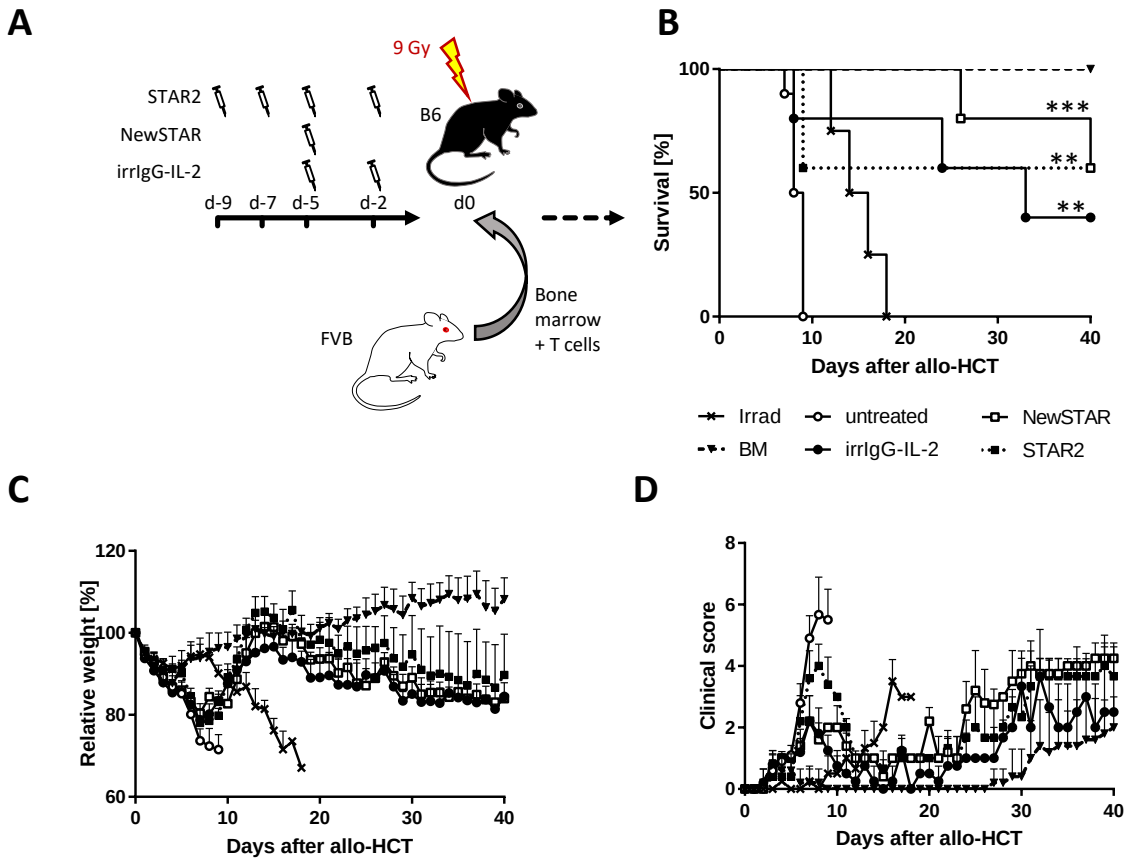

Figure 11: **Exogenous *in vivo* Treg expansion protects from aGvHD.** (A) C57Bl/6 (B6) mice received 75 µg STAR2, 140 µg NewSTAR or 50 µg irrIgG-IL-2 at the indicated time points. Thereafter, the mice were lethally irradiated and received $5x10^6$ bone marrow and $0.6x10^6$ T cells from fully-MHC mismatched FVB donors. The following days (B) survival, (C) weight loss and (D) clinical score were monitored. Weight loss > 20 % for more than two consecutive days or clinical score ≥ 8 were defined as endpoints. Untreated, n = 10; STAR2, NewSTAR, irrIgG-IL-2, bone marrow control, irradiation control, n = 5. **, p ≤ 0.01; ***, p ≤ 0.001.

4.4 Characterization of the tumor microenvironment in PDAC

We reported the beneficial effects of Treg expansion on inflammation in a preclinical mouse model of aGvHD. However, there are immunological diseases, predominantly malignancies, in which the immunosuppression of Tregs worsens the prognosis (Hiraoka et al., 2006) and so we next asked the question how we could target Tregs for the treatment of cancer. To this end, we investigated the syngeneic orthotopic Panc02 model of PDAC (Corbett et al., 1984). In PDAC the negative impact of Tregs on survival is especially dramatic and mouse models suggest therapeutic benefits of Treg depletion (Hiraoka et al., 2006; Jang et al., 2017).

4.4.1 PDAC resists gemcitabine treatment

Resistance to chemotherapy is a hallmark of PDAC. To demonstrate the similarities of the Panc02 model to the human disease and the urgent demand for new therapies we treated tumor-bearing mice with the nucleoside analog gemcitabine. The treatment significantly reduced tumor growth but failed to stop it completely (Figure 12). During gemcitabine treatment the tumors still increased 4-fold in their bioluminescent signal, compared to 15-fold in the control group. In the untreated group 3/5 mice had to be sacrificed versus 1/5 in the gemcitabine treated group because of massive tumor growth in the abdominal area. The limited response to gemcitabine urged us to investigate the tumor microenvironment of PDAC with the aim to develop therapeutic strategies.

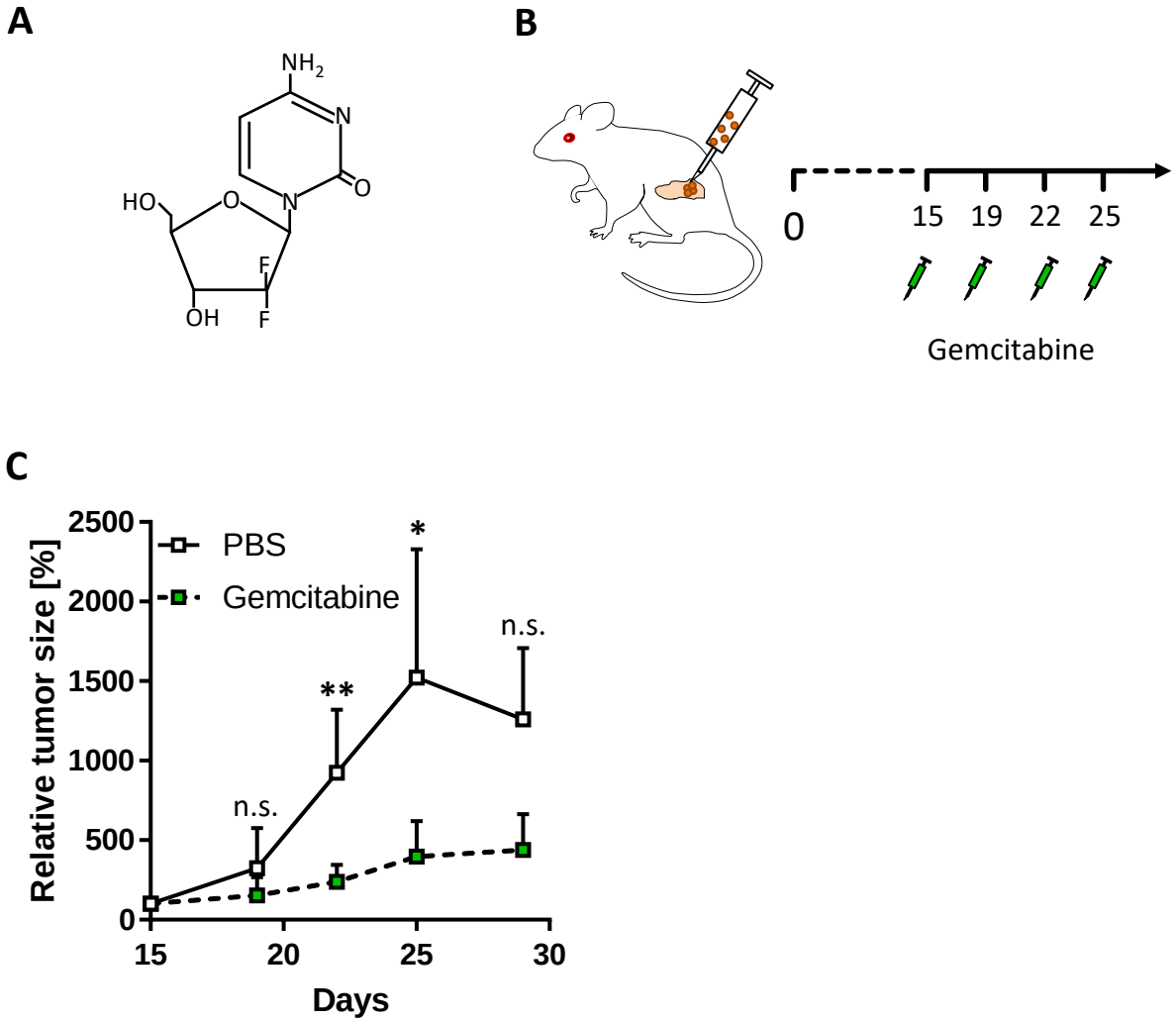

Figure 12**: PDAC resists gemcitabine treatment.** Tumor-bearing mice were treated with 120 mg/kg gemcitabine on day 15, 19, 22 and 25. The control group received PBS. Tumor progression was monitored via BLI. (A, B) Experimental setup, (C) Tumor progression relative to day 15. d15-25: n = 5; d29: PBS, n = 2; gemcitabine, n = 4. *, $p \leq 0.05$; **, $p \leq 0.01$; n.s., not significant.

4.4.2 CD4⁺ cells accumulate at tumor margins without penetrating the tumor core

Salmon *et al.* (2012) investigated lung tumors in mice and reported immune cell islets rather than thorough immune infiltration. We asked whether this immune exclusion also happens in PDAC. Therefore, we employed light-sheet fluorescence microscopy (LSFM) and generated images of healthy and tumor-bearing pancreata (as described in 3.2.10). We confirmed the results from the literature and found CD4⁺ cells to be scarce in healthy pancreata (Clark et al., 2007, Figure 14 A). In contrast to that, CD4⁺ cells highly infiltrated the pancreata of Panc02-bearing mice. The pictures clearly demonstrated that CD4⁺ cells only infiltrate the marginal tumor zone and were absent in the tumor core (Figure 13 B).

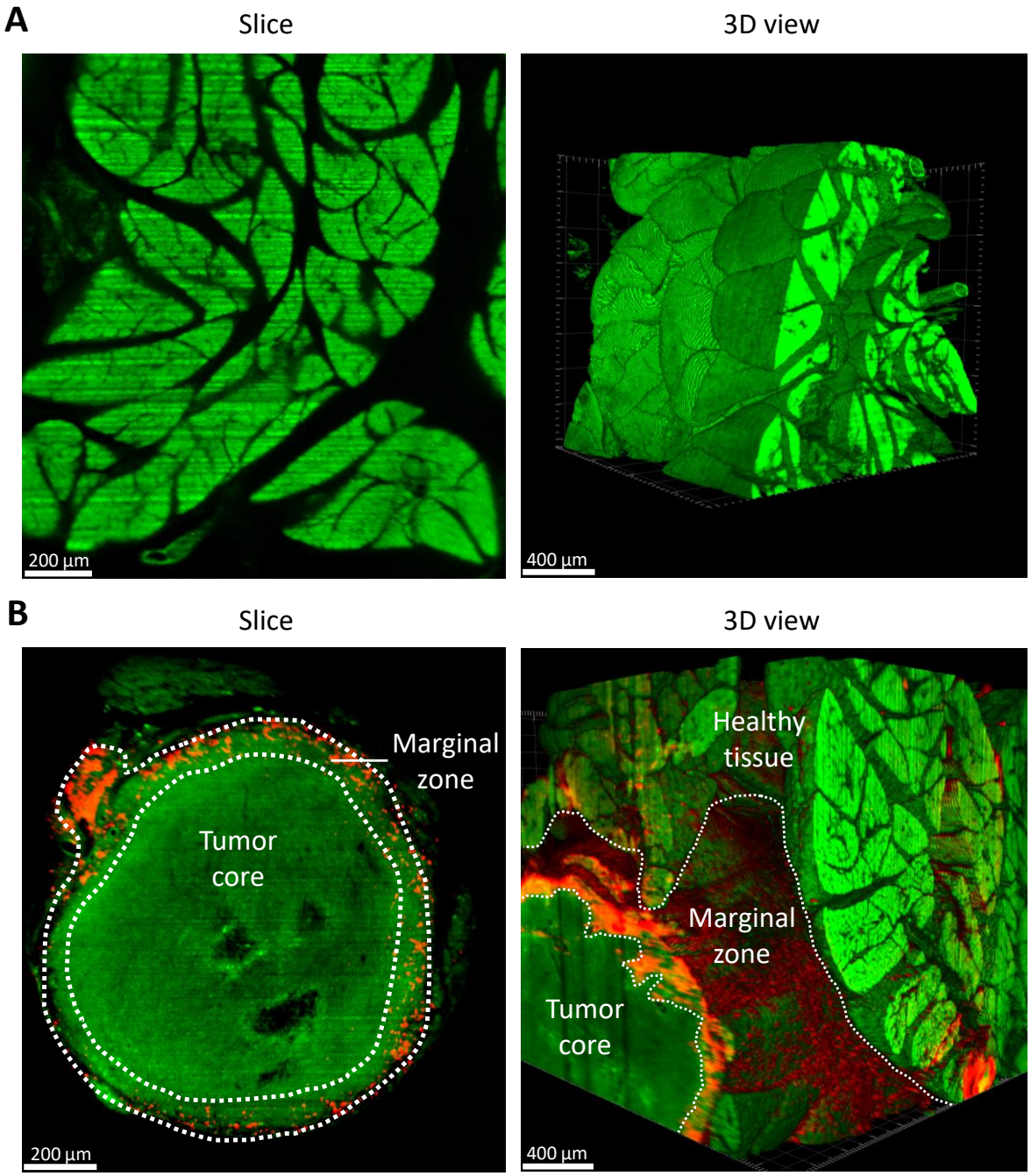

Figure 13: **CD4⁺ cells accumulate at tumor margins without penetrating the tumor core.** Images of (A) healthy untreated pancreas and (B) pancreatic tumors were acquired with a light-sheet microscope. The slices (left) were assembled to 3D images (right). Red, CD4; green, autofluorescence.

4.4.3 Tumor-infiltrating T cells display an activated phenotype

LFSM analysis clearly showed that the immune system reacts to the tumor and infiltrates its marginal zone. Now we further characterized the T cell-immune response and analyzed the infiltrating T cells for activation. Although there were fine differences, all tumor-infiltrating T cells, including Tregs, upregulated activation markers (Figure 14). ICOS and ICAM-1 were highly upregulated. CD69 expression was strong on $CD8^+$ T cells, weaker on $CD4^+$ Tcons and weakest on Tregs. Only a minor fraction of tumor-infiltrating Tregs expressed CD103 (Figure 14 D). $CD8^+$ T cells decreased their CD103 expression after tumor-infiltration. The afore

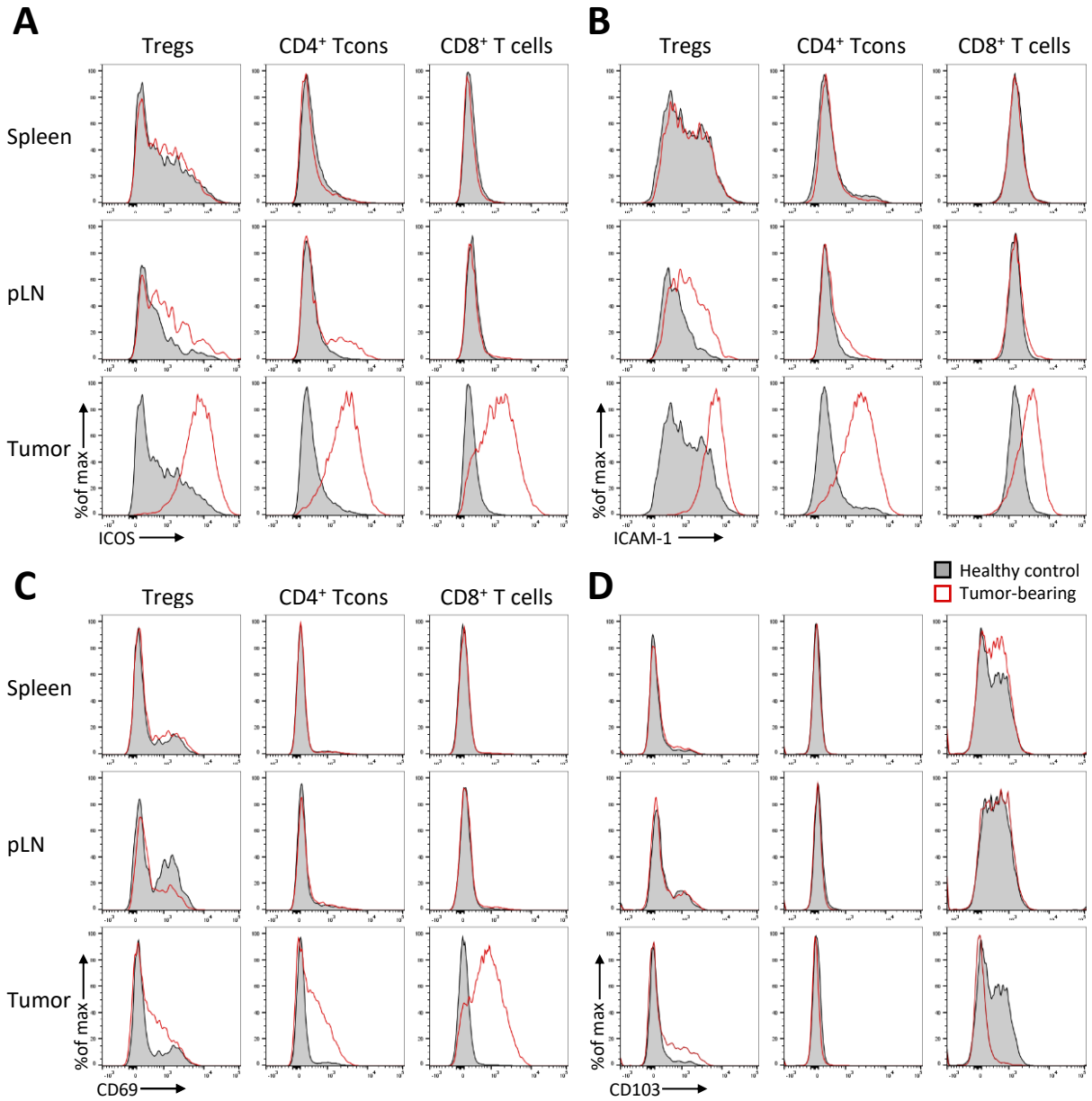

Figure 14: **Tumor-infiltrating T cells display an activated phenotype.** Spleens, pancreatic lymph nodes (pLNs) and tumors were harvested and analyzed via flow cytometry. Healthy mice were used as controls. Tumor-infiltrating T cells were compared to healthy spleen. (A) ICOS, (B) ICAM-1, (C) CD69, (D) CD103. Tregs ($CD3^+$, $CD4^+$, $Foxp3^+$), $CD4^+$ Tcons ($CD3^+$, $CD4^+$, $Foxp3^-$), $CD8^+$ T cells ($CD3^+$, $CD8^+$). Representative images from at least 2 independent experiments are shown. ICOS, ICAM-1, CD69, n = 13; CD103, n = 7.

mentioned activation markers were barely changed in the spleen and tumor-draining pancreatic lymph nodes (pLNs) of tumor-bearing mice. The CD4$^+$ Tcons and CD8$^+$ T cells shifted from a naïve phenotype (CD44^{low}CD62L^{high}) to an effector phenotype (CD44^{high}CD62L^{low}). Tregs on the other hand slightly decreased CD44 and the CD62L^{high} population vanished (Figure 15).

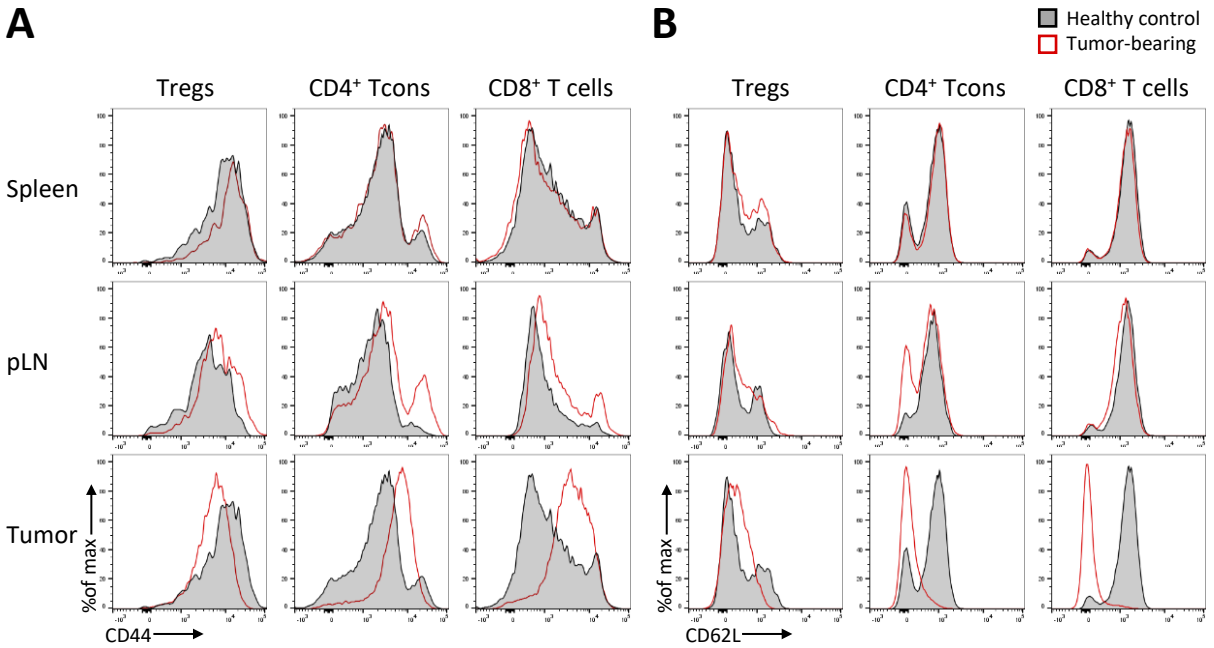

Figure 15: **Tumor-infiltrating T cells shift to an effector phenotype.** Spleens, pancreatic lymph nodes (pLNs) and tumors were harvested and analyzed via flow cytometry. Healthy mice were used as controls. Tumor-infiltrating T cells were compared to healthy spleen. (A) CD44, (B) CD62L. Tregs (CD3$^+$, CD4$^+$, Foxp3$^+$), CD4$^+$ Tcons (CD3$^+$, CD4$^+$, Foxp3$^-$), CD8$^+$ T cells (CD3$^+$, CD8$^+$). Representative images from 3 independent experiments are depicted. n = 13.

4.4.4 Tumor-infiltrating CD8$^+$ T cells coexpress the co-inhibitory receptors PD-1 and Lag-3

In the Panc02 tumors we found activated T cells and tumor progression at the same time. We hypothesized that the CD8$^+$ T cells are strongly regulated by the tumor microenvironment and tested for the expression of exhaustion-associated markers PD-1 and Lag-3 (Blackburn et al., 2009). The majority of tumor-infiltrating CD8$^+$ T cells upregulated both receptors (Figure 16).

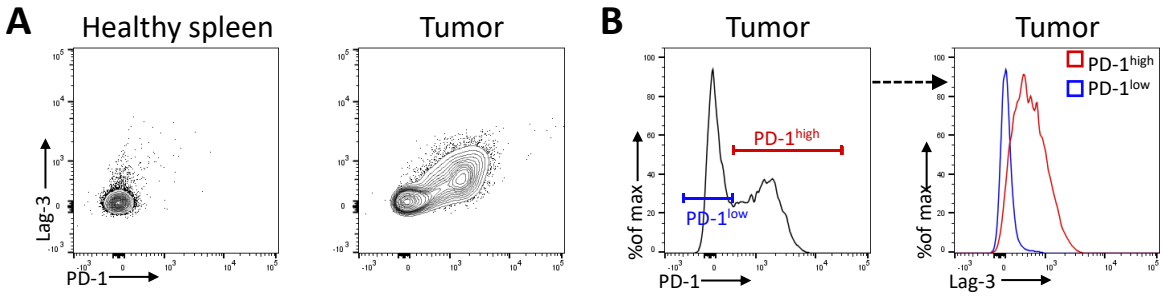

Figure 16: **Tumor-infiltrating CD8$^+$ T cells coexpress the co-inhibitory receptors PD-1 and Lag-3.** Panc02 tumors were analyzed via flow cytometry for PD-1 and Lag-3 expression on tumor-infiltrating CD8$^+$ T cells. CD8$^+$ T cells (CD3$^+$, CD8$^+$). Representative images from two experiment are shown. n = 12.

4.4.5 Treg numbers increase during the progression of PDAC

Searching for the root of immune suppression in PDAC we next investigated tumor-infiltrating Tregs. We employed FoxP3-reporter mice and injected luciferase-negative Panc02 cells into their pancreata (as described in 3.2.8). Starting from day 4 after tumor cell injection, Tregs infiltrated (Figure 17 A, B). While they were on single spots at earlier time points, with the progression of the disease the whole pancreas was more and more densely covered (Figure 17 F). Furthermore, at the advanced stage of the disease at day 16, Tregs also increased in the spleen. Neither did the tumor alter the systemic Treg levels, nor the frequencies of Tregs, $CD4^+$ Tcons and $CD8^+$ T cells in the peripheral blood (Figure 18).

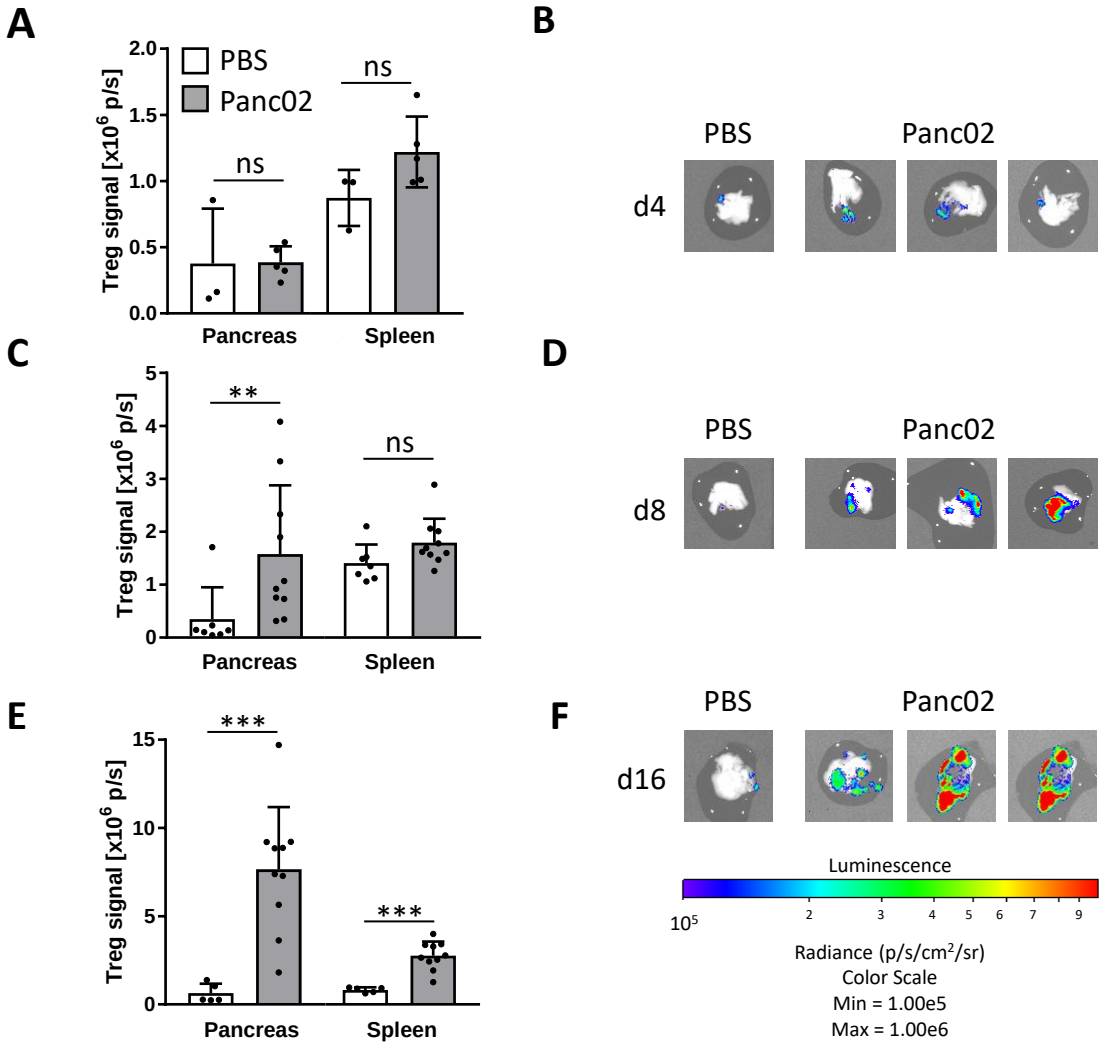

Figure 17: **Treg numbers increase during the progression of PDAC.** Panc02 cells were injected into FoxP3-reporter mic to induce PDAC. Sham operated, and PBS injected mice were used as control. At day 4 (A, B), 8 (C, D) and 16 (E, F) the spleens and tumors were explanted and the bioluminescent signal of the Tregs was acquired. Representative ex vivo images of the pancreas are depicted. d4: PBS, n = 3; Panc02, n = 5; d8: PBS, n = 7; Panc02, n = 10; d16: PBS, n = 5; Panc02, n = 9. *, $p \leq 0.05$; **, $p \leq 0.01$; ***, $p \leq 0.001$; n.s., not significant.

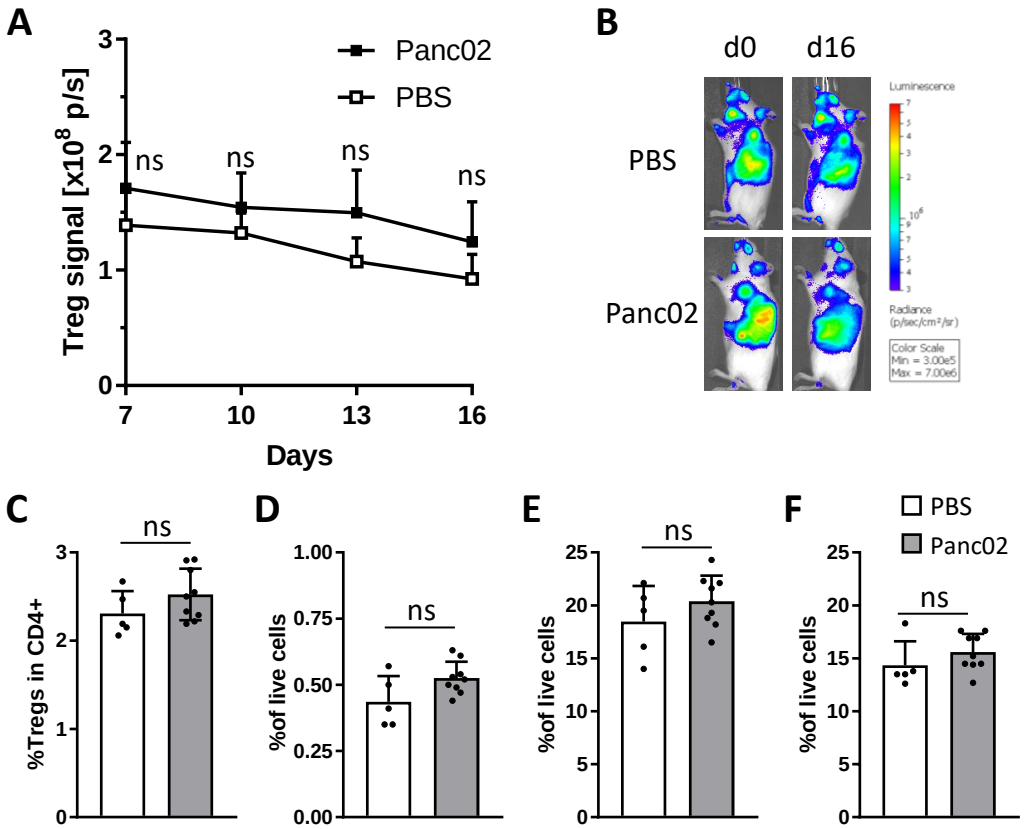

Figure 18: **PDAC does not alter Treg numbers systemically and in the peripheral blood.** (A) Panc02 cells were injected to induce PDAC. Sham operated and PBS injected mice were used as controls. (A, B) The Treg signal was acquired from the lateral side via bioluminescence imaging. At day 16 the blood was analyzed via flow cytometry. (C) %Tregs in $CD4^+$ T cells, (D) Tregs %of live cells, (E) $CD4^+$ Tcons %of live cells, (F) $CD8^+$ T cons. $CD3^+CD4^+FoxP3^+$ (Tregs), $CD3^+CD4^+FoxP3^-$ ($CD4^+$ Tcons), $CD3^+$ $CD8^+$ ($CD8^+$ T cells). PBS, n = 5; Panc02, n = 10. n.s., not significant.

4.4.6 Tregs strongly increase in the immune microenvironment of PDAC

After we knew about the accumulation of Tregs during disease progression we investigated how much they constitute of the tumor-infiltrating T cells. We explanted the tumors, pLNs and spleens and analyzed them via flow cytometry. While splenic $CD4^+$ T cells of healthy and tumor-bearing mice consisted of 9.8 ± 1.2 % Tregs, their numbers increased up to 33.1 ± 7.3 % inside the tumor and ranged from 20 % to almost 50 % (Figure 19 A). In the spleens and pLNs the Treg frequency slightly increased. Inside the tumors we found very few of the tumor critical $CD8^+$ T cells. The mean CD8:Treg ratio of 8.1 ± 1.6 in the spleen and 7.0 ± 1.2 in the pLN decreased to 2.5 ± 1.7 in the tumor (Figure 19 B). Some tumors even showed ratios as low as 1. Nevertheless, also tumors with higher CD8:Treg ratios (maximum 6.2) progressed and were not rejected.

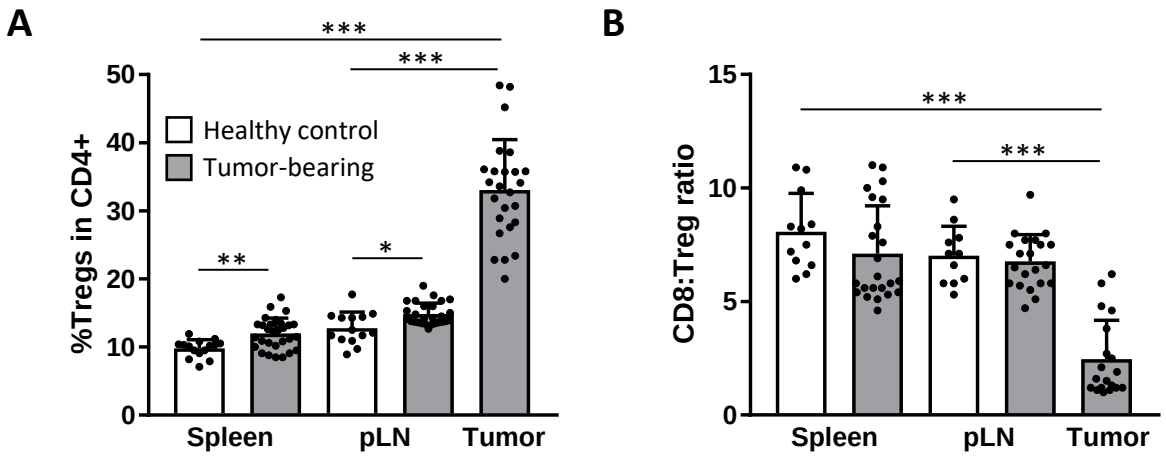

Figure 19: **Tregs strongly increase in the tumor microenvironment of PDAC.** Spleens, pancreatic lymph nodes (pLNs) and tumors were harvested from tumor-bearing mice and analyzed via flow cytometry. T cells from spleen and pLN of tumor-bearing mice were compared to their counterparts in healthy untreated controls. Tumor-infiltrating T cells were compared to healthy spleen. (A) Gating strategy, (B) %Tregs in $CD4^+$ T cells, (C) $CD8^+$ T cell:Treg ratio. Tregs ($CD3^+$, $CD4^+$, $Foxp3^+$), $CD4^+$ Tcons ($CD3^+$, $CD4^+$, $Foxp3^-$), $CD8^+$ T cells ($CD3^+$, $CD8^+$). Pooled data from four independent experiments. Spleen healthy, n = 12; Spleen tumor, n = 23; pLN healthy, n = 11; pLN tumor, n = 21; Tumor, n = 19; *, $p \leq 0.05$; **, $p \leq 0.01$; ***, $p \leq 0.001$.

4.4.7 Tumor-infiltrating Tregs upregulate Helios and downregulate Neuropilin-1

To address the question of the Tregs origin in our model of PDAC we next investigated Helios and Neuropilin-1 expression. The majority of Tregs from the spleen and pLN from healthy mice expressed Helios and Neuropilin-1 (Figure 20). Tumor-burden of the mice did not alter this pattern. Tumor-infiltrating Tregs expressed Helios as high as their splenic companions (Figure 20 A), but the Helios negative subset vanished. For Neuropilin-1 the opposite

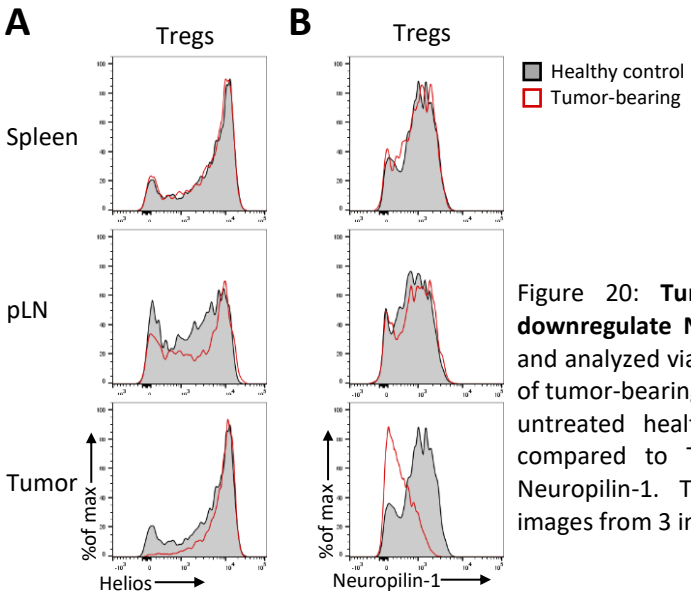

Figure 20: **Tumor-infiltrating Tregs express Helios and downregulate Neuropilin-1.** Panc02 tumors were harvested and analyzed via flow cytometry. Tregs from spleens and pLNs of tumor-bearing mice were compared to their counterparts in untreated healthy controls. Tumor-infiltrating Tregs were compared to Tregs from healthy spleen. (A) Helios (B) Neuropilin-1. Tregs ($CD3^+$, $CD4^+$, $Foxp3^+$). Representative images from 3 independent experiments. n = 13.

happened (Figure 20 B). Expression in tumor-infiltrating Tregs strongly decreased and the dim subset dominated in the tumor bed.

4.4.8 Tumor-infiltrating Treg upregulate immunomodulatory receptors

The incredible high Treg frequencies we found, combined with the literature on their negative impact on PDAC (Hiraoka et al., 2006) encouraged us to develop targeting strategies. Therefore, we first investigated immunomodulatory receptors. Tumor-infiltrating Tregs almost exclusively upregulated CTLA-4 (Figure 21 A). On CD4$^+$ Tcons and CD8$^+$ T cells we observed only slight changes compared to the expression levels in their healthy splenic

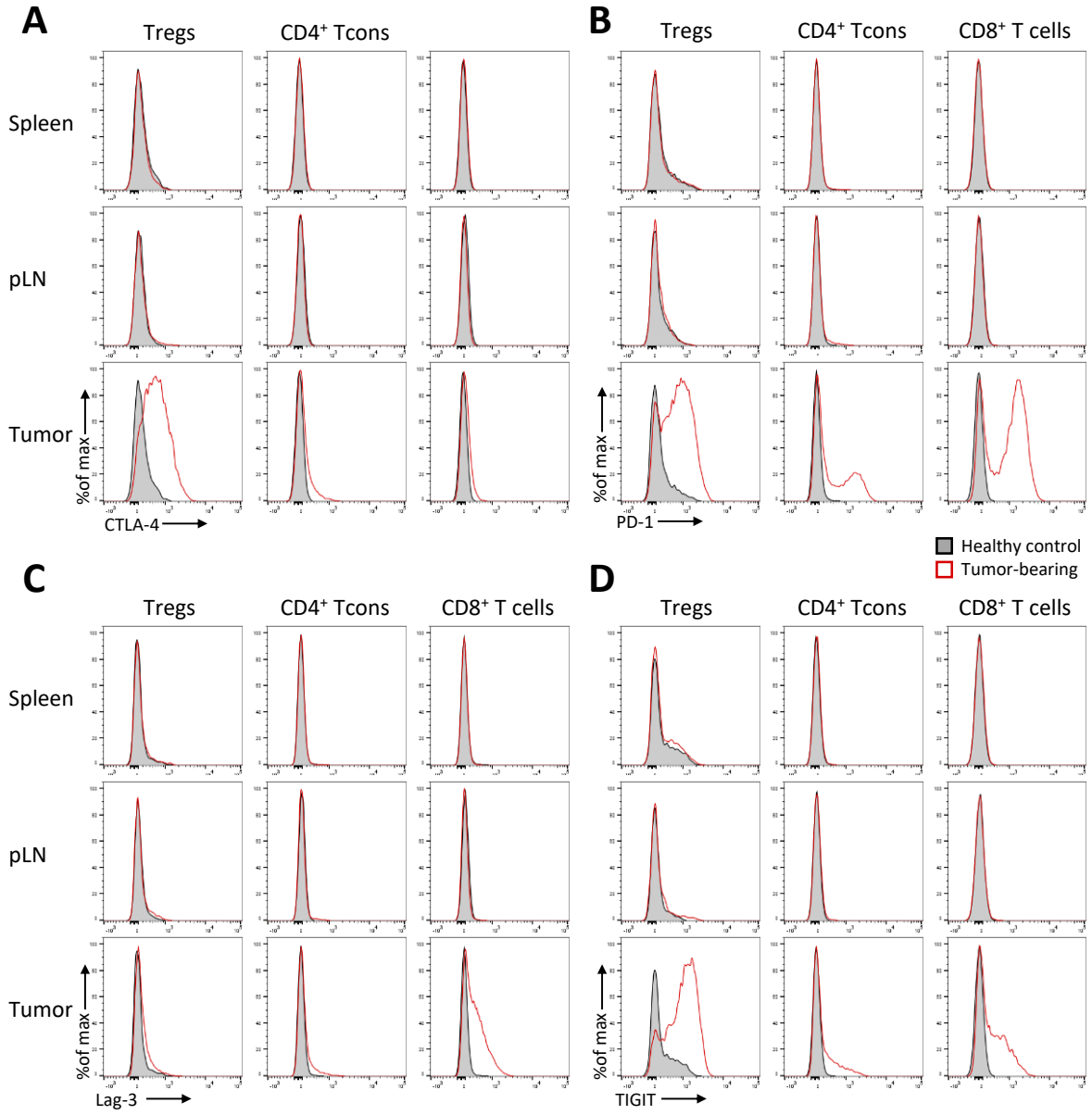

Figure 21: **Tumor-infiltrating Tregs express immunomodulatory receptors.** Spleens, pancreatic lymph nodes (pLNs) and tumors were harvested and analyzed via flow cytometry. Healthy mice were used as controls. Tumor-infiltrating T cells were compared to healthy spleen. (A) PD-1, (B) CTLA-4, (C) Lag-3, (D) TIGIT. Tregs (CD3$^+$, CD4$^+$, Foxp3$^+$), CD4$^+$ T cons (CD3$^+$, CD4$^+$, Foxp3$^-$), CD8$^+$ T cells (CD3$^+$, CD8$^+$). Representative images from at least 2 independent experiments. PD-1, n = 14; CTLA-4, n = 11; Lag-3 n= 18; TIGIT, n = 12.

counterparts. PDAC did not alter the expression pattern of CTLA-4 in pLNs. All tumor-infiltrating T cells divided into a PD-1^{high} and PD1^{low} subset (Figure 21 B). For Tregs and CD8$^+$ T cells the PD1^{high} subset predominated. Most of the CD4$^+$ Tcons remained PD-1^{low}. Lag-3 expression was barely changed in tumor-infiltrating Tregs and CD4$^+$ Tcons compared to their counterparts in spleen and pLN (Figure 21 C). In contrast to that, tumor-infiltrating CD8$^+$ T cells strongly upregulated Lag-3. TIGIT increased on all tumor-infiltrating T cells, however, only slightly on CD4$^+$ Tcons and moderate on CD8$^+$ T cells (Figure 21 D). Tregs on the other hand strongly upregulated this receptor. As seen for the other inhibitory receptors also the TIGT levels of all T cells in spleens and pLNs from tumor-bearing mice remained unaffected compared to healthy animals.

4.4.9 Tumor-infiltrating Tregs express TNF receptor super family members

For targeting reasons, we second analyzed the expression of TNFRSF members on tumor-infiltrating Tregs. In our model we found that Tregs further upregulated their high GITR expression upon tumor infiltration (Figure 22 A). So did the conventional T cells. However, Tregs remained the highest GITR expressors. Tumor-infiltrating Tregs highly upregulated 4-1BB (Figure 22 B). In CD4$^+$ Tcons and CD8$^+$ T cells the expression increased only slightly. CD27 was downregulated on all intratumoral T cells, the most on CD4$^+$ Tcons (Figure 22 C). In Tregs and CD8$^+$ T cells the CD27 loss was less pronounced but still strong. It is of interest, that the pattern of CD27 downregulation was similar in Tregs and CD8$^+$ T cells but different when compared to CD4$^+$ Tcons. The brightest OX40-expressors inside the tumor were the Tregs

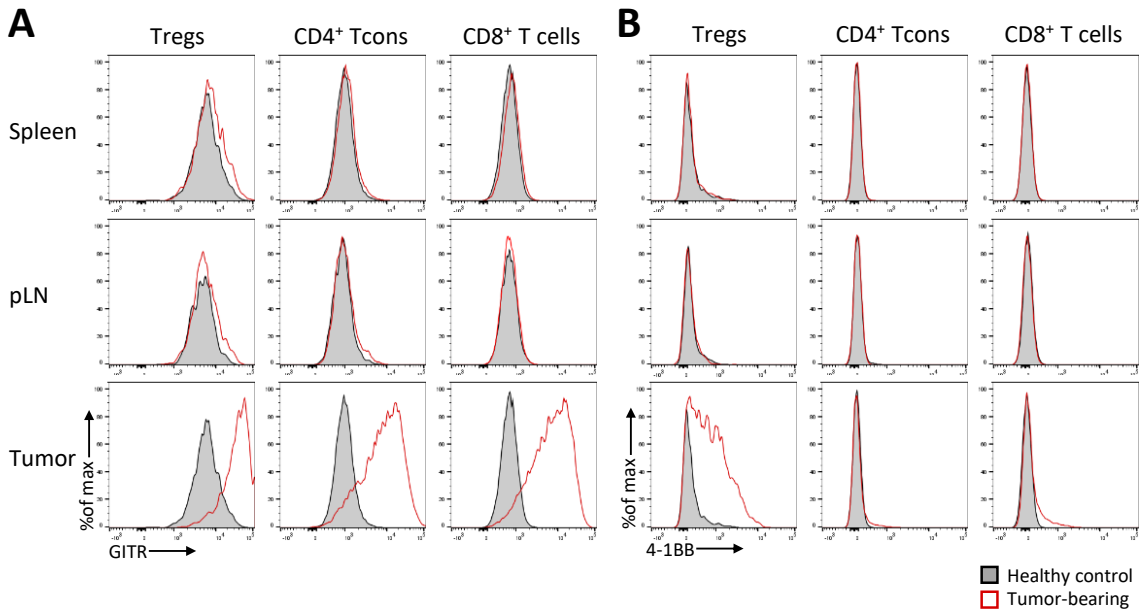

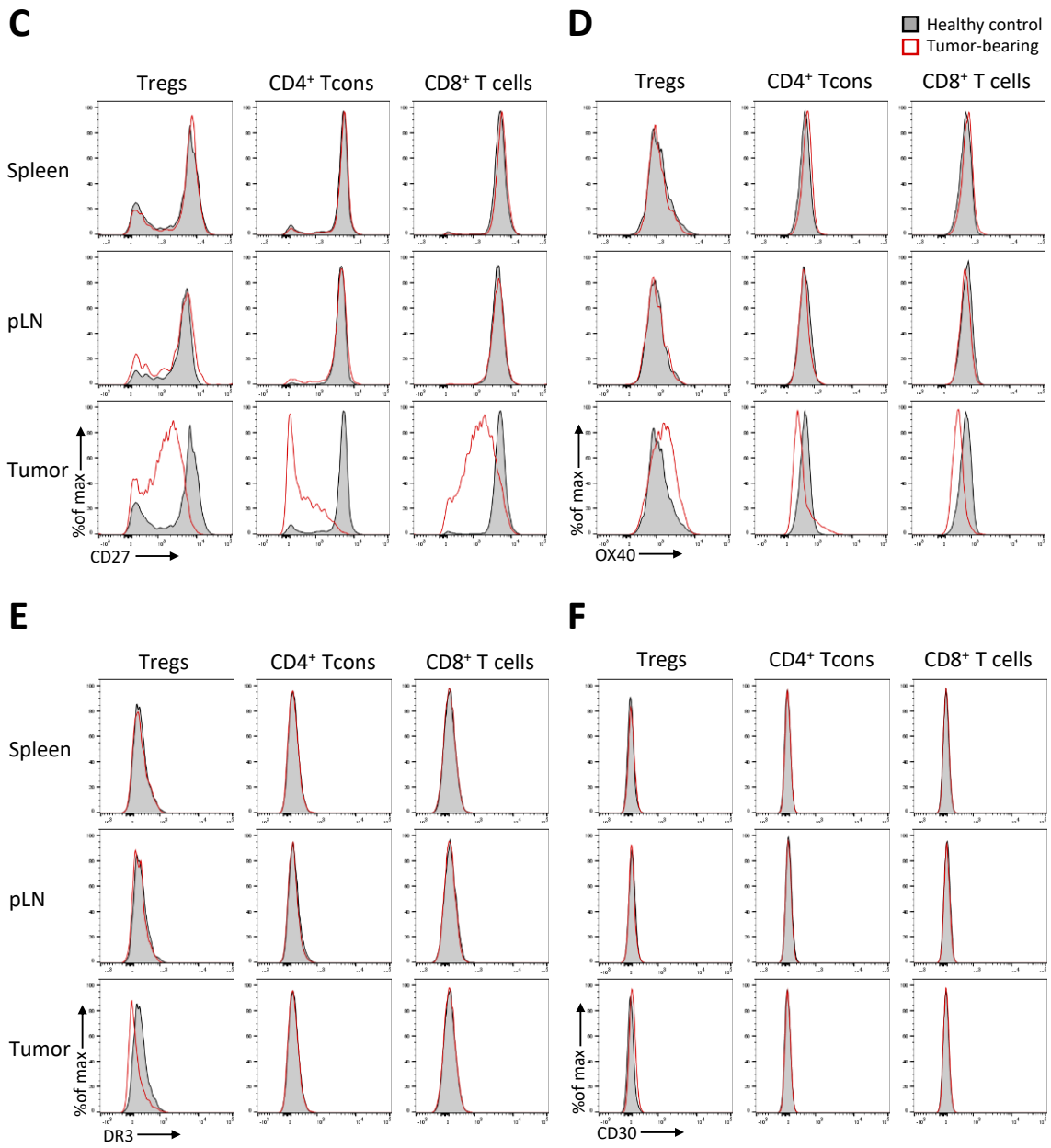

Figure 22: **Tumor-infiltrating Tregs express TNFRSF members.** Spleens, pancreatic lymph nodes (pLNs) and tumors were harvested and analyzed via flow cytometry. Healthy mice were used as controls. Tumor-infiltrating T cells were compared to healthy spleen. (A) GITR, (B) 4-1BB, (C) CD27, (D) Ox40, (E) DR3, (F) CD30. Tregs ($CD3^+$, $CD4^+$, $Foxp3^+$), $CD4^+$ Tcons ($CD3^+$, $CD4^+$, $Foxp3^-$), $CD8^+$ T cells ($CD3^+$, $CD8^+$). Representative images from at least one experiment is shown. GITR, n = 13; 4-1BB, CD27, OX40 n = 12; DR3, CD30, n = 6.

(Figure 22 D). Upon infiltration they upregulated this receptor. Both $CD4^+$ and $CD8^+$ Tcons decreased OX40 when they approached the tumor (Figure 22 D). For DR3 and CD30 we only observed marginal expression alterations in tumor-infiltrating Tregs (Figure 22 E, F). None of the analyzed receptors changed on T cells in the spleen and pLN of tumor-bearing mice compared to healthy untreated controls.

In the first part of this study we demonstrated Treg expansion via TNFR2 agonization. Therefore, we investigated this receptor particularly in detail. TNFR2 was highly upregulated and the TNFR2^{high} subset dominated within the tumor-infiltrating Tregs (Figure 23 A). Also, CD8^{+} T cells upregulated TNFR2, but Tregs remained the brightest expressors. We observed also a small increase in TNFR2 on CD4^{+} Tcons. T cells from huTNFR2 and wt mice showed similar patterns of TNFR2 expression (Figure 23 B). We found that 19.5 ± 1.92 % of the Tregs from healthy spleens expressed Ki-67^{+} and 18 ±- 0.6 % of the Tregs from the spleens of tumor-bearing mice. 2.9 ± 2 % of the tumor-infiltrating Tregs were Ki-67^{+}. Notably, TNFR2^{high} Tregs expressed higher Ki-67. Whereas the overall changes of Ki-67 in tumor-infiltrating T cells were only minor when compared the healthy spleen (Figure 23 C, D). Furthermore, CTLA-4, PD-1 and CD73 increased along with TNFR2 expression on Tregs (Figure 23 D). The findings urged us to target Tregs via TNFR2.

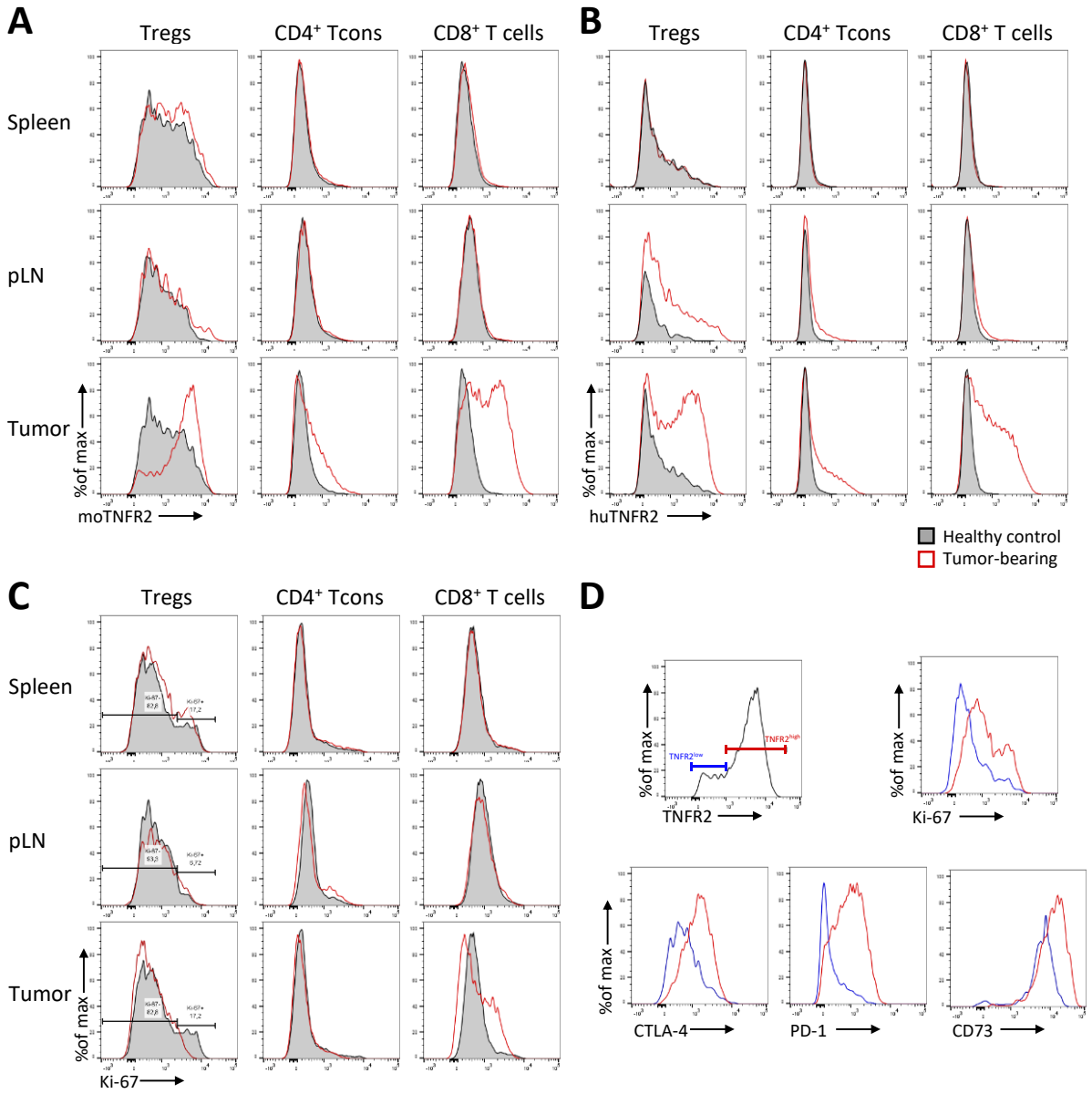

Figure 23: **Proliferating and suppressive Tregs express TNFR2.** Spleens, pancreatic lymph nodes (pLNs) and tumors were harvested and analyzed via flow cytometry. Healthy mice were used as controls. Tumor-infiltrating T cells were compared to healthy spleen. (A) moTNFR2, (B) huTNFR2ecd-ki, (C) Ki-67, (D) tumor-infiltrating Tregs were gated on TNFR2 low and high and further analyzed for the expression of (E) Ki-67, (F) CTLA-4, (G) PD-1 and (H) CD73. Tregs ($CD3^+$, $CD4^+$, $Foxp3^+$), $CD4^+$ Tcons ($CD3^+$, $CD4^+$, $Foxp3^-$), $CD8^+$ T cells ($CD3^+$, $CD8^+$). Representative images from at least one experiment are shown. The threshold for Ki-67^+ Tregs could not be set according to FMO controls and was therefore chosen in a certain degree arbitrary. moTNFR2, n = 12; huTNFR2 n = 10; Ki-67 n = 13, CTLA-4, n = 6; PD-1, n = 4; CD73, n = 5.

4.5 TNFR2 blockade does not reduce tumor-infiltrating Tregs

From our previous analysis we concluded, that the TNFR2-expressing Treg subset is the proliferative source of Tregs inside the tumor bed. The first part of this study taught us that Tregs expand after TNFR2 stimulation. Based on these data we hypothesized that TNFR2 stimulation contributes to the high Treg numbers seen in PDAC and aimed to block TNFR2 to prevent it. To test our hypothesis, we used the anti-huTNFR2 antibody clone C4 from our own antibody pool. C4 binds and blocks TNFR2 without activating it (Medler et al., 2019). To further prevent crosslinking via Fc receptors that then in return activate TNFR2 we introduced the N297A mutation (described in 0). The final construct, C4-N297A, we administered to pancreatic cancer-bearing mice and analyzed the tumors for their Treg frequencies. Neither did C4-N297A change the percentage of Tregs within the CD4$^+$ T cells, nor the CD8$^+$:Treg ratio (Figure 24). Counter-stained with anti-huIgG antibodies the experiment revealed that the C4-huIgG1-N297A efficiently bound tumor-infiltrating Tregs and blocked TNFR2 for antibody (clone 3G7A02) binding (Figure 24 E).

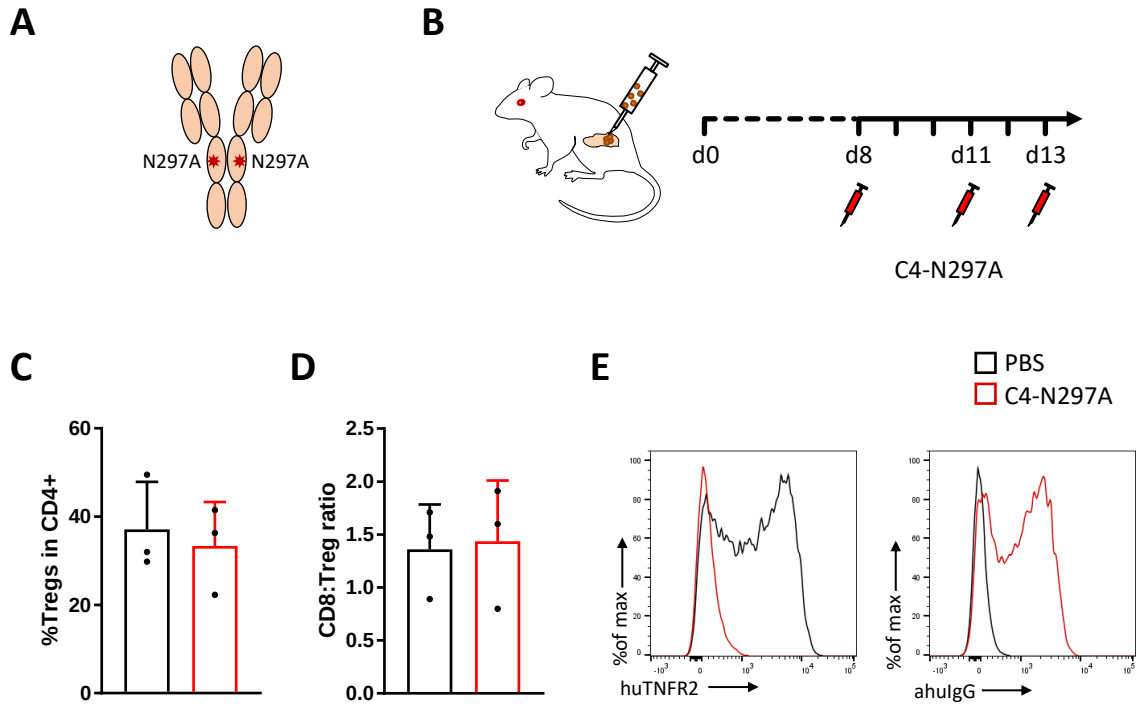

Figure 24: **TNFR2 blockade does not reduce tumor-infiltrating Tregs.** (A, B) PDAC-bearing B6a.huTNFR2 mice were treated with 250 µg C4-huIgG1-N297A on day 8, 11 and 13. On day 14 the tumors were explanted and analyzed via flow cytometry. (C) %Tregs in CD4$^+$ T cells (D) CD8:Treg ratio (E) tumor-infiltrating Tregs stained for huTNFR2 and huIgG1. Tregs (CD3$^+$, CD4$^+$, Foxp3$^+$), CD4$^+$ Tcons (CD3$^+$, CD4$^+$, Foxp3$^-$), CD8$^+$ T cells (CD3$^+$, CD8$^+$). n= 3.

4.6 Targeting the tumor extracellular matrix changes the immune composition in PDAC and reduces tumor infiltrating Tregs

Dense and collagen-rich tumor stroma is a hallmark of PDAC (Hezel et al., 2016). We hypothesized that targeting the stroma might increase the general immune cell-infiltration. To inhibit stroma formation, we treated mice with minoxidil. The treatment did not stop the tumor progression (Figure 25 C). However, it reduced the frequency of Tregs within the $CD4^+$ T cells and the overall content of Tregs inside the tumor (Figure 25 D-F). In addition, the frequency of tumor-infiltrating B cells decreased after minoxidil treatment (Figure 25 I). Conventional T cells, NK cells, macrophages and dendritic cells remained unchanged (Figure 25 G-L). Minoxidil treatment did not alter the immune cell composition of the spleen.

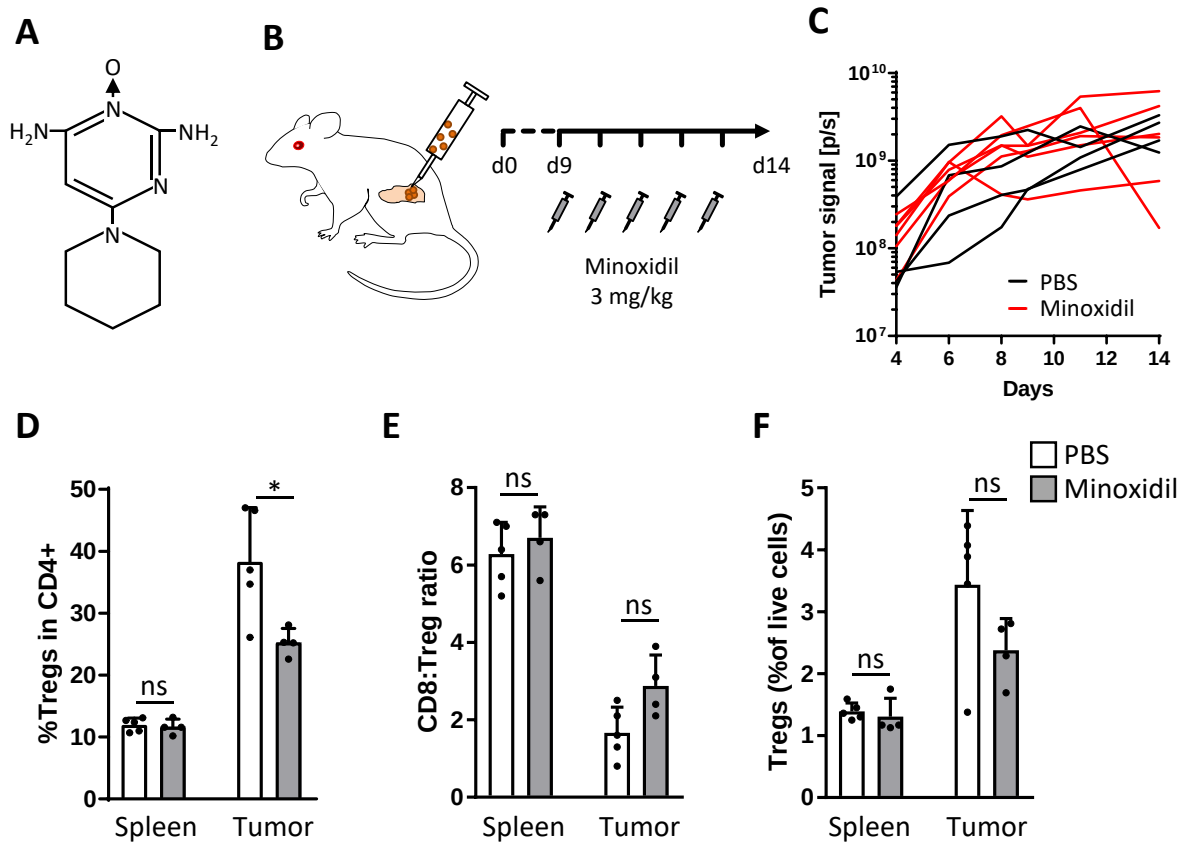

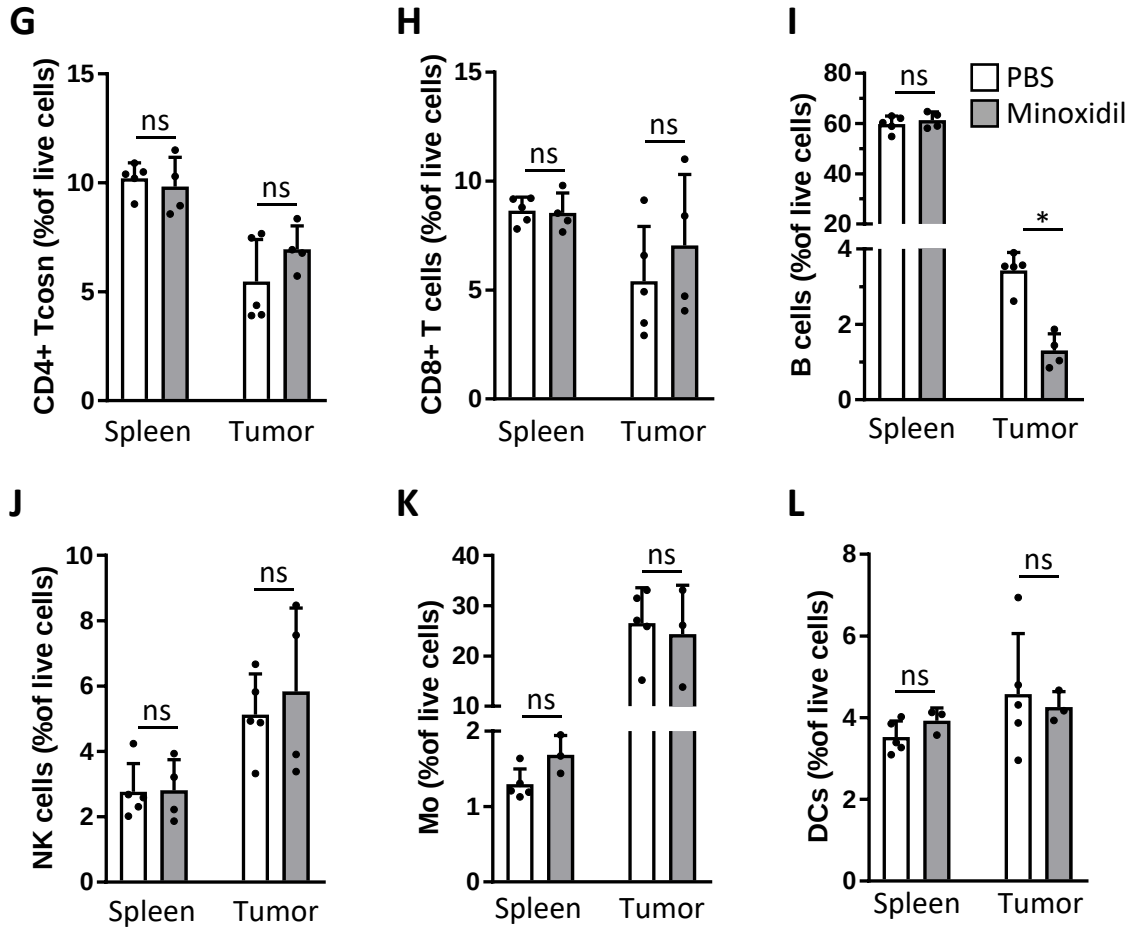

Figure 25: **Targeting the tumor extracellular matrix reduces tumor-infiltrating Tregs.** (A, B) PDAC-bearing mice were treated with 3 mg/kg minoxidil or PBS for 5 consecutive days. (C) The tumor progression was monitored via bioluminescence imaging. (D-L) At day 14 the spleens and tumors were explanted and analyzed via flow cytometry. Tregs ($CD3^+$, $CD4^+$, $Foxp3^+$), $CD4^+$ T cons ($CD3^+$, $CD4^+$, $Foxp3^-$), $CD8^+$ T cells ($CD3^+$, $CD8^+$). B cells ($CD19^+$), NK cells ($NK\text{-}1.1^+$), macrophages ($CD11c^+MHCII^+CD64^+F4/80^+$), dendritic cells ($CD11c^+MHCII^+CD64^-F4/80^-$). n = 4. *, $p \leq 0.05$; **, $p \leq 0.01$; ***, $p \leq 0.001$; n.s., not significant.

5 Discussion

A functional and numerical Treg disbalance has been observed in chronic inflammatory conditions and transplant rejection (Afzali et al., 2007). Therefore, therapeutic strategies to augment Treg function and numbers are highly interesting for the immunotherapy of inflammatory diseases. In contrast to that, induction and accumulation of Tregs inside tumors lead to immune tolerance and predict poor survival (Curiel et al., 2004; Hiraoka et al., 2006; Balsari et al., 2009; Liu et al., 2011). Targeting Tregs might be the key to break tolerance and boost antitumor immunity.

In the first part of this study, we reported novel therapeutic candidates to augment Treg function and numbers. We demonstrated that the TNFR2 pathway is superior to IL-2 and propose it as a crucial receptor for Treg homeostasis. The clinical relevance of augment Treg function and numbers we proved in a mouse model of aGVHD. In the second part, we investigated Tregs in PDAC and introduced TIGIT and TNFRSF members as targets. In addition, and for the first time, we reported that disrupting the extracellular tumor matrix reduces intratumoral Treg accumulation in highly aggressive PDAC.

5.1 Stimulation of TNFR2 activates and expands regulatory T cells

In the first part of this study, we demonstrated the concept of TNFR2 activation for the expansion of Tregs with a TNFR2 agonist termed STAR2. STAR2 consists of three single chain TNF molecules linked to a trimerization domain. This results in a nonameric TNF ligand. In addition, two point mutations in each of the TNF molecules result in specificity for TNFR2, because a steric clash prevents TNFR1 binding (Chopra et al., 2016). In contrast to TNFR1, which becomes activated by both, sTNF and mTNF, TNFR2 activation requires higher receptor clustering (Grell at al. 1995). Under physiological conditions, this is only achieved by mTNF. STAR2 is soluble but the oligomerization of TNF molecules is sufficient to activate the receptor similar to mTNF. This provided us with a powerful tool to study the effects of TNFR2 activation in Tregs. Other groups previously published that TNFR2 is especially important for Tregs and TNFR2 activation results in their expansion (Chen et al., 2007). We proved that STAR2 expanded Tregs. In enriched T cell cultures, we demonstrated that TNFR2 agonization by STAR2 both activated and expanded Tregs. On conventional $CD4^+$ T cells there were only minor effects. To eliminate the possibility of TNFR2-stimulated $CD4^+$ T cells that then in return could stimulate Tregs we performed experiments with FACS-sorted Tregs devoid of Tcons. These

results clearly demonstrated, that TNFR2 agonization on Tregs was sufficient to induce activation and expansion without any further Tcon help or stimulus. Therefore, we conclude that the STAR2-effect is Treg intrinsic. Noteworthy, the activation pattern changed in the presence of Tcons. In the absence of Tcons, STAR2 did not induce CD44 expression on Tregs and decreased ICOS expression. The *in vitro* results prompted us to examine STAR2 in *in vivo* experiments. In FoxP3-reporter mice we demonstrated that STAR2 also expands Treg *in vivo*.

The expansion of Tregs with a selective and soluble TNFR2 agonist gave us the opportunity to examine Treg function in a variety of inflammatory disease models. Expansion of Tregs attenuates symptoms in disease models of allergic lung infiltration, type 1 diabetes, experimental autoimmune encephalomyelitis and transplant rejection (van Maurik et al., 2002; Brusko and Atkinson, 2007; Ephrem et al., 2008; Schreiber et al., 2010). The pathophysiological and clinical relevance along with a clear readout system drew our attention towards GvHD. Tregs oppose GvHD and at the same time preserve the GvL-effect (Hoffmann et al., 2002; Taylor et al. 2002; Edinger et al., 2003; Nguyen et al., 2007). In a fully MHC-mismatch model, STAR2 administration before transplantation reduced clinical GvHD score, weight loss and improved survival (Chopra et al., 2016 and own results). As desired for translation into the patients the GvL effect was preserved (Chopra et al., 2016). After proof of concept, we aimed to further improve our therapeutic strategy. Although, STAR2 activated and expanded Tregs, it seems not yet suited for translation into the clinics. First, the trimerization domain originating from chicken could potentially be immunogenic. Second, and most important, the serum half-life is low and therefore high treatment frequencies are necessary. To address the unfavorable pharmacokinetics of STAR2, we designed NewSTAR. It consists of three TNFR2-selective TNF molecules fused to each heavy chain of an irrelevant human IgG1. This hexameric TNFR2 agonist led to expanded Treg levels for two weeks after a single injection. The expansion itself was faster and higher compared to STAR2. Injected into mice prior to allo-HCT, NewSTAR reduced clinical GvHD score, weight loss and improved survival. The effects were even superior to STAR2. Higher and persisting Treg expansion could explain this.

For translational reasons we raised antibodies directed against TNFR2. Antibodies are frequently used for clinical application. They are stable in serum and compared to most protein therapeutics have an extremely long serum half-life. Antibodies can activate TNFR2

after binding and further crosslinking via Fc receptors (concept reviewed in detail in Wajant 2015). The moTNFR2-specific antibody clone we investigated was C1 in the format mouse isotype IgG1. C1-moIgG1 treatment expanded Tregs in the whole mouse as measured via bioluminescence imaging. After three injections and six days the Treg density increased by 1.4-fold. Compared to that, a single injection of NewSTAR reached the 3.7-fold Treg level on day five. Albeit C1-moIgG1 has the desired pharmacokinetics of an antibody, NewSTAR was by far superior.

TNFα is a key mediator of inflammation (Bradley, 2008). In addition, it plays an important role in immune regulation. The first part of this study clearly showed how TNFR2 mediates this role. In the absence of any other stimulus, TNFR2 agonization activated and expanded Tregs, the masters of immune regulation. With TNFR2 agonization we report a high potential route to suppress over boarding immune responses. Aside from GvHD, inflammatory diseases in general might benefit from it.

5.2 IL-2 fusion proteins for the prevention of aGvHD

IL-2 is indispensable for Treg homeostasis (Sakaguchi et al., 1995; Fontenot et al., 2005) and in multiple disease models low-dose IL-2 or IL-2 antibody complexes increase the function and numbers of Tregs which then in return reduce inflammation (Wilson et al. 2008; Webster et al., 2009; He et al., 2016; Hirakawa et al., 2016; Kim et al. 2016; Peterson et al., 2018; Trotta et al., 2018). However, bad pharmacokinetics of IL-2 (Kontermann, 2012) and severe side effects limit the clinical efficacy (Krieg et al., 2010; Rosenberg et al., 2010). In order to improve pharmacokinetics, we designed an IgG-IL-2-fusion protein. It consists of an huIgG with IL-2 molecules fused to its heavy chains. With IgG-IL-2 we preemptively expanded Tregs prior to allo-HCT and reduced GvHD symptoms afterwards. Along with Tregs we observed a remarkable expansion of NK cells after irrIgG-IL-2 treatment. This phenomenon is frequently reported for IL-2 therapy in humans (Caligiuri et al., 1993; Ito et al., 2014; Hirakawa et al., 2016). NK cells are potent killers of tumor cells (Vivier et al., 2008). With their increase, the tumor might get an additional hit before allo-HCT. This might reduce relapse of the tumor afterwards. It is noteworthy, that the response to viral infections is still intact after Treg expansion via IL-2 (Trotta et al., 2018).

Comparing both of our strategies, we found Treg activation and expansion via TNFR2 stimulation to be superior to IL-2. First, TNFR2 stimulation bypasses the severe side effects of IL-2 administration. Second, the Treg expansion was faster and higher. As seen for IL-2, also Treg activation and expansion via TNFR2 stimulation does not interfere with the response to viral infections (Chopra et al., 2016).

5.3 Targeting Tregs for PDAC therapy

After we demonstrated the benefits of Treg activation and expansion for aGvHD, we next investigated the tumor microenvironment of PDAC where Tregs are highly abundant and negatively impact survival (Hiraoka et al., 2006). For our investigations we used the syngeneic orthotopic Panc02 model in fully immunocompetent mice (Corbett et al., 1984). We identified potential targets on Tregs and disruption of the tumor stroma as mechanism to counteract the high Treg density.

5.3.1 The orthotopic Panc02 model closely resembles the immune microenvironment in PDAC

Our data demonstrates that the Panc02 model mimics the human disease in several aspects. During ten days with four treatments of gemcitabine the tumor growth was strongly reduced. In the control group the tumors 15-fold increased in signal compared to 4-fold under gemcitabine treatment. Nevertheless, the tumors aggressively progressed. In human patients, gemcitabine was one of the first approved therapies and prolonged the median survival to 5.65 months (Burris et al., 1997). The dismal prognosis and the few treatment options urged us to explore the immune microenvironment of the tumor and to expose novel treatment options.

Similar to the human disease we found Treg infiltration and accumulation accompanying disease progression in the Panc02 model (Hiraoka et al., 2006). Tregs seem to protect PDAC from immune responses early on. This underlines the importance of early treatment. However, early diagnosis remains one of the major obstacles in reducing PDAC mortality. For a better understanding of the disease we therefore investigated the T cell composition of established tumors. We found that Tregs constitute 33.1 ± 7.3 % of the $CD4^+$ T cell compartment. This closely matches the 34.6 ± 10.9 % observed in human patients (Hiraoka et al., 2006). In the draining lymph nodes Hiraoka *et al.* did not find elevated Treg levels. We observed a slight but significant increase. Also, in line with our model the group identified dramatically low $CD8^+$ T cell numbers. As Treg numbers increased with the progression of the tumor, the $CD8^+$ T cells decreased. Thus, this demonstrates how similar the Panc02 model resembled the human tumor microenvironment in this devastating disease. In peripheral blood the Treg and T cell frequencies were not altered, whereas in human patients contrasting findings are reported (Liyanage et al., 2002; Yamamoto et al., 2012; Tang et al., 2014). Also unaffected in our experiments were the systemic Treg numbers as assessed by whole body

BLI. Hence, we conclude that the immune suppression in PDAC is not systemic but local at the spleen, tumor-draining lymph nodes and most prominent in the tumor itself. In the analyzed tumors, all T cells showed an activated phenotype. Nevertheless, all tumors continued to grow. The results clearly show that there was an ongoing, but insufficient anti-tumor immune response as the PDAC progressed. Strong regulation of T cells by a tolerogenic tumor microenvironment might contribute to this failure, as we observed and importantly, in line with the literature (Hiraoka et al., 2006) we hypothesize that the highly abundant Tregs suppress the anti-tumor immune response.

5.3.2 Origin and proliferation of highly abundant Tregs in PDAC

One important question we could not answer was where the tumor-infiltrating Tregs originate. High infiltration of tTregs but also the local conversion into pTregs are possible explanations for the high Treg abundance in the Panc02 model. Although controversially discussed, Helios and Neuropilin-1 are frequently used to identify tTregs (Thornton et al., 2010; Yadav et al., 2012). In the Panc02 model we found that all Tregs highly upregulated Helios but decreased Neuropilin-1. With that our results contribute to the currently ongoing controversy about these markers (Gottschalk et al., 2012; Szurek et al., 2015) and we cannot explain the Treg origin. Shevchenko et al. (2013) also raised the question whether tumor-infiltrating Tregs in the Panc02 model are peripherally induced or of thymic origin. They reported that 70 % of the tumor-infiltrating Tregs were Ki-67$^+$. We found that only 2.9 % of the tumor-infiltrating Tregs were Ki-67$^+$ and this was even less than the 19.5 % we observed in healthy spleen. Therefore, we conclude, that Treg expansion inside the tumor cannot explain their accumulation in the Panc02 model alone. However, proliferating Ki-67$^+$ Tregs were TNFR2^{high} and therefore we postulate that the TNFR2$^+$ Treg subset is a pool of locally expanding Tregs. These results suggest that TNFR2 blockade interferes with intra-tumoral Treg expansion. However, when we blocked TNFR2 on Tregs their accumulation inside the Panc02 tumors continued. From that we conclude that other mechanisms must be responsible for the high Treg burden. Tumors establish a Treg fostering metabolic milieu, that in addition impairs Tcons (Speiser et al., 2016). Furthermore, tumor cells express ligands for Treg survival and maintenance (Francisco et al., 2009). Hence, Treg survival and not expansion might lead to their high numbers. The slight changes between healthy splenic Tregs and tumor-infiltrating Tregs in Ki-67 expression favor this hypothesis.

5.3.3 Expression of immunomodulatory receptors on tumor-infiltrating Tregs

To identify potential new targets, we analyzed the expression of immunomodulatory receptors on tumor-infiltrating Tregs. One of the first identified immunomodulatory receptors was CTLA-4. It is constitutively expressed on Tregs and is essential for their suppressive function (Takahashi et al., 2000; Wing et al., 2008). In our orthotopic PDAC model we identified tumor-infiltrating Tregs as the main CTLA-4 upregulating T cell subset. This is in accordance to several other mouse tumor models (Vargas et al., 2018). Until today it is under debate how anti-CTLA-4 antibodies modify the anti-tumor immune response. Although, mouse studies demonstrated Treg reduction by anti-CTLA-4 therapy (Selby et al., 2013; Simpson et al., 2013) the effect is not observed in human patients (Sharma et al. 2019). Since anti-CTLA-4 monotherapy has no significant benefits for patients suffering from PDAC (Royal et al., 2010), we assume that other immunomodulatory receptors may contribute to the suppressive environment. Our study reveals a high PD-1 upregulation on tumor-infiltrating Tregs. PD-1 maintains FoxP3 expression and furthermore can convert $CD4^+$ Tcons into Tregs (Francisco et al., 2009). Rapid conversion might explain why we found only few PD-$1^{high}CD4^+$ Tcons inside the tumor. Along with Tregs we found the majority of $CD8^+$ T cells upregulating PD-1. In T cells PD-1 transduces inhibitory signals (Freeman et al., 2000). Despite these observations in mouse models targeting PD-1 did not improve the outcome of PDAC patients (Brahmer et al., 2012).

In addition to CTLA-4 and PD-1, we included the new emerging immunomodulatory receptors Lag-3 and TIGIT in our study. Lag-3 exerts its function by binding to MHC class II molecules (Anderson et al., 2016). In Tregs it contributes to their suppressive function (Huang et al., 2004). The small increase in Lag-3 expression we observed on Tregs upon tumor infiltration, suggest limited effects of anti-Lag-3 therapy for PDAC. In our hands mainly, tumor-infiltrating $CD8^+$ T cells upregulated Lag-3. Together with Lag-3 also PD-1 increased on the $CD8^+$ T cells. This suggests that the $CD8^+$ T cells are “exhausted” or at least strongly regulated by their tissue environment (Blackburn et al., 2009). Matsuzaki and colleagues (2010) reported infiltrating $CD8^+$PD-1^+Lag-3^+ T cells in cancer patients that produce less IFNγ. The anti-tumor effects of IFNγ are well known (Shankaran et al., 2001) and especially IFNγ-producing $CD8^+$ T cells appear as key players in the rejection of PDAC in mouse models (Jang et al., 2017). Blockade of Lag-3 might enhance their effector functions, but nevertheless the $CD8^+$ T cells still need to overcome an enormous number of opposing Tregs that keep them in check. Thus, targeting

Lag-3 may enhance $CD8^+$ effector functions but may not be sufficient to benefit PDAC patients. As Lag-3 blockade might preserve the effector functions of $CD8^+$ T cells it may therapeutically benefit Treg depleting strategies. Another immunomodulatory receptor on the rise is TIGIT. Similar to CTLA-4 it functions by binding costimulatory receptors and thereby competes with their agonizing ligands (Anderson et al., 2016). In our model, we found TIGIT upregulation on all tumor-infiltrating T cells. However, the TIGIT upregulation on Tregs exceeded the other tumor-infiltrating T cells by far. TIGIT is of paramount importance for Tregs and associated with their protective role in tumors (Kurtulus et al., 2015). Its expression correlates with superior suppressive function and especially higher IL-10 and TGF-β production (Joller et al., 2014). Both are powerful weapons of Tregs to induce T cell exhaustion (Sawant et al., 2019). Concluding from our own results and the literature TIGIT is an attractive target on Tregs for cancer immunotherapy. Currently, there are several ongoing clinical trials that will reveal whether targeting TIGT is safe and effective (reviewed from Solomon and Garrido-Laguna, 2018).

5.3.4 Exposing TNFRSF members as targets for Tregs in PDAC

Besides the immunomodulatory receptors, various members of the TNFRSF are important for Treg function (Shimizu et al., 2002; Chen et al., 2007; So et al., 2008; own results; Nishikii et al., 2016). This urged us to investigate their expression on tumor-infiltrating Tregs. In the Panc02 model we found strong GITR upregulation, which we predicted from the literature (Vargas et al., 2018). For targeting purposes, it is noteworthy that GITR is constitutively expressed on all systemic Tregs (Shimizu et al., 2002) and also strongly upregulated on Tcons upon tumor infiltration. Nevertheless, in preclinical mouse models targeting GITR reduced intratumoral Tregs (Cohen et al., 2010) and clinical trials are ongoing (https://clinicaltrials.gov, identifier: NCT01239134). We found 4-1BB upregulation almost exclusively on tumor-infiltrating Tregs. This makes it a suited target for selective Treg depletion. Several groups reported 4-1BB targeting antibodies with anti-tumoral effects in different models alone and in combination with checkpoint blockade, established antibody therapies and chemotherapies (Melero et al., 1997; May et al., 2002; Miller et al., 2002; Kocak et al., 2006; Ju et al., 2008; Kohrt et al., 2012; Chen et al. 2015). However, severe immunological side effects in mouse models tamed the striking results (Niu et al., 2007; Lee et al., 2009). Clinical trials will now evaluate the safety and efficacy of 4-1BB targeting antibodies in human patients (https://clinicaltrials.gov, identifier: NCT03364348). A mighty and multifunctional pathway for

tumor immune escape is the CD27-CD70 axis. In line with the literature on mouse melanoma we identified Tregs and $CD8^+$ T cells as the highest CD27 expressors (Roberts et al., 2010). Possible effects of CD27 stimulation by CD70 expressing tumors are survival and expansion of Tregs (reviewed in depth by Wajant 2016). *In vitro* Tregs downregulate CD27 after CD70 stimulation (Claus et al., 2012). We therefore conclude that CD70-CD27 interaction on Tregs leads to expansion followed by CD27 reduction afterwards. With this we speculate that blockade of the CD27-CD70 interaction interferes with Treg accumulation. In addition to tumor-infiltrating Tregs, we also found a CD27 decrease on Tcons. We predicted this effect from the literature that links CD27 decrease to shedding after the contact to CD70 expressing tumor cells (Wischhusen et al., 2002). On tumor-infiltrating T cells CD27 stimulation contributes to exhaustion and apoptosis (Wajant 2016). Concluding from our results we urgently propose blocking of the CD27-CD70 interaction for the treatment of PDAC. We predict simultaneous inhibition of Tregs and reduced inhibition of Tcons.

In accordance with the literature we observed the highest OX40 expression in tumor-infiltrating Tregs (Bulliard et al., 2014; Vargas et al., 2018) and thus targeting OX40 seems apparent. OX40 gained interest with reports that its agonization abrogates Treg suppression and turns off FoxP3 expression (Vu et al., 2007; Piconese et al., 2008; Kitamura et al., 2009; Voo et al., 2013). Furthermore, targeting OX40 depletes intra-tumoral Tregs (Bulliard et al., 2014). In our study tumor-infiltrating Tcons downregulated OX40 expression. This is of particular importance for a successful targeting strategy that aims to deplete Tregs but on the other hand spares Tcons and the anti-tumor effects they exert.

We and others reported that particular TNFR2 is important for Treg function and proliferation (Chen et al. 2007, Chen et al. 2008, Chen et al. 2010; Chopra et al., 2016). Also, the high expression on tumor-infiltrating Tregs is well known (Chen et al. 2008). In the Panc02 model we therefore investigated TNFR2 and found an enormous upregulation on Tregs upon tumor-infiltration. As mentioned before higher Ki-67 expression accompanied the TNFR2 upregulation and we propose the $TNFR2^+$ Treg subset is a proliferative reservoir in PDAC. In addition, we observed higher CTLA-4, PD-1 and CD73 expression along with TNFR2 upregulation. All markers are associated with suppressive activity in Tregs (Deaglio et al., 2007; Wing et al., 2008; Francisco et al., 2009). Chen et al. (2008) previously reported the highly suppressive $TNFR2^+$ Tregs in tumor models and thereby strongly supports our position.

Although, Tregs were the brightest TNFR2 expressors, it also increased in $CD8^+$ T cells and to some extent in $CD4^+$ T cells. In summary, we propose TNFR2 as a novel target for Tregs in PDAC for the following reasons. First, TNFR2-expressing Tregs are highly abundant in the tumor bed. Second, in line with the literature we identified TNFR2-expressing Tregs to be highly suppressive (Chen et al. 2008). Third, and unknown so far, they are the main source of Treg proliferation in PDAC. As mentioned before (5.3.2), the blockade of TNFR2 had no effect on this subset and we therefore suggest targeting with depleting antibodies.

In conclusion, we demonstrated the upregulation of TNFRSF members, notably GITR, 4-1BB, OX40 and TNFR2 on tumor-infiltrating Tregs. Not all are exclusively upregulated on tumor-infiltrating Tregs, however, in all cases they had the highest expression. Furthermore, we found CD27 downregulation inside the tumor, which hints on the involvement of this pathway. Our results demonstrate the immense potential of the TNFRSF for tumor immunotherapy directed against Tregs. As targets for PDAC we highly recommend OX40, CD27 and TNFR2. Latter identifies suppressive and proliferative Tregs.

5.3.5 Targeting the tumor extracellular matrix changes the immune composition in PDAC and reduces tumor infiltrating Tregs

Astonishing were the results we obtained with minoxidil treatment in our PDAC model. With its inhibitory effects on collagen synthesis (Murad and Pinnell, 1987) we expected reduced stroma formation and a general increase in immune cell infiltration as a consequence. It was totally unexpected that the tumor-infiltrating Tregs declined and except for B cells the rest of the immune army remained unaffected. The effect seems to be Treg and B cell specific. We can rule out cytotoxic effects, since the frequencies in the spleen were unaffected. Despite the Treg-decreasing effect minoxidil treatment did not affect the tumor growth. This demonstrates that Treg-reduction inside the tumor may not be sufficient for tumor regression and the immune response is still impaired. One possible explanation is that the remaining Tregs are still strong enough to block the tumoricidal part of the immune system and an additional immune stimulation might be necessary to boost the immune response against the poorly immunogenic pancreatic tumors (Vogelstein et al., 2013). Further, we observed T cell exhaustion and highly recommend interfering with it in parallel to Treg depletion. In addition to Tregs, there are several other tolerogenic cells in the tumor microenvironment (described in 1.5.1) and the immune suppression they all together establish might still be functional if the Tregs are reduced or even if they are missing. Another possible explanation is the low

immunogenicity of PDAC (Vogelstein et al., 2013). Even when the Tregs are missing, there might be too few tumor-reactive T cells to combat the tumor. However, our results clearly show that there is T cell activation in our tumor model and so we postulate that the immune response is rather inhibited than not functional. Our findings of exhausted T cells support this claim.

Although minoxidil did not stop tumor growth the results taught us that Tregs, the critical players in PDAC, are vulnerable. Decreasing their vast majority is an important first strike and opens perspectives towards novel treatment options. Minoxidil is approved and well tolerated by the patients.

5.4 Conclusion

Preclinical mouse models and clinical data strongly suggest the benefits of Treg manipulation for the therapy of inflammatory disease and cancer. However, precise strategies and powerful tools to implement them still remain in their infancy. In this study, we explored several approaches to target Tregs *in vivo* and presented new tools that hold great promise for clinical translation.

First, we successfully augmented Treg function and numbers via an IgG-IL-2-fusion protein. In addition, we employed TNFR2 agonists (STAR2, NewSTAR), which appeared superior to IL-2 as *in vivo* Treg expansion and activation was similar effective, yet TNFR2 agonist treatment spared adverse side effects. We propose that the TNFR2 pathway is as important for Treg function as IL-2. Importantly, we proved in a mouse model of aGvHD the clinical relevance of our constructs as treatment reduced symptoms and increased survival.

Second, we investigated and developed targeting strategies for Tregs in cancer. For PDAC we suggest TIGIT and TNFRSF members as novel targets. An important and somewhat surprising finding was that blocking TNFR2 did not interfere with Treg accumulation in orthotopic mouse PDAC. However, we successfully decreased Treg numbers in PDAC when we targeted the tumor extracellular matrix. Notably, even with dramatically reduced Treg numbers the tumors continued to grow and therefore, our results suggest Treg reduction will likely not prevail as a monotherapy but rather to support conventional and immunotherapy for PDAC.

Conclusively, our results clearly demonstrate the benefits of Treg manipulation and point towards novel treatment strategies for patients suffering from inflammatory disease and cancer.

References

Abbas, A.K., Benoist, C., Bluestone, J.A., Campbell, D.J., Ghosh, S., Hori, S., Jiang, S., Kuchroo, V.K., Mathis, D., Roncarolo, M.G., et al. (2013). Regulatory T cells: Recommendations to simplify the nomenclature. Nat. Immunol. *14*, 307–308.

Afzali, B., Lombardi, G., Lechler, R.I., and Lord, G.M. (2007). The role of T helper 17 (Th17) and regulatory T cells (Treg) in human organ transplantation and autoimmune disease. Clin. Exp. Immunol. *148*, 32–46.

Akimova, T., Beier, U.H., Wang, L., Levine, M.H., and Hancock, W.W. (2011). Helios expression is a marker of T cell activation and proliferation. PLoS One *6*, e24226.

Anderson, A.C., Joller, N., and Kuchroo, V.K. (2016). Lag-3, Tim-3, and TIGIT: Co-inhibitory Receptors with Specialized Functions in Immune Regulation. Immunity *44*, 989–1004.

Anz, D., Mueller, W., Golic, M., Kunz, W.G., Rapp, M., Koelzer, V.H., Ellermeier, J., Ellwart, J.W., Schnurr, M., Bourquin, C., et al. (2011). CD103 is a hallmark of tumor-infiltrating regulatory T cells. Int. J. Cancer *129*, 2417–2426.

Apostolou, I., Sarukhan, A., Klein, L., and Von Boehmer, H. (2002). Origin of regulatory T cells with known specificity for antigen. Nat. Immunol. *3*, 756–763.

Aspalter, R.M., Eibl, M.M., and Wolf, H.M. (2003). Regulation of TCR-mediated T cell activation by TNF-RII. J. Leukoc. Biol. *74*, 572–582.

Balsari, A., Merlo, A., Casalini, P., Carcangiu, M.L., Malventano, C., Triulzi, T., Menard, S., and Tagliabue, E. (2009). FOXP3 expression and overall survival in breast cancer. J. Clin. Oncol. *27*, 1746–1752.

Barnett, B., Kryczek, I., Cheng, P., Zou, W., and Curiel, T.J. (2005). Regulatory T Cells in Ovarian Cancer: Biology and Therapeutic Potential. Am. J. Reprod. Immunol. *54*, 369–377.

Baron, U., Floess, S., Wieczorek, G., Baumann, K., Grützkau, A., Dong, J., Thiel, A., Boeld, T.J., Hoffmann, P., Edinger, M., et al. (2007). DNA demethylation in the human FOXP3 locus discriminates regulatory T cells from activated FOXP3+conventional T cells. Eur. J. Immunol. *37*, 2378–2389.

Baruch, K., Rosenzweig, N., Kertser, A., Deczkowska, A., Sharif, A.M., Spinrad, A., Tsitsou-Kampeli, A., Sarel, A., Cahalon, L., and Schwartz, M. (2015). Breaking immune tolerance by targeting Foxp3(+) regulatory T cells mitigates Alzheimer's disease pathology. Nat. Commun. *6*, 7967.

Bennett, C.L., Christie, J., Ramsdell, F., Brunkow, M.E., Ferguson, P.J., Whitesell, L., Kelly, T.E., Saulsbury, F.T., Chance, P.F., and Ochs, H.D. (2001). The immune dysregulation, polyendocrinopathy, enteropathy, X-linked syndrome (IPEX) is caused by mutations of FOXP3. Nat. Genet. *27*, 20–21.

Bettelli, E., Carrier, Y., Gao, W., Korn, T., Strom, T.B., Oukka, M., Weiner, H.L., and Kuchroo, V.K. (2006). Reciprocal developmental pathways for the generation of pathogenic effector TH17 and regulatory T cells. Nature *441*, 235–238.

Beyer, M., Kochanek, M., Giese, T., Endl, E., Weihrauch, M.R., Knolle, P.A., Classen, S., and Schultze, J.L. (2006). In vivo peripheral expansion of naive CD4+CD25high FoxP3+ regulatory T cells in patients with multiple myeloma. Blood *107*.

Black, R.A., Rauch, C.T., Kozlosky, C.J., Peschon, J.J., Slack, J.L., Wolfson, M.F., Castner, B.J., Stocking, K.L., Reddy, P., Srinivasan, S., et al. (1997). A metalloproteinase disintegrin that releases tumour-necrosis factor-α from cells. Nature *385*, 729–733.

Blackburn, S.D., Shin, H., Haining, W.N., Zou, T., Workman, C.J., Polley, A., Betts, M.R., Freeman, G.J., Vignali, D.A.A., and Wherry, E.J. (2009). Coregulation of CD8+T cell exhaustion by multiple inhibitory receptors during chronic viral infection. Nat. Immunol. *10*, 29–37.

Bodmer, J.-L., Schneider, P., and Tschopp, J. (2002). The molecular architecture of the TNF superfamily. Trends Biochem. Sci. *27*, 19–26.

Bos, P.D., Plitas, G., Rudra, D., Lee, S.Y., and Rudensky, A.Y. (2013). Transient regulatory T cell ablation deters oncogene-driven breast cancer and enhances radiotherapy. J. Exp. Med. *210*, 2435–2466.

Bradley, J.R. (2008). TNF-mediated inflammatory disease. J. Pathol. *214*, 149–160.

Brahmer, J.R., Tykodi, S.S., Chow, L.Q.M., Hwu, W.-J., Topalian, S.L., Hwu, P., Drake, C.G., Camacho, L.H., Kauh, J., Odunsi, K., et al. (2012). Safety and Activity of Anti–PD-L1 Antibody in Patients with Advanced Cancer. N. Engl. J. Med. *366*, 2455–2465.

Brede, C., Friedrich, M., Jordán-Garrote, A.-L., Riedel, S.S., Bäuerlein, C.A., Heinze, K.G., Bopp, T., Schulz, S., Mottok, A., Kiesel, C., et al. (2012). Mapping immune processes in intact tissues at cellular resolution. J. Clin. Invest. *122*, 4439–4446.

Brunkow, M.E., Jeffery, E.W., Hjerrild, K.A., Paeper, B., Clark, L.B., Yasayko, S.-A., Wilkinson, J.E., Galas, D., Ziegler, S.F., and Ramsdell, F. (2001). Disruption of a new forkhead/winged-helix protein, scurfin, results in the fatal lymphoproliferative disorder of the scurfy mouse. Nat. Genet. *27*, 68–73.

Brunstein, C.G., Miller, J.S., Cao, Q., McKenna, D.H., Hippen, K.L., Curtsinger, J., DeFor, T., Levine, B.L., June, C.H., Rubinstein, P., et al. (2011). Infusion of ex vivo expanded T regulatory cells in adults transplanted with umbilical cord blood: Safety profile and detection kinetics. Blood *117*, 1061–1070.

Brusko, T., and Atkinson, M. (2007). Treg in type 1 diabetes. Cell Biochem. Biophys. *48*, 165–175.

Bulliard, Y., Jolicoeur, R., Zhang, J., Dranoff, G., Wilson, N.S., and Brogdon, J.L. (2014). OX40 engagement depletes intratumoral Tregs via activating FcγRs, leading to antitumor efficacy. Immunol. Cell Biol. *92*, 475–480.

Burris, H.A., Moore, M.J., Andersen, J., Green, M.R., Rothenberg, M.L., Modiano, M.R., Cripps, M.C., Portenoy, R.K., Storniolo, A.M., Tarassoff, P., et al. (1997). Improvements in Survival and Clinical Benefit With Gemcitabine as First-Line Therapy for Patients With Advanced Pancreas Cancer: A Randomized Trial.

Burton, J.L., and Marshall, A. (1979). Hypertrichosis due to minoxidil. Br. J. Dermatol. *101*, 593–595.

Cabral, H., Matsumoto, Y., Mizuno, K., Chen, Q., Murakami, M., Kimura, M., Terada, Y., Kano, M.R., Miyazono, K., Uesaka, M., et al. (2011). Accumulation of sub-100 nm polymeric micelles in poorly permeable tumours depends on size. Nat. Nanotechnol. *6*, 815–823.

Caligiuri, M.A., Murray, C., Robertson, M.J., Wang, E., Cochran, K., Cameron, C., Schow, P., Ross, M.E., Klumpp, T.R., and Soiffer, R.J. (1993). Selective modulation of human natural killer cells in vivo after prolonged infusion of low dose recombinant interleukin 2. J. Clin. Invest. *91*, 123–132.

Chen, D.S., and Mellman, I. (2013). Oncology meets immunology: The cancer-immunity cycle. Immunity *39*, 1–10.

Chen, S., Lee, L.-F., Fisher, T.S., Jessen, B., Elliott, M., Evering, W., Logronio, K., Tu, G.H., Tsaparikos, K., Li, X., et al. (2015). Combination of 4-1BB agonist and PD-1 antagonist promotes antitumor effector/memory CD8 T cells in a poorly immunogenic tumor model. Cancer Immunol. Res. *3*, 149–160.

Chen, W., Jin, W., Hardegen, N., Lei, K.-J., Li, L., Marinos, N., McGrady, G., and Wahl, S.M. (2003). Conversion of Peripheral CD4+ CD25− Naive T Cells to CD4+ CD25+ Regulatory T Cells by TGF-β Induction of Transcription Factor Foxp3. J. Exp. Med. *198*, 1875–1886.

Chen, X., Baumel, M., Mannel, D.N., Howard, O.M.Z., and Oppenheim, J.J. (2007). Interaction of TNF with TNF Receptor Type 2 Promotes Expansion and Function of Mouse CD4+CD25+ T Regulatory Cells. J. Immunol. *179*, 154–161.

Chen, X., Subleski, J.J., Kopf, H., Howard, O.M.Z., Mannel, D.N., and Oppenheim, J.J. (2008). Cutting Edge: Expression of TNFR2 Defines a Maximally Suppressive Subset of Mouse CD4+CD25+FoxP3+ T Regulatory Cells: Applicability to Tumor-Infiltrating T Regulatory Cells. J. Immunol. *180*, 6467–6471.

Chen, X., Subleski, J.J., Hamano, R., Howard, O.M.Z., Wiltrout, R.H., and Oppenheim, J.J. (2010). Co-expression of TNFR2 and CD25 identifies more of the functional CD4 +FOXP3+ regulatory T cells in human peripheral blood. Eur. J. Immunol. *40*, 1099–1106.

Chopra, M., Lang, I., Salzmann, S., Pachel, C., Kraus, S., Bäuerlein, C.A., Brede, C., Garrote, A.-L.J.,

Mattenheimer, K., Ritz, M., et al. (2013). Tumor necrosis factor induces tumor promoting and anti-tumoral effects on pancreatic cancer via TNFR1. PLoS One *8*, e75737.

Chopra, M., Biehl, M., Steinfatt, T., Brandl, A., Kums, J., Amich, J., Vaeth, M., Kuen, J., Holtappels, R., Podlech, J., et al. (2016). Exogenous TNFR2 activation protects from acute GvHD via host T reg cell expansion. J. Exp. Med. *213*, 1881–1900.

Clark, C.E., Hingorani, S.R., Mick, R., Combs, C., Tuveson, D.A., and Vonderheide, R.H. (2007). Dynamics of the immune reaction to pancreatic cancer from inception to invasion. Cancer Res. *67*, 9518–9527.

Claus, C., Riether, C., Schurch, C., Matter, M.S., Hilmenyuk, T., Ochsenbein, A.F., Schürch, C., Matter, M.S., Hilmenyuk, T., and Ochsenbein, A.F. (2012). CD27 signaling increases the frequency of regulatory T cells and promotes tumor growth. Cancer Res. *72*, 3664–3676.

Coe, D., Begom, S., Addey, C., White, M., Dyson, J., and Chai, J.G. (2010). Depletion of regulatory T cells by anti-GITR mAb as a novel mechanism for cancer immunotherapy. Cancer Immunol. Immunother. *59*, 1367–1377.

Cohen, A.D., Schaer, D.A., Liu, C., Li, Y., Hirschhorn-Cymmerman, D., Kim, S.C., Diab, A., Rizzuto, G., Duan, F., Perales, M.A., et al. (2010). Agonist anti-GITR monoclonal antibody induces melanoma tumor immunity in mice by altering regulatory T cell stability and intra-tumor accumulation. PLoS One *5*, e10436.

Condeelis, J., and Weissleder, R. (2010). In vivo imaging in cancer. Cold Spring Harb. Perspect. Biol. *2*, a003848.

Corbett, T.H., Roberts, B.J., Leopold, W.R., Peckham, J.C., Wilkoff, L.J., Griswold, D.P., and Schabel, F.M. (1984). Induction and chemotherapeutic response of two transplantable ductal adenocarcinomas of the pancreas in C57BL/6 mice. Cancer Res. *44*, 717–726.

Curiel, T.J., Coukos, G., Zou, L., Alvarez, X., Cheng, P., Mottram, P., Evdemon-Hogan, M., Conejo-Garcia, J.R., Zhang, L., Burow, M., et al. (2004). Specific recruitment of regulatory T cells in ovarian carcinoma fosters immune privilege and predicts reduced survival. Nat. Med. *10*, 942–949.

Deaglio, S., Dwyer, K.M., Gao, W., Friedman, D., Usheva, A., Erat, A., Chen, J.-F., Enjyoji, K., Linden, J., Oukka, M., et al. (2007). Adenosine generation catalyzed by CD39 and CD73 expressed on regulatory T cells mediates immune suppression. J. Exp. Med. *204*, 1257–1265.

Dong, H., Strome, S.E., Salomao, D.R., Tamura, H., Hirano, F., Flies, D.B., Roche, P.C., Lu, J., Zhu, G., Tamada, K., et al. (2002). Tumor-associated B7-H1 promotes T-cell apoptosis: A potential mechanism of immune evasion. Nat. Med. *8*, 793–800.

Dong, Y., Fischer, R., Naudé, P.J.W., Maier, O., Nyakas, C., Duffey, M., Van der Zee, E.A., Dekens, D., Douwenga, W., Herrmann, A., et al. (2016). Essential protective role of tumor necrosis factor receptor 2 in neurodegeneration. Proc. Natl. Acad. Sci. U. S. A. *113*, 12304–12309.

Dopp, J.M., Mackenzie-Graham, A., Otero, G.C., and Merrill, J.E. (1997). Differential expression, cytokine modulation, and specific functions of type-1 and type-2 tumor necrosis factor receptors in rat glia. J. Neuroimmunol. *75*, 104–112.

Ducreux, M., Seufferlein, T., Van Laethem, J.-L., Laurent-Puig, P., Smolenschi, C., Malka, D., Boige, V., Hollebecque, A., and Conroy, T. (2018). Systemic treatment of pancreatic cancer revisited. Semin. Oncol.

Edinger, M., Hoffmann, P., Ermann, J., Drago, K., Garrison Fathman, C., Strober, S., and Negrin, R.S. (2003). CD4+CD25+ regulatory T cells preserve graft-versus-tumor activity while inhibiting graft-versus-host disease after bone marrow transplantation. Nat. Med. *9*, 1144–1150.

Ephrem, A., Chamat, S., Miquel, C., Fisson, S., Mouthon, L., Caligiuri, G., Delignat, S., Elluru, S., Bayry, J., Lacroix-Desmazes, S., et al. (2008). Expansion of CD4+CD25+ regulatory T cells by intravenous immunoglobulin: a critical factor in controlling experimental autoimmune encephalomyelitis. Blood *111*.

Esni, F., Shi, G., Habbe, N., Feldmann, G., Konieczny, S.F., Stoffers, D.A., Fendrich, V., Meguid, R.A., Leach, S.D., Maitra, A., et al. (2008). Spontaneous induction of murine pancreatic intraepithelial neoplasia (mPanIN) by acinar cell targeting of oncogenic Kras in adult mice. Proc. Natl. Acad. Sci. *105*, 18913–18918.

Ferrara, J.L., Levine, J.E., Reddy, P., and Holler, E. (2009). Graft-versus-host disease. Lancet *373*, 1550–1561.

Fontenot, J.D., Rasmussen, J.P., Gavin, M.A., and Rudensky, A.Y. (2005). A function for interleukin 2 in Foxp3-expressing regulatory T cells. Nat. Immunol. *6*, 1142–1151.

Francisco, L.M., Salinas, V.H., Brown, K.E., Vanguri, V.K., Freeman, G.J., Kuchroo, V.K., and Sharpe, A.H. (2009). PD-L1 regulates the development, maintenance, and function of induced regulatory T cells. J. Exp. Med. *206*, 3015–3029.

Freeman, G.J., Long, A.J., Iwai, Y., Bourque, K., Chernova, T., Nishimura, H., Fitz, L.J., Malenkovich, N., Okazaki, T., Byrne, M.C., et al. (2000). Engagement of the PD-1 immunoinhibitory receptor by a novel B7 family member leads to negative regulation of lymphocyte activation. J. Exp. Med. *192*, 1027–1034.

Gottlieb, T.B., Thomas, R.C., and Chidsey, C.A. (1972). Pharmacokinetic studies of minoxidil. Clin. Pharmacol. Ther. *13*, 436–441.

Gottschalk, R.A., Corse, E., and Allison, J.P. (2012). Expression of Helios in Peripherally Induced Foxp3+ Regulatory T Cells. J. Immunol. *188*, 976–980.

Grell, M., Scheurich, P., Meager, A., and Pfizenmaier, K. (1993). TR60 and TR80 tumor necrosis factor (TNF)-receptors can independently mediate cytolysis. Lymphokine Cytokine Res. *12*, 143–148.

Grell, M., Douni, E., Wajant, H., Löhden, M., Clauss, M., Maxeiner, B., Georgopoulos, S., Lesslauer, W., Kollias, G., Pfizenmaier, K., et al. (1995). The transmembrane form of tumor necrosis factor is the prime activating ligand of the 80 kDa tumor necrosis factor receptor. Cell *83*, 793–802.

Grilo, A.L., and Mantalaris, A. (2019). The Increasingly Human and Profitable Monoclonal Antibody Market. Trends Biotechnol. *37*, 9–16.

Grimm, J., Potthast, A., Wunder, A., and Moore, A. (2003). Magnetic resonance imaging of the pancreas and pancreatic tumors in a mouse orthotopic model of human cancer. Int. J. Cancer *106*, 806–811.

Han, Y., He, T., Huang, D.R., Pardo, C.A., and Ransohoff, R.M. (2001). TNF-alpha mediates SDF-1 alpha-induced NF-kappa B activation and cytotoxic effects in primary astrocytes. J. Clin. Invest. *108*, 425–435.

He, J., Zhang, X., Wei, Y., Sun, X., Chen, Y., Deng, J., Jin, Y., Gan, Y., Hu, X., Jia, R., et al. (2016). Low-dose interleukin-2 treatment selectively modulates CD4 + T cell subsets in patients with systemic lupus erythematosus. Nat. Med. *22*, 991–993.

Hezel, A.F., Kimmelman, A.C., Stanger, B.Z., Bardeesy, N., and Depinho, R.A. (2016). Genetics and biology of pancreatic ductal adenocarcinoma. Genes Dev. *1*, 355–385.

Hidalgo, M. (2010). Pancreatic Cancer. N. Engl. J. Med. *362*, 1605–1617.

Hingorani, S.R., Wang, L., Multani, A.S., Combs, C., Deramaudt, T.B., Hruban, R.H., Rustgi, A.K., Chang, S., and Tuveson, D.A. (2005). Trp53R172H and KrasG12D cooperate to promote chromosomal instability and widely metastatic pancreatic ductal adenocarcinoma in mice. Cancer Cell *7*, 469–483.

Hirakawa, M., Matos, T., Liu, H., Koreth, J., Kim, H.T., Paul, N.E., Murase, K., Whangbo, J., Alho, A.C., Nikiforow, S., et al. (2016). Low-dose IL-2 selectively activates subsets of CD4+ Tregs and NK cells. JCI Insight *1*, e89278.

Hiraoka, N., Onozato, K., Kosuge, T., and Hirohashi, S. (2006). Prevalence of FOXP3+ regulatory T cells increases during the progression of pancreatic ductal adenocarcinoma and its premalignant lesions. Clin. Cancer Res. *12*, 5423–5434.

Von Hoff, D.D., Ervin, T., Arena, F.P., Chiorean, E.G., Infante, J., Moore, M., Seay, T., Tjulandin, S.A., Ma, W.W., Saleh, M.N., et al. (2013). Increased Survival in Pancreatic Cancer with nab-Paclitaxel plus Gemcitabine. N. Engl. J. Med. *369*, 1691–1703.

Hoffmann, P., Ermann, J., Edinger, M., Fathman, C.G., and Strober, S. (2002). Donor-type CD4(+)CD25(+) regulatory T cells suppress lethal acute graft-versus-host disease after allogeneic bone marrow transplantation. J. Exp. Med. *196*, 389–399.

Hori, S., Nomura, T., and Sakaguchi, S. (2003). Control of regulatory T cell development by the transcription factor Foxp3. Science *299*, 1057–1061.

Hu, X., Li, B., Li, X., Zhao, X., Wan, L., Lin, G., Yu, M., Wang, J., Jiang, X., Feng, W., et al. (2014). Transmembrane TNF-α Promotes Suppressive Activities of Myeloid-Derived Suppressor Cells via TNFR2. J. Immunol. *192*.

Huang, C.T., Workman, C.J., Flies, D., Pan, X., Marson, A.L., Zhou, G., Hipkiss, E.L., Ravi, S., Kowalski, J., Levitsky, H.I., et al. (2004). Role of LAG-3 in regulatory T cells. Immunity *21*, 503–513.

Di Ianni, M., Falzetti, F., Carotti, A., Terenzi, A., Castellino, F., Bonifacio, E., Del Papa, B., Zei, T., Ostini, R.I., Cecchini, D., et al. (2011). Tregs prevent GVHD and promote immune reconstitution in HLA-haploidentical transplantation. Blood *117*, 3921–3928.

Idriss, H.T., and Naismith, J.H. (2000). TNFα and the TNF receptor superfamily: Structure-function relationship(s). Microsc. Res. Tech. *50*, 184–195.

Ito, S., Bollard, C.M., Carlsten, M., Melenhorst, J.J., Biancotto, A., Wang, E., Chen, J., Kotliarov, Y., Cheung, F., Xie, Z., et al. (2014). Ultra-low dose interleukin-2 promotes immune-modulating function of regulatory t cells and natural killer cells in healthy volunteers. In Molecular Therapy, (Cell Press), pp. 1388–1395.

Jacomb, R.G., and Brunnberg, F.J. (1976). The use of Minoxidil in the Treatment of Severe Essential Hypertension: A Report on 100 Patients. Clin. Sci. *51*, 579s-581s.

Jang, J.E., Hajdu, C.H., Liot, C., Miller, G., Dustin, M.L., and Bar-Sagi, D. (2017). Crosstalk between Regulatory T Cells and Tumor-Associated Dendritic Cells Negates Anti-tumor Immunity in Pancreatic Cancer. Cell Rep. *20*, 558–571.

Jiang, J., Zhou, H., Ni, C., Hu, X., Mou, Y., Huang, D., and Yang, L. (2019). Immunotherapy in pancreatic cancer: new hope or mission impossible? Cancer Lett.

Johnson, G.A., Barsuhn, K.J., and McCall, J.M. (1982). Sulfation of minoxidil by liver sulfotransferase. Biochem. Pharmacol. *31*, 2949–2954.

Joller, N., Lozano, E., Burkett, P.R., Patel, B., Xiao, S., Zhu, C., Xia, J., Tan, T.G., Sefik, E., Yajnik, V., et al. (2014). Treg cells expressing the coinhibitory molecule TIGIT selectively inhibit proinflammatory Th1 and Th17 cell responses. Immunity *40*, 569–581.

Jordan, M.S., Boesteanu, A., Reed, A.J., Petrone, A.L., Holenbeck, A.E., Lerman, M.A., Naji, A., and Caton, A.J. (2001). Thymic selection of CD4+CD25+ regulatory T cells induced by an agonist self-peptide. Nat. Immunol. *2*, 301–306.

Joshi, N.S., Akama-Garren, E.H., Lu, Y., Lee, D.-Y., Chang, G.P., Li, A., DuPage, M., Tammela, T., Kerper, N.R., Farago, A.F., et al. (2015). Regulatory T Cells in Tumor-Associated Tertiary Lymphoid Structures Suppress Anti-tumor T Cell Responses. Immunity.

Ju, S.-A., Cheon, S.-H., Park, S.-M., Tam, N.Q., Kim, Y.M., An, W.G., and Kim, B.-S. (2008). Eradication of established renal cell carcinoma by a combination of 5-fluorouracil and anti-4-1BB monoclonal antibody in mice. Int. J. Cancer *122*, 2784–2790.

Kamisawa, T., Wood, L.D., Itoi, T., and Takaori, K. (2016). Pancreatic cancer. Lancet *388*, 73–85.

Kaplan, G. (1983). In vitro differentiation of human monocytes. Monocytes cultured on glass are cytotoxic to tumor cells but monocytes cultured on collagen are not. J. Exp. Med. *157*, 2061–2072.

Kim, E.Y., and Teh, H.S. (2001). TNF type 2 receptor (p75) lowers the threshold of T cell activation. J. Immunol. *167*, 6812–6820.

Kim, M.P., Evans, D.B., Wang, H., Abbruzzese, J.L., Fleming, J.B., and Gallick, G.E. (2009). Generation of orthotopic and heterotopic human pancreatic cancer xenografts in immunodeficient mice. Nat. Protoc. *4*, 1670–1680.

Kim, N., Jeon, Y.-W., Nam, Y.-S., Lim, J.-Y., Im, K.-I., Lee, E.-S., and Cho, S.-G. (2016). Therapeutic potential of low-dose IL-2 in a chronic GVHD patient by in vivo expansion of regulatory T cells. Cytokine *78*, 22–26.

Kitamura, N., Murata, S., Ueki, T., Mekata, E., Reilly, R.T., Jaffee, E.M., and Tani, T. (2009). OX40 costimulation can abrogate Foxp3+ regulatory T cell-mediated suppression of antitumor immunity. Int. J. Cancer *125*, 630–638.

Kleeff, J., Korc, M., Apte, M., La Vecchia, C., Johnson, C.D., Biankin, A. V., Neale, R.E., Tempero, M., Tuveson, D.A., Hruban, R.H., et al. (2016). Pancreatic cancer (Nature Publishing Group).

Kocak, E., Lute, K., Chang, X., May, K.F., Exten, K.R., Zhang, H., Abdessalam, S.F., Lehman, A.M., Jarjoura, D., Zheng, P., et al. (2006). Combination therapy with anti-CTL antigen-4 and anti-4-1BB antibodies enhances cancer immunity and reduces autoimmunity. Cancer Res. *66*, 7276–7284.

Kohrt, H.E., Houot, R., Weiskopf, K., Goldstein, M.J., Scheeren, F., Czerwinski, D., Colevas, A.D., Weng, W.-K., Clarke, M.F., Carlson, R.W., et al. (2012). Stimulation of natural killer cells with a CD137-specific antibody enhances trastuzumab efficacy in xenotransplant models of breast cancer. J. Clin. Invest. *122*, 1066–1075.

Komatsu, N., and Hori, S. (2007). Full restoration of peripheral Foxp3+ regulatory T cell pool by radioresistant host cells in scurfy bone marrow chimeras. Proc. Natl. Acad. Sci. *104*, 8959–8964.

Kontermann, R.E. (2009). Strategies to extend plasma half-lives of recombinant antibodies. BioDrugs *23*, 93–109.

Kontermann, R.E. (2012). Antibody-cytokine fusion proteins. Arch. Biochem. Biophys. *526*, 194–205.

Krieg, C., Letourneau, S., Pantaleo, G., and Boyman, O. (2010). Improved IL-2 immunotherapy by selective stimulation of IL-2 receptors on lymphocytes and endothelial cells. Proc. Natl. Acad. Sci. *107*, 11906–11911.

Kriegler, M., Perez, C., DeFay, K., Albert, I., and Lu, S.D. (1988). A novel form of TNF/cachectin is a cell surface cytotoxic transmembrane protein: Ramifications for the complex physiology of TNF. Cell *53*, 45–53.

Kurtulus, S., Sakuishi, K., Ngiow, S.F., Joller, N., Tan, D.J., Teng, M.W.L., Smyth, M.J., Kuchroo, V.K., and Anderson, A.C. (2015). TIGIT predominantly regulates the immune response via regulatory T cells. J. Clin. Invest. *125*, 4053–4062.

Lee, S.-W., Salek-Ardakani, S., Mittler, R.S., and Croft, M. (2009). Hypercostimulation through 4-1BB distorts homeostasis of immune cells. J. Immunol. *182*, 6753–6762.

Lehmann, J., Huehn, J., de la Rosa, M., Maszyna, F., Kretschmer, U., Krenn, V., Brunner, M., Scheffold, A., and Hamann, A. (2002). Expression of the integrin E 7 identifies unique subsets of CD25+ as well as CD25- regulatory T cells. Proc. Natl. Acad. Sci. *99*, 13031–13036.

Lencer, W.I., and Blumberg, R.S. (2005). A passionate kiss, then run: exocytosis and recycling of IgG by FcRn. Trends Cell Biol. *15*, 5–9.

Lewis, M., Tartaglia, L.A., Lee, A., Bennett, G.L., Rice, G.C., Wong, G.H., Chen, E.Y., and Goeddel, D. V (1991). Cloning and expression of cDNAs for two distinct murine tumor necrosis factor receptors demonstrate one receptor is species specific. Proc. Natl. Acad. Sci. U. S. A. *88*, 2830–2834.

Liu, F., Lang, R., Zhao, J., Zhang, X., Pringle, G.A., Fan, Y., Yin, D., Gu, F., Yao, Z., and Fu, L. (2011). CD8+ cytotoxic T cell and FOXP3+ regulatory T cell infiltration in relation to breast cancer survival and molecular subtypes. Breast Cancer Res. Treat. *130*, 645–655.

Liyanage, U.K., Moore, T.T., Joo, H.-G., Tanaka, Y., Herrmann, V., Doherty, G., Drebin, J.A., Strasberg, S.M., Eberlein, T.J., Goedegebuure, P.S., et al. (2002). Prevalence of regulatory T cells is increased in peripheral blood and tumor microenvironment of patients with pancreas or breast adenocarcinoma. J. Immunol. *169*, 2756–2761.

Locksley, R.M., Killeen, N., and Lenardo, M.J. (2001). The TNF and TNF receptor superfamilies: integrating mammalian biology. Cell *104*, 487–501.

Lu, L.L., Suscovich, T.J., Fortune, S.M., and Alter, G. (2018). Beyond binding: Antibody effector functions in infectious diseases. Nat. Rev. Immunol. *18*, 46–61.

Lund, J., Takahashi, N., Pound, J.D., Goodall, M., Nakagawa, H., and Jefferis, R. (1995). Oligosaccharide-protein interactions in IgG can modulate recognition by Fc gamma receptors. FASEB J. *9*, 115–119.

Lund, J., Takahashi, N., Pound, J.D., Goodall, M., and Jefferis, R. (1996). Multiple interactions of IgG with its core oligosaccharide can modulate recognition by complement and human Fc gamma receptor I and influence the synthesis of its oligosaccharide chains. J. Immunol. *157*, 4963–4969.

Lutz, E.R., Wu, A.A., Bigelow, E., Sharma, R., Mo, G., Soares, K., Solt, S., Dorman, A., Wamwea, A., Yager, A., et al. (2014). Immunotherapy Converts Nonimmunogenic Pancreatic Tumors into Immunogenic Foci of Immune Regulation. Cancer Immunol. Res. *2*, 616–631.

Malek, T.R. (2008). The Biology of Interleukin-2. Annu. Rev. Immunol. *26*, 453–479.

Mamaeva, V., Dimcevski, G., Delalande, A., McCormack, E., Postema, M., Popa, M., Gilja, O.H., Gjertsen, B.T., and Kotopoulis, S. (2013). Sonoporation-Enhanced Chemotherapy Significantly Reduces Primary Tumour Burden in an Orthotopic Pancreatic Cancer Xenograft. Mol. Imaging Biol. *16*, 53–62.

Mason, A.T., McVicar, D.W., Smith, C.A., Young, H.A., Ware, C.F., and Ortaldo, J.R. (1995). Regulation of NK cells through the 80-kDa TNFR (CD120b). J Leukoc Biol *58*, 249–255.

Matsuzaki, J., Gnjatic, S., Mhawech-Fauceglia, P., Beck, A., Miller, A., Tsuji, T., Eppolito, C., Qian, F., Lele, S., Shrikant, P., et al. (2010). Tumor-infiltrating NY-ESO-1-specific CD8+ T cells are negatively regulated by LAG-3 and PD-1 in human ovarian cancer. Proc. Natl. Acad. Sci. U. S. A. *107*, 7875–7880.

van Maurik, A., Herber, M., Wood, K.J., and Jones, N.D. (2002). Cutting edge: CD4+CD25+ alloantigen-specific immunoregulatory cells that can prevent CD8+ T cell-mediated graft rejection: implications for anti-CD154 immunotherapy. J Immunol *169*, 5401–5404.

May, K.F., Chen, L., Zheng, P., and Liu, Y. (2002). Anti-4-1BB monoclonal antibody enhances rejection of large tumor burden by promoting survival but not clonal expansion of tumor-specific CD8+ T cells. Cancer Res. *62*, 3459–3465.

McHugh, R.S., Whitters, M.J., Piccirillo, C.A., Young, D.A., Shevach, E.M., Collins, M., and Byrne, M.C. (2002). CD4+CD25+Immunoregulatory T Cells: Gene expression analysis reveals a functional role for the glucocorticoid-induced TNF receptor. Immunity *16*, 311–323.

Medler, J., Nelke, J., Weisenberger, D., Steinfatt, T., Rothaug, M., Berr, S., Hünig, T., Beilhack, A., and Wajant, H. (2019). TNFRSF receptor-specific antibody fusion proteins with targeting controlled FcγR-independent agonistic activity. Cell Death Dis. *10*, 224.

Mehta, P.K., Mamdani, B., Shansky, R.M., Mahurkar, S.D., and Dunea, G. (1975). Severe Hypertension: Treatment With Minoxidil. JAMA J. Am. Med. Assoc. *233*, 249–252.

Meisheri, K.D., Cipkus, L.A., and Taylor, C.J. (1988). Mechanism of action of minoxidil sulfate-induced vasodilation: a role for increased K+ permeability. J. Pharmacol. Exp. Ther. *245*, 751–760.

Meisheri, K.D., Johnson, G.A., and Puddington, L. (1993). Enzymatic and non-enzymatic sulfation mechanisms in the biological actions of minoxidil. Biochem. Pharmacol. *45*, 271–279.

Melero, I., Shuford, W.W., Newby, S.A., Aruffo, A., Ledbetter, J.A., Hellström, K.E., Mittler, R.S., and Chen, L. (1997). Monoclonal antibodies against the 4-1BB T-cell activation molecule eradicate established tumors. Nat. Med. *3*, 682–685.

Messenger, A.G., and Rundegren, J. (2004). Minoxidil: Mechanisms of action on hair growth. Br. J. Dermatol. *150*, 186–194.

Miller, R.E., Jones, J., Le, T., Whitmore, J., Boiani, N., Gliniak, B., and Lynch, D.H. (2002). 4-1BB-specific monoclonal antibody promotes the generation of tumor-specific immune responses by direct activation of CD8 T cells in a CD40-dependent manner. J. Immunol. *169*, 1792–1800.

Mizoguchi, E., Mizoguchi, A., Takedatsu, H., Cario, E., De Jong, Y.P., Ooi, C.J., Xavier, R.J., Terhorst, C., Podolsky, D.K., and Bhan, A.K. (2002). Role of tumor necrosis factor receptor 2 (TNFR2) in colonic epithelial hyperplasia and chronic intestinal inflammation in mice. Gastroenterology *122*, 134–144.

Monjazeb, A.M., Zamora, A.E., Grossenbacher, S.K., Mirsoian, A., Sckisel, G.D., and Murphy, W.J. (2013). Immunoediting and Antigen Loss: Overcoming the Achilles Heel of Immunotherapy with Antigen Non-Specific Therapies. Front. Oncol. *3*, 197.

Morikane, K., Tempero, R.M., Sivinski, C.L., Nomoto, M., Van Lith, M.L., Muto, T., and Hollingsworth, M.A. (1999). Organ-specific pancreatic tumor growth properties and tumor immunity. Cancer Immunol.

Immunother. *47*, 287–296.

Moss, M.L., Jin, S.-L.L.C., Milla, M.E., Burkhart, W., Carter, H.L., Chen, W.J., Clay, W.C., Didsbury, J.R., Hassler, D., Hoffman, C.R., et al. (1997). Cloning of a disintegrin metalloproteinase that processes precursor tumour-necrosis factor-α. Nature *385*, 733–736.

Murad, S., and Pinnell, S.R. (1987). Suppression of fibroblast proliferation and lysyl hydroxylase activity by minoxidil. J. Biol. Chem. *262*, 11973–11978.

Murad, S., Walker, L.C., Tajima, S., and Pinnell, S.R. (1994). Minimum Structural Requirements for Minoxidil Inhibition of Lysyl Hydroxylase in Cultured Fibroblasts. Arch. Biochem. Biophys. *308*, 42–47.

Nassereddine, S., Rafei, H., Elbahesh, E., and Tabbara, I. (2017). Acute Graft Versus Host Disease: A Comprehensive Review. Anticancer Res. *37*, 1547–1555.

Natsume, A., Niwa, R., and Satoh, M. (2009). Improving effector functions of antibodies for cancer treatment: Enhancing ADCC and CDC. Drug Des. Devel. Ther. *3*, 7–16.

Naudé, P.J.W., den Boer, J.A., Luiten, P.G.M., and Eisel, U.L.M. (2011). Tumor necrosis factor receptor cross-talk. FEBS J. *278*, 888–898.

Naylor, M.S., Stamp, G.W., Foulkes, W.D., Eccles, D., and Balkwill, F.R. (1993). Tumor necrosis factor and its receptors in human ovarian cancer. Potential role in disease progression. J. Clin. Invest. *91*, 2194–2206.

Nguyen, V.H., Zeiser, R., DaSilva, D.L., Chang, D.S., Beilhack, A., Contag, C.H., and Negrin, R.S. (2007). In vivo dynamics of regulatory T-cell trafficking and survival predict effective strategies to control graft-versus-host disease following allogeneic transplantation. Blood *109*, 2649–2656.

Nishikii, H., Kim, B.S., Yokoyama, Y., Chen, Y., Baker, J., Pierini, A., Alvarez, M., Mavers, M., Maas-Bauer, K., Pan, Y., et al. (2016). DR3 signaling modulates the function of Foxp3+ regulatory T cells and the severity of acute graft-versus-host disease. Blood *128*, 2846–2858.

Niu, L., Strahotin, S., Hewes, B., Zhang, B., Zhang, Y., Archer, D., Spencer, T., Dillehay, D., Kwon, B., Chen, L., et al. (2007). Cytokine-mediated disruption of lymphocyte trafficking, hemopoiesis, and induction of lymphopenia, anemia, and thrombocytopenia in anti-CD137-treated mice. J. Immunol. *178*, 4194–4213.

Overdijk, M.B., Verploegen, S., Ortiz Buijsse, A., Vink, T., Leusen, J.H.W., Bleeker, W.K., and Parren, P.W.H.I. (2012). Crosstalk between Human IgG Isotypes and Murine Effector Cells. J. Immunol. *189*, 3430–3438.

Owen, D.L., Mahmud, S.A., Vang, K.B., Kelly, R.M., Blazar, B.R., Smith, K.A., and Farrar, M.A. (2018). Identification of Cellular Sources of IL-2 Needed for Regulatory T Cell Development and Homeostasis. J. Immunol. ji1800097.

Paleolog, E., Delasalle, S., Buurman, W., and Feldmann, M. (1994). Functional activities of receptors for tumor necrosis factor-alpha on human vascular endothelial cells. Blood *84*.

Park, J.-S., Lim, K.-M., Park, S.G., Jung, S.Y., Choi, H.-J., Lee, D.H., Kim, W.-J., Hong, S.-M., Yu, E.-S., and Son, W.-C. (2014). Pancreatic Cancer Induced by In Vivo Electroporation-Enhanced Sleeping Beauty Transposon Gene Delivery System in Mouse. Pancreas *43*, 614–618.

Partecke, L.I., Sendler, M., Kaeding, A., Weiss, F.U., Mayerle, J., Dummer, A., Nguyen, T.D., Albers, N., Speerforck, S., Lerch, M.M., et al. (2011). A syngeneic orthotopic murine model of pancreatic adenocarcinoma in the C57/BL6 mouse using the panc02 and 6606PDA cell lines. Eur. Surg. Res. *47*, 98–107.

Peterson, L.B., Bell, C.J.M., Howlett, S.K., Pekalski, M.L., Brady, K., Hinton, H., Sauter, D., Todd, J.A., Umana, P., Ast, O., et al. (2018). A long-lived IL-2 mutein that selectively activates and expands regulatory T cells as a therapy for autoimmune disease. J. Autoimmun.

Piconese, S., Valzasina, B., and Colombo, M.P. (2008). OX40 triggering blocks suppression by regulatory T cells and facilitates tumor rejection. J. Exp. Med. *205*, 1505–1505.

Rahib, L., Smith, B.D., Aizenberg, R., Rosenzweig, A.B., Fleshman, J.M., and Matrisian, L.M. (2014). Projecting cancer incidence and deaths to 2030: the unexpected burden of thyroid, liver, and pancreas cancers in the United States. Cancer Res. *74*, 2913–2921.

Rauert, H., Wicovsky, A., Müller, N., Siegmund, D., Spindler, V., Waschke, J., Kneitz, C., and Wajant, H. (2010). Membrane tumor necrosis factor (TNF) induces p100 processing via TNF receptor-2 (TNFR2). J. Biol. Chem. *285*, 7394–7404.

Roberts, D.J., Franklin, N.A., Kingeter, L.M., Yagita, H., Tutt, A.L., Glennie, M.J., and Bullock, T.N.J. (2010). Control of established melanoma by cd27 stimulation is associated with enhanced effector function and persistence, and reduced PD-1 expression of tumor infiltrating CD8+ T cells. J. Immunother. *33*, 769–779.

Rogers, W.O., Weaver, C.T., Kraus, L.A., Li, J., Li, L., and Bucy, R.P. (1997). Visualization of antigen-specific T cell activation and cytokine expression in vivo. J. Immunol. *158*, 649–657.

Rosenberg, S.A., Lotze, M.T., Muul, L.M., Leitman, S., Chang, A.E., Ettinghausen, S.E., Matory, Y.L., Skibber, J.M., Shiloni, E., Vetto, J.T., et al. (2010). Observations on the Systemic Administration of Autologous Lymphokine-Activated Killer Cells and Recombinant Interleukin-2 to Patients with Metastatic Cancer. N. Engl. J. Med. *313*, 1485–1492.

Rothe, M., Wong, S.C., Henzel, W.J., and Goeddel, D. V. (1994). A novel family of putative signal transducers associated with the cytoplasmic domain of the 75 kDa tumor necrosis factor receptor. Cell *78*, 681–692.

Rothe, M., Pan, M.G., Henzel, W.J., Ayres, T.M., and V. Goeddel, D. (1995). The TNFR2-TRAF signaling complex contains two novel proteins related to baculoviral inhibitor of apoptosis proteins. Cell *83*, 1243–1252.

Royal, R.E., Levy, C., Turner, K., Mathur, A., Hughes, M., Kammula, U.S., Sherry, R.M., Topalian, S.L., Yang, J.C., Lowy, I., et al. (2010). Phase 2 trial of single agent ipilimumab (Anti-CTLA-4) for locally advanced or metastatic pancreatic adenocarcinoma. J. Immunother. *33*, 828–833.

Ruspi, G., Schmidt, E.M., McCann, F., Feldmann, M., Williams, R.O., Stoop, A.A., and Dean, J.L.E. (2014). TNFR2 increases the sensitivity of ligand-induced activation of the p38 MAPK and NF-κB pathways and signals TRAF2 protein degradation in macrophages. Cell. Signal. *26*, 683–690.

Sakaguchi, S., Sakaguchi, N., Asano, M., Itoh, M., and Toda, M. (1995). Immunologic self-tolerance maintained by activated T cells expressing IL-2 receptor alpha-chains (CD25). Breakdown of a single mechanism of self-tolerance causes various autoimmune diseases. J. Immunol. *155*, 1151–1164.

Salmon, H., Franciszkiewicz, K., Damotte, D., Dieu-Nosjean, M.C., Validire, P., Trautmann, A., Mami-Chouaib, F., and Donnadieu, E. (2012). Matrix architecture defines the preferential localization and migration of T cells into the stroma of human lung tumors. J. Clin. Invest. *122*, 899–910.

Sawant, D. V., Yano, H., Chikina, M., Zhang, Q., Liao, M., Liu, C., Callahan, D.J., Sun, Z., Sun, T., Tabib, T., et al. (2019). Adaptive plasticity of IL-10+ and IL-35+ Treg cells cooperatively promotes tumor T cell exhaustion. Nat. Immunol. 1.

Schreiber, T.H., Wolf, D., Tsai, M.S., Chirinos, J., Deyev, V. V, Gonzalez, L., Malek, T.R., Levy, R.B., and Podack, E.R. (2010). Therapeutic Treg expansion in mice by TNFRSF25 prevents allergic lung inflammation. J. Clin. Invest. *120*, 3629–3640.

Seitz, U., Wagner, M., Vogg, A.T., Glatting, G., Neumaier, B., Greten, F.R., Schmid, R.M., and Reske, S.N. (2001). In vivo evaluation of 5-[18F]fluoro-2′-deoxyuridine as tracer for positron emission tomography in a murine pancreatic cancer model. Cancer Res. *61*, 3853–3857.

Selby, M.J., Engelhardt, J.J., Quigley, M., Henning, K.A., Chen, T., Srinivasan, M., and Korman, A.J. (2013). Anti-CTLA-4 Antibodies of IgG2a Isotype Enhance Antitumor Activity through Reduction of Intratumoral Regulatory T Cells. Cancer Immunol. Res. *1*, 32–42.

Serbina, N. V, Salazar-Mather, T.P., Biron, C.A., Kuziel, W.A., and Pamer, E.G. (2003). TNF/iNOS-producing dendritic cells mediate innate immune defense against bacterial infection. Immunity *19*, 59–70.

Shankaran, V., Ikeda, H., Bruce, A.T., White, J.M., Swanson, P.E., Old, L.J., and Schreiber, R.D. (2001). IFNγ, and lymphocytes prevent primary tumour development and shape tumour immunogenicity. Nature *410*, 1107–1111.

Sharma, P., and Allison, J.P. (2015). The future of immune checkpoint therapy. Science (80-.). *348*, 56–61.

Sharma, A., Subudhi, S.K., Blando, J., Scutti, J., Vence, L., Wargo, J., Allison, J.P., Ribas, A., and Sharma, P. (2019). Anti-CTLA-4 immunotherapy does not deplete Foxp3 þ regulatory T cells (Tregs) in human cancers. Clin. Cancer Res. *25*, 1233–1238.

Shevchenko, I., Karakhanova, S., Soltek, S., Link, J., Bayry, J., Werner, J., Umansky, V., and Bazhin, A. V. (2013). Low-dose gemcitabine depletes regulatory T cells and improves survival in the orthotopic Panc02 model of pancreatic cancer. Int. J. Cancer *133*, 98–107.

Shimizu, J., Yamazaki, S., Takahashi, T., Ishida, Y., and Sakaguchi, S. (2002). Stimulation of CD25+CD4+ regulatory T cells through GITR breaks immunological self-tolerance. Nat. Immunol. *3*, 135–142.

Siegel, R.L., Miller, K.D., and Jemal, A. (2017). Cancer Statistics, 2017. CA. Cancer J. Clin. *67*, 7–30.

Simpson, T.R., Li, F., Montalvo-Ortiz, W., Sepulveda, M.A., Bergerhoff, K., Arce, F., Roddie, C., Henry, J.Y., Yagita, H., Wolchok, J.D., et al. (2013). Fc-dependent depletion of tumor-infiltrating regulatory T cells co-defines the efficacy of anti-CTLA-4 therapy against melanoma. J. Exp. Med. *210*, 1695–1710.

Smith, C.A., Davis, T., Anderson, D., Solam, L., Beckmann, M.P., Jerzy, R., Dower, S.K., Cosman, D., and Goodwin, R.G. (1990). A receptor for tumor necrosis factor defines an unusual family of cellular and viral proteins. Science *248*, 1019–1023.

So, T., Lee, S.-W., and Croft, M. (2008). Immune regulation and control of regulatory T cells by OX40 and 4-1BB. Cytokine Growth Factor Rev. *19*, 253–262.

Solomon, B.L., and Garrido-Laguna, I. (2018). TIGIT: a novel immunotherapy target moving from bench to bedside. Cancer Immunol. Immunother. *67*, 1659–1667.

Spain, L., Diem, S., and Larkin, J. (2016). Management of toxicities of immune checkpoint inhibitors. Cancer Treat. Rev. *44*, 51–60.

Speiser, D.E., Ho, P.C., and Verdeil, G. (2016). Regulatory circuits of T cell function in cancer. Nat. Rev. Immunol. *16*, 599–611.

Steffen, M., Ottmann, O.G., and Moore, M.A. (1988). Simultaneous production of tumor necrosis factor-alpha and lymphotoxin by normal T cells after induction with IL-2 and anti-T3. J. Immunol. *140*, 2621–2624.

Stegner, D., Vaneeuwijk, J.M.M., Angay, O., Gorelashvili, M.G., Semeniak, D., Pinnecker, J., Schmithausen, P., Meyer, I., Friedrich, M., Dütting, S., et al. (2017). Thrombopoiesis is spatially regulated by the bone marrow vasculature. Nat. Commun. *8*, 127.

Stein, M., and Gordon, S. (1991). Regulation of tumor necrosis factor (TNF) release by murine peritoneal macrophages: role of cell stimulation and specific phagocytic plasma membrane receptors. Eur. J. Immunol. *21*, 431–437.

Suffner, J., Hochweller, K., Kühnle, M.-C., Li, X., Kroczek, R.A., Garbi, N., and Hämmerling, G.J. (2010). Dendritic cells support homeostatic expansion of Foxp3+ regulatory T cells in Foxp3.LuciDTR mice. J. Immunol. *184*, 1810–1820.

Szurek, E., Cebula, A., Wojciech, L., Pietrzak, M., Rempala, G., Kisielow, P., and Ignatowicz, L. (2015). Differences in expression level of Helios and neuropilin-1 do not distinguish thymus-derived from extrathymically-induced CD4+Foxp3+regulatory T cells. PLoS One *10*, e0141161.

Takahashi, T., Tagami, T., Yamazaki, S., Uede, T., Shimizu, J., Sakaguchi, N., Mak, T.W., and Sakaguchi, S. (2000). Immunologic Self-Tolerance Maintained by CD25+ CD4+ Regulatory T Cells Constitutively Expressing Cytotoxic T Lymphocyte–Associated Antigen 4. J. Exp. Med. *192*, 303–310.

Tan, M.C.B., Goedegebuure, P.S., Belt, B.A., Flaherty, B., Sankpal, N., Gillanders, W.E., Eberlein, T.J., Hsieh, C.-S., and Linehan, D.C. (2009). Disruption of CCR5-Dependent Homing of Regulatory T Cells Inhibits Tumor Growth in a Murine Model of Pancreatic Cancer. J. Immunol. *182*, 1746–1755.

Tang, Y., Xu, X., Guo, S., Zhang, C., Tang, Y., Tian, Y., Ni, B., Lu, B., and Wang, H. (2014). An increased abundance of tumor-infiltrating regulatory t cells is correlated with the progression and prognosis of pancreatic ductal adenocarcinoma. PLoS One *9*, e91551.

Taylor, P.A., Lees, C.J., and Blazar, B.R. (2002). The infusion of ex vivo activated and expanded CD4(+)CD25(+) immune regulatory cells inhibits graft-versus-host disease lethality. Blood *99*, 3493–3499.

Thornton, A.M., Korty, P.E., Tran, D.Q., Wohlfert, E.A., Murray, P.E., Belkaid, Y., and Shevach, E.M. (2010). Expression of Helios, an Ikaros transcription factor family member, differentiates thymic-derived from peripherally induced Foxp3+ T regulatory cells. J. Immunol. *184*, 3433–3441.

Timpson, P., Sansom, O.J., Lowy, A.M., Frame, M.C., Brunton, V.G., Oien, K.A., Jamieson, N.B., Ridgway, R.A., Morton, J.P., Athineos, D., et al. (2009). Mutant p53 drives metastasis and overcomes growth arrest/senescence in pancreatic cancer. Proc. Natl. Acad. Sci. *107*, 246–251.

Trotta, E., Bessette, P.H., Silveria, S.L., Ely, L.K., Jude, K.M., Le, D.T., Holst, C.R., Coyle, A., Potempa, M., Lanier, L.L., et al. (2018). A human anti-IL-2 antibody that potentiates regulatory T cells by a structure-based mechanism. Nat. Med. 1.

Vargas, F.A., Furness, A.J.S., Litchfield, K., Joshi, K., Rosenthal, R., Ghorani, E., Solomon, I., Lesko, M.H., Ruef, N., Roddie, C., et al. (2018). Fc Effector Function Contributes to the Activity of Human Anti-CTLA-4 Antibodies. Cancer Cell *33*, 649-663.e4.

Vieira, P., and Rajewsky, K. (1986). The bulk of endogenously produced IgG2a is eliminated from the serum of adult C57BL/6 mice with a half-life of 6–8 days. Eur. J. Immunol. *16*, 871–874.

Vieira, P., and Rajewsky, K. (1988). The half-lives of serum immunoglobulins in adult mice. Eur. J. Immunol. *18*, 313–316.

Vignali, D.A.A., Collison, L.W., and Workman, C.J. (2008). How regulatory T cells work. Nat. Rev. Immunol. *8*, 523–532.

Vivier, E., Tomasello, E., Baratin, M., Walzer, T., and Ugolini, S. (2008). Functions of natural killer cells. Nat. Immunol. *9*, 503–510.

Vogelstein, B., Papadopoulos, N., Velculescu, V.E., Zhou, S., Diaz, L.A., and Kinzler, K.W. (2013). Cancer genome landscapes. Science (80-.). *340*, 1546–1558.

Voo, K.S., Bover, L., Harline, M.L., Vien, L.T., Facchinetti, V., Arima, K., Kwak, L.W., and Liu, Y.J. (2013). Antibodies Targeting Human OX40 Expand Effector T Cells and Block Inducible and Natural Regulatory T Cell Function. J. Immunol. *191*, 3641–3650.

Vu, M.D., Xiao, X., Gao, W., Degauque, N., Chen, M., Kroemer, A., Killeen, N., Ishii, N., and Chang Li, X. (2007). OX40 costimulation turns off Foxp3+ Tregs. Blood *110*, 2501–2510.

Wajant, H. (2015). Principles of antibody-mediated TNF receptor activation. Cell Death Differ. *22*, 1727–1741.

Wajant, H. (2016). Therapeutic targeting of CD70 and CD27. Expert Opin. Ther. Targets *20*, 959–973.

Wajant, H., Pfizenmaier, K., and Scheurich, P. (2003). Tumor necrosis factor signaling. Cell Death.Differ. *10*, 45–65.

Wang, Y., Wang, M., Abarbanell, A.M., Weil, B.R., Herrmann, J.L., Tan, J., Novotny, N.M., Coffey, A.C., and Meldrum, D.R. (2009). MEK mediates the novel cross talk between TNFR2 and TGF-EGFR in enhancing vascular endothelial growth factor (VEGF) secretion from human mesenchymal stem cells. Surgery *146*, 198–205.

Webster, K.E., Walters, S., Kohler, R.E., Mrkvan, T., Boyman, O., Surh, C.D., Grey, S.T., and Sprent, J. (2009). In vivo expansion of T reg cells with IL-2–mAb complexes: induction of resistance to EAE and long-term acceptance of islet allografts without immunosuppression. J. Exp. Med. *206*, 751–760.

Weiner, L.M., Surana, R., and Wang, S. (2010). Monoclonal antibodies: Versatile platforms for cancer immunotherapy. Nat. Rev. Immunol. *10*, 317–327.

Wilson, M.S., Pesce, J.T., Ramalingam, T.R., Thompson, R.W., Cheever, A., and Wynn, T.A. (2008). Suppression of murine allergic airway disease by IL-2:anti-IL-2 monoclonal antibody-induced regulatory T cells. J. Immunol. *181*, 6942–6954.

Wilson, R.A.M., Evans, T.R.J., Fraser, A.R., and Nibbs, R.J.B. (2018). Immune checkpoint inhibitors: new

strategies to checkmate cancer. Clin. Exp. Immunol. *191*, 133–148.

Wing, K., Onishi, Y., Prieto-Martin, P., Yamaguchi, T., Miyara, M., Fehervari, Z., Nomura, T., and Sakaguchi, S. (2008). CTLA-4 control over Foxp3+ regulatory T cell function. Science (80-.). *322*, 271–275.

Wischhusen, J., Jung, G., Radovanovic, I., Beier, C., Steinbach, J.P., Rimner, A., Huang, H., Schulz, J.B., Ohgaki, H., Aguzzi, A., et al. (2002). Identification of CD70-mediated apoptosis of immune effector cells as a novel immune escape pathway of human glioblastoma. Cancer Res. *62*, 2592–2599.

Yadav, M., Louvet, C., Davini, D., Gardner, J.M., Martinez-Llordella, M., Bailey-Bucktrout, S., Anthony, B.A., Sverdrup, F.M., Head, R., Kuster, D.J., et al. (2012). Neuropilin-1 distinguishes natural and inducible regulatory T cells among regulatory T cell subsets in vivo. J. Exp. Med. *209*, 1713–1722.

Yamamoto, T., Yanagimoto, H., Satoi, S., Toyokawa, H., Hirooka, S., Yamaki, S., Yui, R., Yamao, J., Kim, S., and Kwon, A.-H. (2012). Circulating CD4+CD25+ Regulatory T Cells in Patients With Pancreatic Cancer. Pancreas *41*, 409–415.

Yang, L., Lindholm, K., Konishi, Y., Li, R., and Shen, Y. (2002). Target Depletion of Distinct Tumor Necrosis Factor Receptor Subtypes Reveals Hippocampal Neuron Death and Survival through Different Signal Transduction Pathways. J. Neurosci. *22*.

Zeiser, R., and Blazar, B.R. (2017). Acute Graft-versus-Host Disease — Biologic Process, Prevention, and Therapy. N. Engl. J. Med. *377*, 2167–2179.

Publication list

Chopra, M., Biehl, M., Steinfatt, T., Brandl, A., Kums, J., Amich, J., Vaeth, M., Kuen, J., Holtappels, R., Podlech, J., et al. (2016). **Exogenous TNFR2 activation protects from acute GvHD via host T reg cell expansion.** J. Exp. Med. *213, 1881–1900*.

Medler, J., Nelke, J., Weisenberger, D., Steinfatt, T., Rothaug, M., Berr, S., Hünig, T., Beilhack, A., and Wajant, H. (2019). **TNFRSF receptor-specific antibody fusion proteins with targeting controlled FcγR-independent agonistic activity.** Cell Death Dis. *10, 224*.

Wajant, H., Beilhack, A., Medler, J., Steinfatt, T.
Monospecific bimodular TNF-receptor activating antibodies (mobiTRaAbs)
Invention report May 2019

Curriculum vitae